Signal Transduction in Tandem HAMP Domains

Dissertation

der Mathematisch-Naturwissenschaftlichen Fakultät

der Eberhard Karls Universität Tübingen

zur Erlangung des Grades eines

Doktors der Naturwissenschaften

(Dr. rer. nat.)

vorgelegt von

Janani Natarajan

Chennai, Indien

Tübingen

2014

Tag der mündlichen Qualifikation:	06.05.2014
Dekan:	Prof. Dr. Wolfgang Rosenstiel
1. Berichterstatter:	Prof.Dr. Joachim E. Schultz
2. Berichterstatter:	Prof.Dr. Peter Ruth

Acknowledgement

I would like to thank my supervisor, Prof. Dr. J. E. Schultz, for letting me work on an interesting topic, for opportunities to attend conferences, for helping me understand and think about research and for being such a competent supervisor. This thesis work would not have been possible without his guidance.

I thank Prof. Dr. Peter Ruth for taking part in the evaluation of my thesis.

It is an honor to have Prof. Dr. Peter Ruth, Prof. Dr. Harald Groß, Prof. Dr. Klaus Hantke and Prof Dr. J. E. Schultz for my thesis evaluation.

I would like to thank Prof. Dr. Klaus Hantke for his insight and discussions on the project.

I would like to thank Anita Schultz for her expertise and help with all my difficult clones.

I'm grateful to Ursula Kurz for her excellent technical support. Thank you for being ever so kind with my German. I would also like to thank Dr. Yinlan Guo for all her help and tips.

I would like to thank all my co-workers from Prof. Ruth group; Prof. Drews group and Clement for the nice atmosphere in the 7th floor.

Ana, Karin, Laura and Kajal, thank you for the wonderful times we had. It's always more fun to work with friends. Thank you for all the discussions on science and everything else under the sun. I thank you guys and Bissan whole heartedly. I appreciate Simon-Peter Skopek and all other diploma students for good times.

I would like to thank Stephanie Beltz, Simone Breitkopf and Miriam Ziegler for good atmosphere in the lab. It was fun with you guys. Thanks for your assistance in writing the Zusammenfassung.

Im extremly indebted to KBK, frank, kash, mani, lalli, drazen, vaish, bala, anu, sunny, martina, and shruti for being there during my tough times and all your support especially in the last few months. I'm also thankful to all my friends for their constant support and cheer throughout.

Im grateful to my husband Siva and his family for their support. Siva thank you for your reassurance and faith in me. You made it a lot easier.

Amma, appa, pappu and dharu your support, constant inspiration and confidence in me has made this possible. I thank you with my whole heart for letting me follow my dream. At last but not the least I would like to thank my whole family back in India, USA and London. Without their encouragement and best wishes I would never have been able to finish my work successfully.

TABLE OF CONTENTS

Accession numbers I
Amino acid sequence and the domain representation of various chimeras II
Nomenclature of the constructs. V
Abbreviations VI
1 INTRODUCTION 1
1.1 Chemotactic and phototactic signal transduction 2
1.1.1 The chemoreceptors of *E. coli* 3
1.1.2 The phototaxis transducers of archaea 4
1.2 HAMP domains 5
1.2.1 Classification of HAMP domains 6
1.2.2 Mechanism of signal transduction via HAMP domains 6
1.2.3 Signal transduction in poly-HAMP modules. 7
1.3 Adenylyl cyclases 8
1.3.1 Mycobacterial Rv3645 cyclase 8
1.3.2 Cyanobacterial CyaG cyclase 9
1.4 Question of this thesis 10
2 MATERIALS and METHODS 11
2.1 Chemicals 11
2.2 Equipments 12
2.3 Plasmids 12
2.4 Bacterial strains 13
2.5 Molecular biology methods 13
2.5.1 Isolation of DNA (miniprep) 13
2.5.2 PCR 13
2.5.3 Purification of DNA from gel 14
2.5.4 Estimation of DNA concentration 14
2.5.5 Restriction digestion of DNA 15
2.5.6 Phosphorylation 15
2.5.7 Dephosphorylation of vectors 15
2.5.8 Ligation 15
2.5.9 Transformation of recombinant DNA 15
2.5.10 Isolation and purification of DNA 15
2.5.11 DNA sequencing 16
2.5.12 Permanent cultures 16
2.5.13 Cloning 16

2.6 Protein chemistry 17
2.6.1 Expression 17
2.6.2 Cell harvest. 17
2.6.3 Cell lysis 17
2.6.4 Preparation of membrane fractions 19
2.6.5 Bio-Rad Protein determination. 19
2.6.6 SDS-PAGE 20
2.6.7 Western Blot 20
2.7 Adenylyl cyclase assay 22
2.8 Bioinformatics 23
3 Map of all constructs 24
3.1 NpHAMP domains in test system. 24
3.2 $NpHAMP_{1\text{-}mut5}$ 25
3.3 Comparison of HAMP tandems. 26
3.4 $AS1_1$ mutational analysis. 35
3.5 Connector mutants of NpHAMP tandem 38
3.6 NpHtrII inter-HAMP linker mutants 40
3.7 Structural analysis of the tandems. 40
3.8 Oligonucleotides 42
4 RESULTS 49
4.1 Biochemical analysis of tandem HAMP from *Natronomonas pharaonis*. 49
4.1.1 Tandem HAMP from *N. pharaonis* 49
4.1.2 Triple chimera generation. 50
4.2 Comparison of tandem HAMP domains 57
4.2.1 Tsr HAMP-$NpHAMP_2$ tandem 57
4.2.2 Af1503 HAMP - $NpHAMP_2$ tandem 58
4.2.3 $HAMP_1$ chimeras $HAMP_{Tsr}$-$NpHAMP_1$. 59
4.2.4 $HAMP_1$ chimeras $HAMP_{Af1503}$ -$NpHAMP_1$ 60
4.2.5 Effect of $HAMP_1$ AS1 on signal sign. 61
4.3 $AS1_1$ and signal sign 65
4.3.1 Critical mutations 65
4.3.2 Insignificant mutants 67
4.3.3 Significant mutations 71
4.3.4 Lethal mutations. 73
4.4 Connector in NpHAMP 75
4.4.1 $NpHAMP_1$ connector 75
4.4.2 $NpHAMP_2$ connector 77

4.5 Inter-HAMP linker in NpHAMP tandem. 78
4.5.1 Significance of the length of the linker. 78
4.5.2 The function of all HtrII inter-helical linkers. 80
4.6 Structural analysis of the tandems. 82
4.6.1 CD spectrum of tandem HAMP domains. 82
4.6.2 Homology model of the tandem HAMPs 84
5 DISCUSSION 86
5.1 Tandem HAMP domains. 86
5.2 NpHtrII HAMP tandem does not inverse the signal sign 87
5.3 Oppositely signaling tandems. 87
5.4 Five residues determine the signal sign in tandem. 88
5.4.1 Effect of an M/M or L/I in a/d positions in $AS1_1$ 90
5.5 Importance of connector 91
5.6 Inter-HAMP linker 92
5.7 Model for signal transmission via tandem HAMPs 94
6 SUMMARY 96
7 Zusammenfassung 98
8 References 101

Accession numbers

Tsr receptor (*E. coli*)

gi: 16132176

Tar receptor (*E. coli*)

gi: 16129838

Af1503 protein (*Archaeoglobus fulgidus*)

gi: 159163751

NpHtrII (*Natronomonas pharaonis*)

gi: 161761092

Rv3645 (*Mycobacterium tuberculosis*)

gi: 15610781

CyaG (*Arthrospira platensis*)

gi: 11990887

Amino acid sequence and the domain representation of various chimeras.

The sequence of the domains used is shown below. The numbering of the protein sequence corresponds to the respective native protein.

The transmembrane sensor domains used were:

1) Tsr sensor (1-215)

MLKRIKIVTSLLLVLAVFGLLQLTSGGLFFNALKNDKENFTVLQTIRQQQSTLNGSWVALLQTRNTLNR
AGIRYMMDQNNIGSGSTVAELMESASISLKQAEKNWADYEALPRDPRQSTAAAAEIKRNYDIYHNALA
ELIQLLGAGKINEFFDQPTQGYQDGFEKQYVAYMEQNDRLHDIAVSDNNASYSQAMWILVGVMIVVL
AVIFAVWFGIK

2) Tar sensor (1-213)

MINRIRVVTLLVMVLGVFALLQLISGSLFFSSLHHSQKSFVVSNQLREQQGELTSTWDLMLQTRINLSRS
AVRMMMDSSNQQSNAKVELLDSARKTLAQAATHYKKFKSMAPLPEMVATSRNIDEKYKNYYTALTE
LIDYLDYGNTGAYFAQPTQGMQNAMGEAFAQYALSSEKLYRDIVTDNADDYRFAQWQLAVIALVVVL
ILLVAWYGIR

The HAMP domains used in the study were:

1) Tsr HAMP (216-268)

ASLVAPMNRLIDSIRHIAG GDLVKPIEVDGS NEMGQLAESLRHMQGELMRTVG
-------- AS 1 (216-234) ------- connector (235-246) ---------- AS 2 (247-268) --------

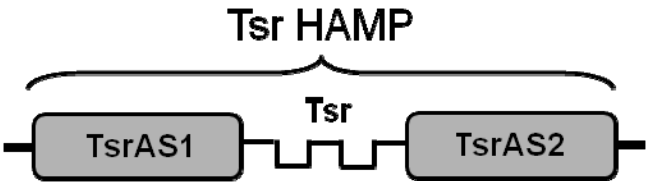

2) Tar HAMP (214-266)

RMLLTPLAKIIAHIREIAG GNLANTLTIDGR SEMGDLAQSVSHMQRSLTDTVT
-------- AS 1 (214-232) ------ connector (233-244) ---------- AS 2 (245-266) --------

3) Af1503 HAMP (278-331)

STITRPIIELSNTADKIAE GNLEAEVPHQNRA DEIGILAKSIERLRRSLKVAME
-------- AS 1 (278-296) ---- connector (297-309) ---------- AS 2 (310-331) -------

4) Af1503$_{mut2}$ HAMP (278-331)

STITRPIIELINTIDKIAE GNLEAEVPHQNRA DEIGILAKSIERLRRSLKVAME
-------AS 1 (278-296) ---- connector (297-309) ---------- AS 2 (310-331) -------

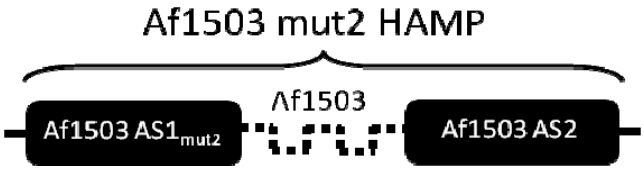

5) NpHAMP$_1$ (84-136)

GDTAASLSTLAAKASRMGD GDLDVELETRRE DEIGDLYAAFDEMRQSVRTSLE
-------- AS 1 (84-102) ---------- connector (103-114) ---------- AS 2 (115-136) --------

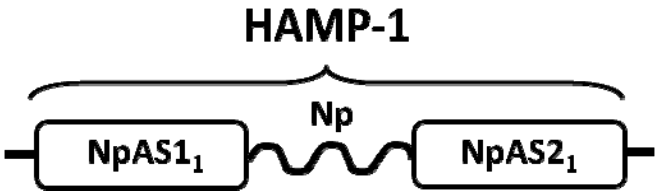

6) NpHAMP$_2$ (157-210)

TELQAEAERFGEVMDRCAD GDFTQRLDAETDN EAMQSIEGSFNEMMDGIEALVG
-------- AS 1 (157-175) ---------- connector (176-188) ---------- AS 2 (189-210) --------

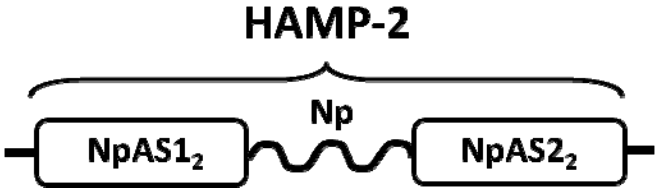

7) NpHAMP tandem (84-210)

The $NpHAMP_1$ and -2 are shown above. The inter-HAMP linker is a 20 amino acid stretch from 137-156, is shown in bold.

GDTAASLSTLAAKASRMGDGDLDVELETRREDEIGDLYAAFDEMRQSVRTSLE**DAKNAREDAEQAQ**
KRAEEINTELQAEAERFGEVMDRCADGDFTQRLDAETDNEAMQSIEGSFNEMMDGIEALVG

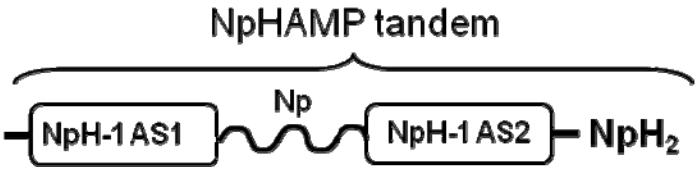

The output domains used in this study were:

1) Rv3645 CHD (331-549)

LRDLFGRYVGEDVARRALERGTELGGQERDVAVLFVDLVGSTQLAATRPPAEVVQLLNEFFRVVVETV
ARHGGFVNKFQGDAALAIFGAPIEHPDGAGAALSAARELHDELIPVLGSAEFGIGVSAGRAIAGHIGAQ
ARFEYTVIGDPVNEAARLTELAKLEDGHVLASAIAVSGALDAEALCWDVGEVVELRGRAAPTQLARP
MNLAAPEEVSSEVRG.

2) CyaG CHD (431-672)

ALENTNRELEQRVLERTAALLQEKERSEELLLNVLPKPIADQLKANKKAIASAIEEVTILFADIVGFTPLS
ARMHPIDLVSLLNEMFSIFDHLAEKHKLEKIKTIGDAYMVVGGLPLPQDNHAEAIADMALEMQAAMK
QFQGSYLVGSESFQIRIGINTGSVVAGVIGIKKFIYDLWGDAVNIASRMESSGTPGSIQVTEETYNRLKKN
YIFKERGPIPVKGKGQMTTYWLLGKKPVVDIS

General sequence pattern of constructs:

e.g., 1) Tsr_{1-215} -**NpHAMP tandem$_{84-210}$** -$Rv3645_{331-549}$

*MRGSHHHHHHGS*MLKRIKIVTSLLLVLAVFGLLQLTSGGLFFNALKNDKENFTVLQTIRQQQSTLNGSW
VALLQTRNTLNRAGIRYMMDQNNIGSGSTVAELMESASISLKQAEKNWADYEALPRDPRQSTAAAAEI
KRNYDIYHNALAELIQLLGAGKINEFFDQPTQGYQDGFEKQYVAYMEQNDRLHDIAVSDNNASYSQA
MWILVGVMIVVLAVIFAVWFGIK**GDTAASLSTLAAKASRMGDGDLDVELETRREDEIGDLYAAFDE**
MRQSVRTSLEDAKNAREDAEQAQKRAEEINTELQAEAERFGEVMDRCADGDFTQRLDAETDNEA
MQSIEGSFNEMMDGIEALVGLRDLFGRYVGEDVARRALERGTELGGQERDVAVLFVDLVGSTQLAA
TRPPAEVVQLLNEFFRVVVETVARHGGFVNKFQGDAALAIFGAPIEHPDGAGAALSAARELHDELIPVL
GSAEFGIGVSAGRAIAGHIGAQARFEYTVIGDPVNEAARLTELAKLEDGHVLASAIAVSGALDAEALCW
DVGEVVELRGRAAPTQLARPMNLAAPEEVSSEVRG.

The sequence in italics is the His-tag that is added to the protein sequence for purification and identification in Western blots.

Nomenclature of the constructs.

Clone name	Details of the clone
NpHAMP tandem	Tandem HAMP domain from *N. pharaonis* transducer HtrII
$NpH_{1\text{-}mut5}$	$NpHAMP_1$ with 5 mutations in the $HAMP_1$ AS1
$NpH_{1\text{-}mut5}$ tandem	$NpHAMP_1$ with 5 mutations in tandem with $NpHAMP_2$
$Af1503_{mut2}$ tandem	Af1503 HAMP with 2 mutations in tandem with $NpHAMP_2$
$AS1_{1\text{-}Tsr}/NpH_1$	HAMP with AS1 from Tsr and connector and AS2 from $NpHAMP_1$
$AS1_{1\text{-}Tsr}/NpH_1$ tandem	$HAMP_1$ with AS1 from Tsr and connector and AS2 from $NpHAMP_1$ in tandem with $NpHAMP_2$
$AS1_{1\text{-}Tar}/NpH_1$ tandem	$HAMP_1$ with AS1 from Tar and connector and AS2 from $NpHAMP_1$ in tandem to $NpHAMP_2$

Abbreviations

AC	Adenylyl cyclase
Af1503 HAMP	*Archaeoglobus fulgidus* HAMP
$AS1_1$	Amphipathic helix 1 from $HAMP_1$
$AS2_1$	Amphipathic helix 2 from $HAMP_1$
$AS1_2$	Amphipathic helix 1 from $HAMP_2$
$AS2_2$	Amphipathic helix 2 from $HAMP_2$
aa	Amino acid
CHD	Cyclase homology domain
IPTG	Isopropylthiogalactosid
LB medium	Luria-Bertani culture medium
Ni^{2+}-IDA	Nickel-iminodiacetic acid
Ni^{2+}-NTA	Nickel-nitrilotriacetic acid
OD	Optical density
SEM	Standard error of the mean
TEV	Tobacco Etch Virus
TEMED	N,N,N',N'-Tetramethyl-ethylene-diamine
TM	Transmembrane
Tar	Aspartate receptor in *E. coli*
Tsr	Serine receptor in *E. coli*

1 INTRODUCTION

Microorganisms seeking optimal living conditions for survival have adapted to track constantly various environmental cues. The surroundings with various small molecules are sensed directly by a receptor or indirectly by changes in membrane fluidity. The response to the stimulus involves signal transmission across the cytoplasm starting the signal cascade which can be either covalent modification like in histidine kinases or by second messengers such as cAMP. Most of these tracking proteins are modular and operate as a receiver-transmitter complex aka two component systems which have been subject to several studies in the recent times. The information of the past stimulus apart from the transfer of the signal is critical as signal transduction is not an "on-off switch" but rather a continuous adaptation to assess the current situation.[1]

Adaptation of the organism to stimuli thereby plays a critical role. Most abundant cues are light and chemicals. The movement of motile bacteria in response to these stimuli is called phototaxis and chemotaxis, respectively (Fig. 1-1B/C). Motility aids in continuous tracking of the most optimal conditions for survival. The proteins involved in phototaxis and chemotaxis have been studied in detail in the recent years. The bacteria fluctuate between random tumble and a smooth run depending on the direction of the rotation of the flagellar rotor either counterclockwise (CCW) or clockwise (CW) enabling random sensing of the concentration gradient around them (Fig. 1-1A) . In both phototaxis and chemotaxis, the presence of an attractant leads to a more smooth straight movement and the presence of repellant switches to a more random tumble to move away.

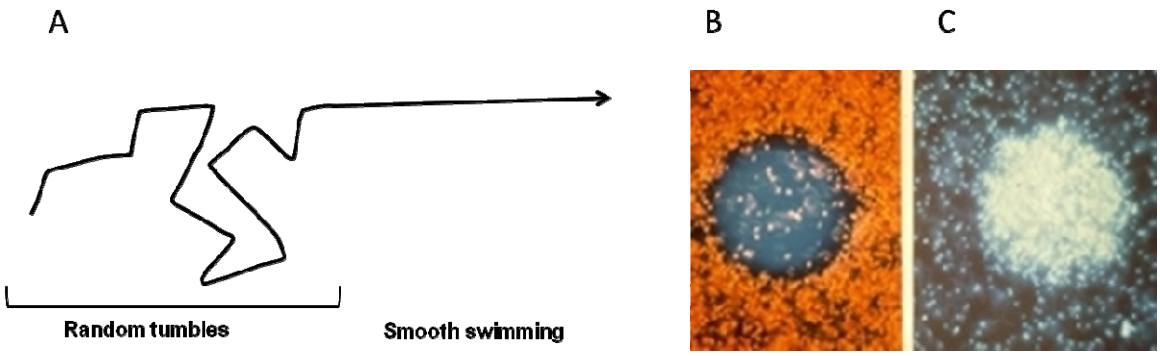

Figure 1-1. (A) Representation of the direction of the movement of bacteria in the random tumbling and a smooth straight walk. (B & C) Light trap experiments with *Halobacterium salinarum* [2]. Cells escape from a central spot of blue light (B) or accumulate in a central spot of orange light (false color representation, C).

1.1 Chemotactic and phototactic signal transduction

The signal transduction via the chemotactic or the phototactic sensors is very similar (Fig. 1-2). The light and chemical stimuli are received by membrane-embedded receptors, sensory rhodopsin (SR) and Tsr/Tar, respectively [3-6]. The sensory rhodopsin, SR-I/SR-II transfers the light signal to its cognate transducers HtrI/HtrII, respectively [7]. Tsr, Tar, HtrI and HtrII belong to a family of two-transmembrane helical proteins and are termed methyl-accepting chemotaxis protein (MCP) and MCP-like protein (MLP), respectively [6, 8]. MCP and MLP exist as homodimers composed of a signal sensor region, transmitter region and a kinase control module which interacts with kinase CheA, and an adaptor protein, CheW [8, 9]. The presence of attractants leads to a "kinase-on" state and presence of repellents leads to a "kinase-off" state. In the "kinase-on" state the rate of autophosphorylation of the histidine kinase CheA is increased several fold and the "kinase-off" state leads to a decrease in the level of autophosphorylation of CheA.

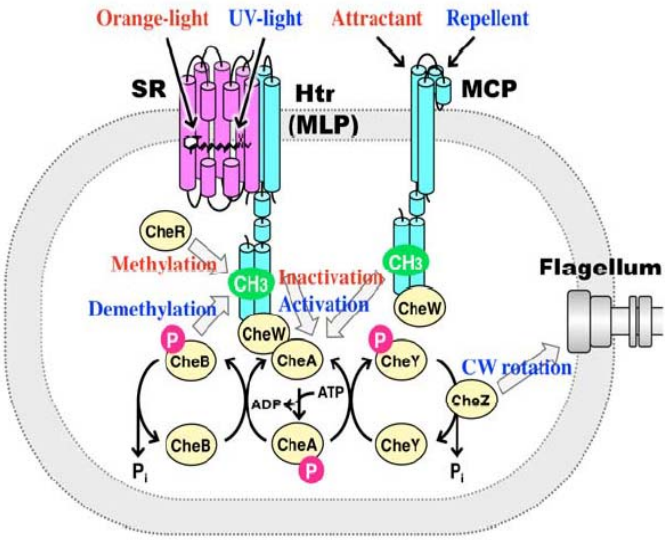

Figure 1-2. Light and chemical signal transfer cascades in microorganisms [10]. Chemicals (attractant and repellent) bind to the extracellular domain of the chemoreceptors (MCP) and the binding induces the structural changes of MCP. Light stimulation activates sensory rhodopsins (SRs). SRs transmit light signals to their cognate transducer proteins (Htrs) in the membrane.

The flux between the "kinase-on and kinase-off" caused changes in the level of CheA phosphorylation leading to modulation of phosphorylation of these two response regulators CheY (motor control) and CheB (sensory adaptation). The phosphorylated CheY binds to the flagellar rotor, leading to the switch in the default CCW (random tumbles) to a CW direction leading to a smooth straight run. The levels of the CheA mediated phosphorylation is

monitored by the levels of phospho-CheY. A phosphatase CheZ hydrolyses phospho-CheY. The cells track the levels of different gradients by a reversible methylation of the glutamyl residues in the adaptation region of the receptor monitored by the MCP specific proteins CheR and CheB-P [9]. The methyltransferase CheR methylates the glutamate residues, whereas the methylesterase CheB-P is responsible for removal of methyl groups [9]. The interplay between motor control and sensory adaptation results in directed motile behavior (Fig. 1-2, [8]).

1.1.1 The chemoreceptors of *E. coli*

The positive and negative taxis in bacteria has been reported already in the 1880´s by Wilhelm Pfeffer [11]. There are five chemosensors identified in *E. coli* namely Tsr (taxis towards serine, away from leucine, indole and weak acids), Tar (taxis towards aspartate and maltose, away from nickel and cobalt), Tap (taxis towards dipeptides), Trg (taxis towards ribose and galactose) and Aer (for redox potentials). Tsr and Tar are most abundant as the other sensors Tap, Trg and Aer are expressed only at residual 10% [12, 13]. The ligands i.e., serine, aspartate and citrate are sensed directly by the periplasmic domain of the sensors Tsr, Tar and Tcp [14]. The Tcp receptor for citrate is unique to *Salmonella typhimurium* [15]. Ligands like maltose, galactose, glucose, ribose, dipeptide and Ni(II) are sensed with the help of a binding protein by the Tsr, Tar, Trg or Tap receptors [16]. The chemoreceptors form helical, intertwined homodimers [8, 17]. Functionally these receptors can be divided into three parts with modules for transmembrane sensing, signal conversion and kinase control, respectively. Attractant binding to the periplasmic loop of the receptor initiates a downward piston-like movement of the second transmembrane span [8, 18-20]. This conformational change is then propagated via the HAMP domains to the downstream kinase control module finally leading to a change in direction of the flagellar rotor thereby change in the direction of movement of bacteria. Thousands of these receptors are clustered at cell poles together with CheA and CheW [9, 21-23]. The chemoreceptors form mixed trimers of dimer arrays across the membrane during signal transduction [8, 17, 24-26]. The receptors communicate with one another via allosteric interactions within the clusters [8, 9, 25, 27, 28]. The communication between the clusters is crucial for adaptation and amplification of the signal with high sensitivity [9, 22].

1.1.2 The phototaxis transducers of archaea

The extreme conditions of salt and sunlight have facilitated the archaea like *Natronomonas pharaonis, Halobacterium salinarium, and Halobacterium halobium* to develop receptors that exploit the available severe conditions. The motility towards the optimal light conditions is very critical for their survival. The phototaxis receptor complex consists of a sensory rhodopsin, SR-I and -II coupled to its innate transducers, HtrI and II respectively. The sensory rhodopsin and transducers are specific to one another and the stoichiometric ratio is 2:2 in an active state [7]. The SR-I:HtrI complex is involved in attractant taxis to orange light and a short lived repellant taxis to near UV light [2, 6, 29]. The SR-II:HtrII complex is involved in the repellant movement away from the oxidizing sunlight (blue-green light [6]).

Studies on the SR-I and SR-II have demonstrated that in the absence of their tightly coupled transducers, SR-I and -II can function as proton pumps [7, 30, 31]. The SR-I and -II like their counterparts BR (Bacterial Rhodopsins) have seven transmembrane helices (helix A-G, Fig. 1-3). The light activated changes in the SR-II results in the movement of the penultimate transmembrane span outward [32-37]. This movement results in counterclockwise rotation of second transmembrane span of the transducer, HtrII [35]. The counterclockwise rotation and the downward piston movement of the second transmembrane span starts the signal cascade propagated via the tandem HAMP domains to the kinase control module resulting in change in the direction of motility of the archaeon. It has been speculated that in the SR-I:HtrI signaling the conformational changes are opposite (Fig. 1-3). The second transmembrane of HtrI supposedly rotates clockwise [38].

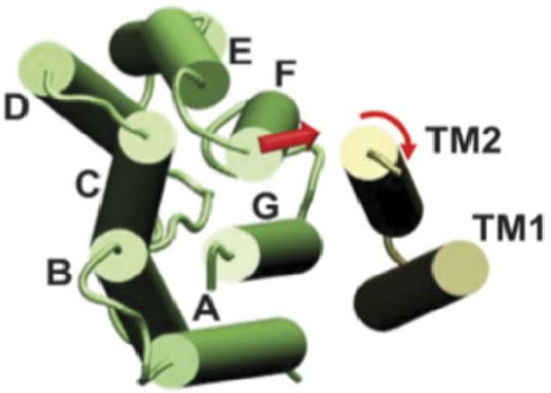

Figure 1-3. Model for SR-I:HtrI signaling [38]. Modeled helix positions in SR-I:HtrI based on the crystal structure of the SR-II:HtrII complex (PDB code 1H2S [39]). The photoreceptor and the transmembrane domain (TM1 and TM2) of the transducer are shown in green and gray, respectively. Helix F of the photoreceptor is in direct contact with TM2.

1.2 HAMP domains

HAMP domains are signal transducing modules, named after their presence in **H**istidine kinases, **A**denylyl cyclases, **M**ethyl-accepting chemotaxis proteins and **P**hosphatases [40, 41]. They are also present in diguanylate cyclases, phosphodiesterases, metal dependant phosphohydrolases and Ser/Thr kinases [42]. About 26,000 of these domains have been annotated in the SMART-EMBL database so far. The HAMP domains are signal transducing modules typically connecting an input sensor to an output domain, thereby facilitating the signal transfer from one domain to another. The NMR structure of an archaeal HAMP of unknown function, Af1503 indicated that they are homodimeric coiled coils (Fig. 1-4, [43]). These modules are typically 55 amino acids in length with a heptad repeat pattern. Each HAMP has structurally three components; the amphipathic alpha helix 1 (AS1), the amphipathic alpha helix 2 (AS2) connected by a flexible loop of about 12 amino acids. In a heptad repeat pattern the residues are labeled from a to g. This pattern corresponds to the heptad periodicity postulated by Crick as the hallmark of a coiled coil structure [44, 45]. The residue positions `a´ and `d´ are predominantly occupied by a hydrophobic residue (Fig. 1-4, [42, 43]).

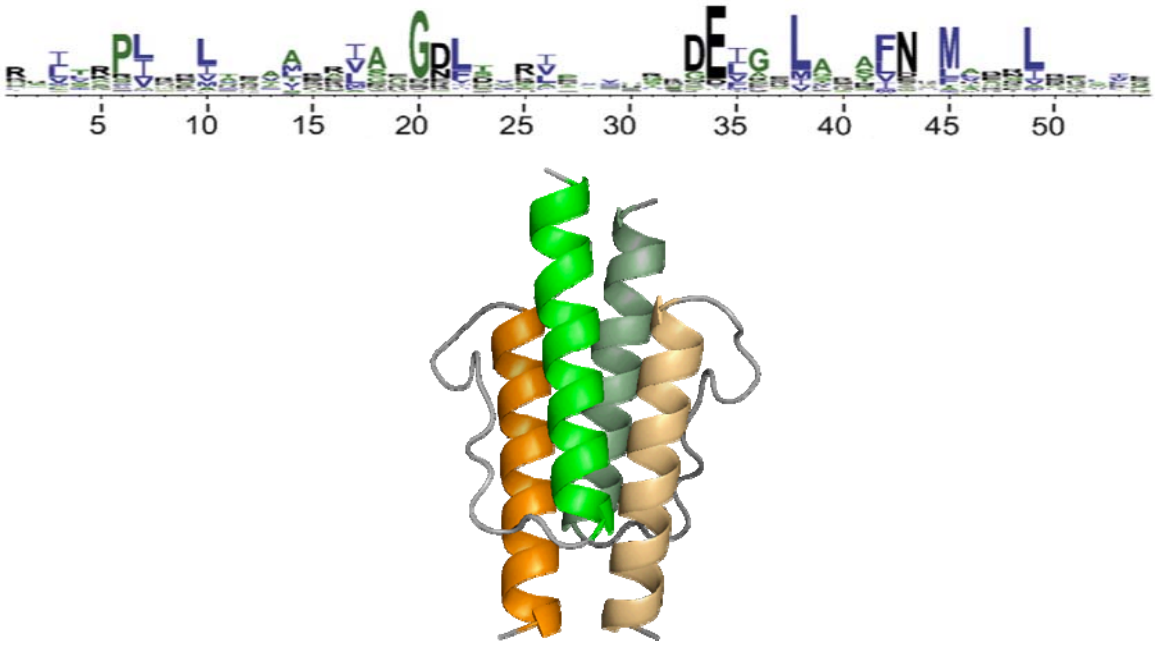

Figure 1-4. *Top:* consensus sequence of the HAMP domains [42]. *Below*: NMR structure of the archeal HAMP Af1503 [43]. The NMR structure depicts the homodimeric state of the HAMP. The AS1 (green) and AS2 (yellow) of one HAMP and the AS1' and AS2' of the second HAMP form tetrahelical coiled coils. The connector residues form a loop that interconnects the AS1 and AS2.

1.2.1 Classification of HAMP domains

An exhaustive bioinformatic analysis of HAMP domains identified certain specific sequence conservation in HAMP domains [42]. Among various positions, the position ´a´ and ´g´ of the heptad is predominantly a hydrophobic residue. The HAMP domains with sequences that retain the conserved positions were classified as canonical HAMP domains and the HAMP sequences that did not retain the conserved positions were termed divergent. In poly-HAMP domains, predominantly the HAMP that picks up the signal from the input sensor is from the canonical group and the HAMP succeeding one from the divergent group.

1.2.2 Mechanism of signal transduction via HAMP domains

The HAMP domains are predicted to adopt two interchangeable conformational states that are facilitated by binding of ligand to the sensor. There are two major proposals for the mechanism of the signal transduction via these modules:

A) Rotation of the helices: The hydrophobic ´a´ and ´d´ positions in coiled coil structures from knobs-into-holes geometry to stabilize the helices. The NMR structure revealed a different geometry of the HAMP domains, the "x-da" geometry. In addition to the core 'a' and 'd' positions, the positions 'g' from AS1 and 'e' from AS2 are also involved in signaling. This led to the proposal of rotation as the mechanism of the signal transmission via HAMP domains. The helices rotate 26º interchanging into the respective geometries (Fig. 1-5, [43]).

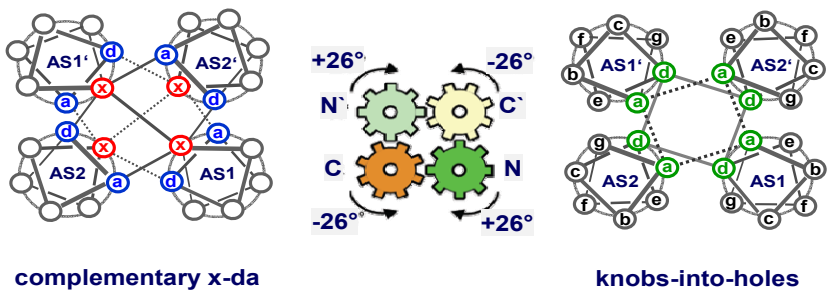

Figure 1-5. Gear box model for signal transduction via HAMP domains. The two conformations, "complementary x-da" and "knobs-into-holes" are interconvertible by a rotation of 26º [43]. The AS1, AS2, AS1' and AS2' are N, C, N', C' helices respectively.

B) Helix-bundle stability: In a different proposal the signal output is determined by the stability of the helices in the HAMP domain. HAMP domains may adopt two alternative

conformations both of which seem to cause CCW output in Tsr. When the two HAMP structures rapidly inter-convert, or when neither is stable, output supposedly is CW [46, 47].

1.2.3 Signal transduction in poly-HAMP modules.

In poly-HAMPs the sign of the signal output was proposed to be reversed with each additional HAMP [48]. With the gearbox model as a likely mechanism of signal transmission, the direction of rotation of the helices AS1 and AS2 is opposite in a mono-HAMP (Fig. 6, mono-HAMP). In a tandem HAMP, the $AS2_1$ is continuous with the $AS1_2$. This means that their direction of rotation is unidirectional; i.e., the direction of rotation of helices $AS1_1$ and $AS2_2$ are the same (Fig. 1-6, HAMP tandem). This was assumed to indicate a change in the signal sign from a mono to a tandem HAMP. We tested the hypothesis by using a tandem HAMP from the halophilic archaea *Natronomonas pharaonis*. The $NpHAMP_1$ along with $HAMP_{Tsr}$ and $HAMP_{Af1503}$ belongs to the canonical group while $NpHAMP_2$ belongs to the divergent group. The sign of signal output from the canonical $HAMP_{Tsr}$ and $HAMP_{Af1503mut2}$ in the reporter system is inhibition to serine. According to the predicted model $NpHAMP_1$ would result in inhibition by serine which would be inverted by $NpHAMP_2$.

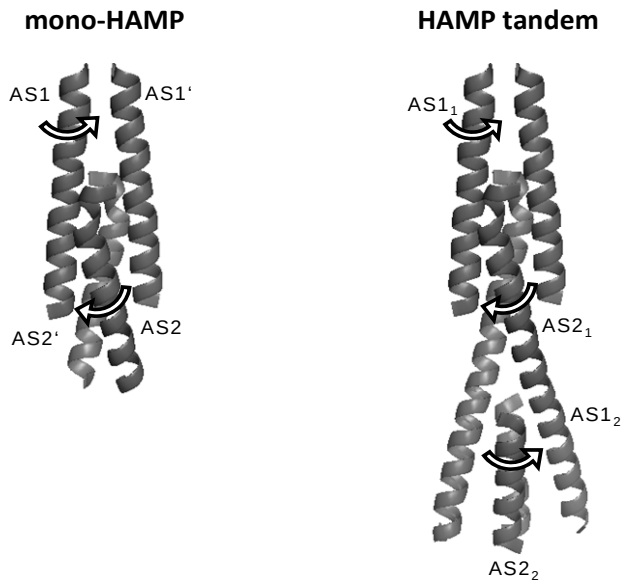

Fig 1-6. The model for signal transduction via mono- and tandem HAMP domains (adapted from [48]). The block white arrows indicate the probable direction of rotation of the helices.

1.3 Adenylyl cyclases

cAMP is an ubiquitous second messenger influencing gene expression and regulation, regulation of enzymes across all kingdoms of life except for archaea. Adenylyl cyclases which synthesize cAMP from ATP yielding pyrophosphate as a byproduct can be grouped into six classes based on their sequence identity [49]. Class I ACs are involved in catabolite repression in enteric bacteria, e.g. *E. coli.* [49, 50]. Class II ACs are toxins secreted by bacterial pathogens like *Bacillus anthracis, Bordetella pertussis* and *Pseudomonas aeruginosa* [49, 51]. Class III ACs are the most abundant enzymes. The classes IV, V, VI are minor classes as only few members are known and have been studied [52-54]. Class III cyclases are further subdivided into a-d based on different signature motifs present at the dimer interface and the length of an arm region, that is the distance between a conserved glycine and the substrate defining aspartate and threonine/serine residues [55].

Bacterial class III ACs are typically multi-domain proteins and are functional only upon homodimerization, forming two catalytic centers (*51, 52*). In contrast to mammalian ACs the mode of regulation of bacterial ACs is not well understood. Most of the N-terminal domains of the bacterial ACs are believed to regulate the cyclases but the mechanism of signal regulation is enigmatic. In mammalian ACs the two CHDs in a single protein form a pseudoheterodimer with a single ATP binding pocket [56]. Bacterial class III ACs have a single CHD hence all six catalytic residues are present on a single protein chain. Six amino acids have been identified to be important for catalysis. Two aspartate residues coordinate two metal co-factors (Mg^{2+} or Mn^{2+}). The four other residues are a substrate specifying lysine and aspartate pair and a transition state stabilizing arginine and asparagine couple [57, 58].

1.3.1 Mycobacterial Rv3645 cyclase

cAMP plays a major role in the biology of mycobacteria [59]. All 16 AC identified in the genome of *M. tuberculosis* H37Rv belong to class III [60, 61]. In Rv3645 a class IIIb AC, the six TM helices are connected to the catalytic domains via a HAMP domain [55, 62]. The catalytic activity of Rv3645 is enhanced in conjunction with its N-terminal HAMP region. The tripartite organisation of the cyclase is similar to the chemosensors and hence, these cyclases provided an interesting tool to study the HAMP domains.

1.3.2 Cyanobacterial CyaG cyclase

Whole genomes of 38 cyanobacterial strains have been sequenced so far demonstrating an abundance of ACs and other signaling proteins. cAMP is an important signaling molecule in cyanobacteria [63]. *A. platensis* encodes 22 ACs as revealed from recent genome sequencing [64]. CyaG AC from Arthrospira, a class IIIa AC, has two TM spans, a HAMP domain, and a CHD. The primary structure of the CHD of CyaG is more closely related to transmembrane ACs and guanylyl cyclases (GCs) [65]. In addition the CyaG AC contains an S-helix which connects the HAMP to the catalytic domain. The S-helix has been shown to modulate the sign of the signal output [66]. This cyclase along with the S-helix provides another interesting system to test the HAMP domains.

1.4 Question of this thesis

The tripartite domain organisation of methyl-accepting chemotaxis proteins like Tsr from *E. coli* and the class III cyclases like Rv3645 is similar. The bacterial cyclases are homodimers in an active state and have twelve transmembrane spans like their mammalian counterparts. Since the discovery of cyclases the function of the huge membrane spans which make about 40% of the protein is still unknown [67]. Following the membrane helices both the proteins have the signal transducing modules HAMP continuing into the output domains. The HAMP domains have been shown to be exchangeable between MCPs and cyclases and hence structural changes occurring during signal transduction seem to be similar [68].
It has been already shown that the Tsr or Tar receptors can be modified to have a cAMP readout. A chimera was generated of the Tsr receptor with the kinase module replaced by the CHD domain of mycobacterial cyclase Rv3645. The cyclase activity of this chimera was affected by the concentration of serine binding to the Tsr receptor (Fig. 1-7, [69]). This setup provides an excellent system to analyze biochemically a specific HAMP of interest [66, 68].

The thesis work is centered around the following questions:

- How is the signal sign in a Tsr-tandem HAMP-Rv3645 AC chimera?
- Biochemically characterize the tandem HAMP domains from *N. pharaonis* HtrII.

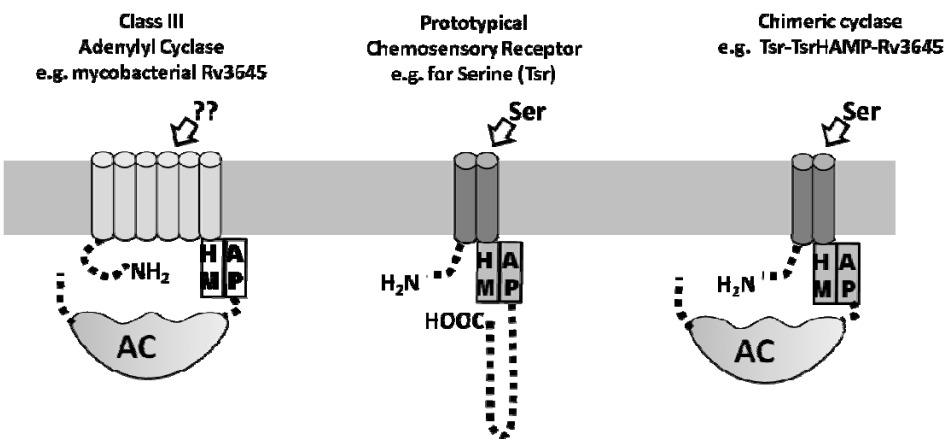

Figure 1-7. Model of a chimeric cyclase construct (monomer).

2 MATERIALS and METHODS

The materials and methods were adapted from the dissertation of Dr. Laura Garcia Mondéjar.

2.1 Chemicals

Amersham Pharmacia Biotech, Freiburg (2,8-^{3}H)-cAMP, ECL Plus Western blotting detection system, hyperfilm ECL, Formamide.

Appligene, Heidelberg: Taq DNA-polymerase with 10x reaction buffer

Applied biosystems,California(USA): BigDye Terminator v3.1 cycle sequencing kit.

Biomers.net GmbH, Ulm: Oligonucleotides (PCR and sequencing primers)

BIO RAD, Munich: BIO-RAD protein assay reagents, Profinity^{TM} IMAC Ni-charged resin.

Dianova, Hamburg: Secondary goat antimouse IgG-F_c horseradish peroxidase conjugated antibodies.

GE Healthcare, Freiburg: Secondary ECL Plex Goat-α-Mouse IgG-Cy3, Thermo sequence Primer Cycle Sequencing Kit, GFX PCR DNA and Gel band purification kit, ECL plus Western blotting detection system.

Hartmann Analytik, Braunschweig: (α-^{32}P)-ATP.

Macherey-Nagel, Düren: Nucleotrap kit, Parablot PDVF-blotting membrane (2 µm pore size)

Millipore, Molsheim (France): Amicon Ultra centrifuge-filters.

New England Biolabs, Schwalbach/Taunus: BSA for molecular biology, restriction endonucleases, T4-Polynucleotide kinase and 10x kinase buffer

PEQ LAB, Erlangen: KAPA HiFi proofreading DNA Polymerase, peqGOLD-Protein marker IV.

Perkin Elmer, Massachusetts (USA): (α-^{32}P)-ATP, LSC-scintillator cocktail Ultima GOLD XR.

Promega, Madison (USA): Wizard plus SV Plasmid Purification Kit (Minipreps)

Qbiogene, Heidelberg: Taq- and QBio Taq-polymerase with 10X buffer.

Qiagene, Hilden: Ni^{2+}-NTA Agarose, pQE30, PQE60, PQE80 and pETDUET expression vectors, purified mouse monoclonal RGS-His_4 antibody and Tetra-His antibody, Taq-DNA-polymerase.

Roche Diagnostics GmbH, Mannheim: alkaline phosphatase, ATP, dNTPs, λ-DNA, restriction endonucleases, Klenow-polymerase, Rapid DNA (dephosphorylation) ligation Kit.

Schleicher& Schuell, Dassel: Protran BA 83 cellulose nitrate 0.2 µm (200 x 200 mm) nucleic acid and protein transfer media.

Serva, Heidelberg: Visking Dialyse-membrane 8/32 (pore size 6mm)

Süd-Laborbedarf GmbH: Hi Yield R PCR Clean-Up / Gel Extraction Kit

Vivascience, Hannover: Vivaspin 500 µL and 2 mL (for protein concentration)

Whatman International Ltd, Maidstone (England): Whatmann 3 MM paper.

2.2 Equipments

ÄKTA Applied biosystems, California (USA): ABI3130xl Sequencer, sequence scanner v 1.0

BIO RAD, Munich: Blotapparatus *trans*-Blot SD *Semi Dry Transfer Cell*.

DNASTAR, Wisconsin (USA): *Lasergene*® Software package.

GE Healthcare Freiburg (Amersham Pharmacia, San Francisco, USA): Ettan Dige imager. ÄKTA-FPLC™ , Superdex-200 10/30 and 16/60 60, Scintillation counter rackbeta 1209, *GSTtrap™* FF columns.

Millipore, Schwalbach am Taunus : *MilliQ* and *Elix* waterfiltration systems.

Kontron-Hermle, Gosheim: Centrikon *H401 & ZK401*, Rotors *A6.14 (SS34) and A8.24* (GSA)

SLM, Instruments, Urbana (USA): French Pressure Cell Press *FA-078-E1*, French Press cylinder, nylon balls and rubber ring.

2.3 Plasmids

The plasmids that have been used in the cloning of different constructs are: pBluescript II SK(-) (Stratagene), pQE30, pQE80L (Qiagen) and pETDUET (Novagen). pETDUET 3(MCS1-pQE30) was modified by A.Schultz.

2.4 Bacterial strains

Different strains of bacterial competent cells have been used.

Strain	Supplier	Characteristics	Genotype
XL-I-Blue	Stratagene	Cloning cells (Tetracyclin resistant)	recA1 endA1 gyrA96 thi-1 hsdR17 supE44 relA1 lac [F´ proAB lacIqZΔM15 Tn10 (Tetr)]
DH5α	Invitrogen	Cloning cells (Amphicillin resistant)	F^- ϕ80lacZΔM15 Δ(lac ZYA-argF) U169 recA1 endA1 hsdR17(rk-, mk+) phoA supE44 thi-1 gyrA96 relA1 λ
BL21 DE3 (pRep 4)	Novagen	Protein Expression	F^- *omp* T *hsd* SB(rB–, mB–) *gal dcm* (DE3) pRep4 :KanR, lacI

2.5 Molecular biology methods

2.5.1 Isolation of DNA (miniprep)

A single colony from a LB-agarose plate with appropriate antibiotics or a small amount of inoculum from permanent culture is taken and grown in LB medium with antibiotics for 6-16hrs at 37ºC in a shaker. The plasmid DNA is then isolated from the culture using *Wizard® plus SV plasmid purification kit.* The isolated DNA is then eluted in 50-100µL of milliQ water. The DNA is then stored either at 4ºC or -20 ºC.

Solutions

TAE : 40 mM Tris/ Acetate pH 8.0, 1 mM EDTA.

TE buffer : 10 mM Tris/ HCl pH 7.5, 1 mM EDTA.

10x TBE buffer : 1000 mM Tris, 890 mM Boric acid, 25 mM EDTA.

dNTP's : 25 mM of each dNTP

4x sample buffer (BX) : 0.05 % Bromophenol blue, 0.05 % Xylenecyanol, 50 % Glycerol

2.5.2 PCR

The DNA was amplified by standard PCR. The following components were used:

Plasmid DNA of about 50ng was used as a template. In case of fusion PCR, the primary PCR amplified fragments were used at a concentration of 10 ng each and with a molar ratio of 1:1. Primers (sense and anti-sense) 500 nM each, dNTP´s mixture 250 µM and buffer with $MgCl_2$

were used. 5% DMSO was always added. The enzyme (Taq polymerase 1U or kappa polymerase 2U) was added last to the reaction mixture. The volume is made up to required volume with water (autoclaved).

The last 18 bp from the 3´ end of the primer is used for calculating the annealing temperature according to:

$$Tm\ (°C) = 4*(GC) + 2*(AT)$$

The conditions used for amplification are as follows:

Programm for Taq polymerase.			
Cycling parameters	T (°C)	Time (min)	cycle
Initial denaturation	95	5	
Denaturation	95	1	30
Anealing	Tm	1	
Extension	72	1/kb	
Final extension	72	10	
Cooling	4	hold	

Programm for kappa polymerase.			
Cycling parameters	T (°C)	Time (sec)	cycle
Initial denaturation	95	120	
Denaturation	95	20	30
Anealing	Tm	15	
Extension	68	30/kb	
Final extension	68	300	
Cooling	4	hold	

In conditions were the Tm of the primers are not close then the amplification is done in two steps. In the first round, 5 cycles are performed at the lower temperature then 20 cycles are performed at a higher temperature. The amplified fragments are then run on an agarose gel and processed further.

2.5.3 Purification of DNA from gel

The DNA fragment is run on an agarose gel (0.8 - 2 %). A DNA marker (λ-DNA marker) is used. The gel is visualized under UV light. The DNA fragment of interest is cut from the gel. The isolated fragment was purified with *HiYield PCR clean up & Gel extraction kit*. The DNA is eluted in 15-20 µl water (autoclaved) and stored at 4° or at -20°C.

2.5.4 Estimation of DNA concentration

The concentration of DNA is measured in a photometer at wavelength 260 nm. The purity of the DNA sample is compared by checking the E_{260nm}/E_{280nm} ratio which should be around 1.5 to 1.9. The measurement at 280 nm is to check for protein contamination.

2.5.5 Restriction digestion of DNA

About 100-500 ng of DNA is digested with 1U of appropriate enzymes (from NEB, Roche or Fermentas). After 1-3 hrs the reaction is run on an agarose gel. The DNA in gel is viewed under UV light to assess the insert presence and then cut and purified.

2.5.6 Phosphorylation

The 5´ends of the insert require phosphorylated for ligation. DNA fragment (500 ng), 1 mM ATP, 10U of T4 polynucleotide kinase and 1X T4-PNK buffer in 15 µl reaction were incubated at 37°C for 1hr for phosphorylation.

2.5.7 Dephosphorylation of vectors

To inhibit the vector fragment from re-ligating, and to increase the efficiency of ligation the 5´ end of the vector is dephosphorylated. The reaction of 10 µl consists of DNA (500 ng), 1U/pmol of alkaline phosphatase and 1X de-phosphorylation buffer is incubated at 37°C for 1hr.

2.5.8 Ligation

The ligation of the DNA fragments (vector and insert(s)) was done with the rapid ligation kit. The vector insert molar ratio used was either 1:3 or 1:1. The ligation mixture is kept at room temperature for 30 mins or overnight at 4ºC.

2.5.9 Transformation of recombinant DNA

The entire DNA ligation reaction was added to competent cells (100 µl), mixed gently and incubated on ice for 10 min, cells were then heat-shocked at 42°C for exactly 1 min and then incubated on ice for 2 min. 500 µl of the LB-broth (without antibiotic) were added and cells were incubated for one hour with shaking. 100-200 µl of the mixture were spread on an LB agar plate with the appropriate antibiotic. Plates were incubated for 12-16 hrs at 37°C.

2.5.10 Isolation and purification of DNA

Plasmid DNA was isolated from bacterial cultures using *Wizard Plus Minipreps DNA Purification system* (PROMEGA). The DNA was eluted with 50-100 µl of water (autoclaved). The plasmid could be used directly for DNA sequencing and restriction digestion.

2.5.11 DNA sequencing

DNA was sequenced either with GATC or with the ABI Big Dye terminator v3.1 cycle sequencing kit.

GATC sanger sequencing: An Eppendorf (1.5 ml) tube with 5 µl of sample DNA (50-100 ng) along with 5 µl of appropriate primer (5 pmol) was sent to the GATC sequencing facility. The sequence of the DNA was available online which could be downloaded for further analysis.

ABI Big Dye sequencing: Double stranded DNA 150-300 ng of DNA was usually taken. 5 µl of DNA was taken and mixed with 4 µl of ABI mix provided in the kit and then 0.6 picomoles of sequencing primers were added. The volume of the reaction was adjusted to 10 µl. The Eppendorf tube with this reaction mixture was given a short spin and run in the thermocycler. The conditions were: initial denaturation at 96ºC for 1 min, denaturation at 96ºC for 10 sec, annealing at 50ºC for 5 sec, extension at 60ºC for 10 sec and final extension at 60ºC for 4 mins. 25 cycles were performed of these conditions. After the PCR reaction the mixture was given a short spin and the mix was transferred to 1.5 ml Eppendorf tubes. 40 µl of 75% isopropanol was added and incubated at room temperature for 10 min and then centrifuged at 13,000 rpm for 30 min. Isopropanol was taken out carefully without touching the pellet. The pellet was washed with 140 µl of 80% ethanol and then centrifuged at 13,000 rpm for 5 min, vacuum dried and re suspended in 15 µl of HiDi buffer. The pellet was kept in HiDi buffer for 15 min and then sequenced.

2.5.12 Permanent cultures

600 µ1 of overnight bacterial culture and 400 µl of autoclaved glycerol were thoroughly mixed and then stored at -80°C.

2.5.13 Cloning

All cloning was done into the expression vector pETDUET3 with pQE30 MCS1 (with or without MCS2). Either fusion PCR or quick mutagenesis PCR was used to introduce specific mutations in the chimera.

2.6 Protein chemistry

All proteins were expressed in *E. coli* BL-21 (DE3) [pREP4]. For pre-culture 5 ml of LB-broth containing 100 µg/ml Ampicillin and 50 µg/ml Kanamycin were inoculated with a small amount of permanent culture (overnight, 37°C, 210 rpm).

2.6.1 Expression

The 5 ml pre-culture was the inoculum for 200 ml LB-broth containing 100 µg/ml Ampicillin and 50 µg/ml Kanamycin (30°C, 210 rpm). It was grown to an OD_{600} between 0.4-0.6 (approx. 2-3 hrs). The expression of chimeras was induced with 0.1 mM IPTG (18°C, 210 rpm) for 12-14 hours.

Solutions.

LB-Agar : 35 g/L LB Agar.

LB-antibiotic-Agar plates : 100 µg Ampicillin/ml LB Agar, 50 µg Kanamycin/mL LB agar.

LB-broth : 20 g/L LB broth powder.

2.6.2 Cell harvest.

Cells were harvested (15 min., 5000 x g, 4°C), the supernatant was discarded and the pellet washed with 20 ml of cell wash buffer, centrifuged (15 min, 5000 x g, 4°C) and stored at - 80°C.

Pellet washing buffer : 50 mM Tris/ HCl pH 8.0, 1 mM EDTA.

2.6.3 Cell lysis

The frozen pellets were thawed on ice (10-15 min), suspended in 25 ml of cell lysis buffer, passed twice through a French Press (1000 psi) and the homogenate was centrifuged (30 min, 20000 x g, 4°C). The supernatant was either pelleted for membranes or purified further with immobilized metal affinity chromatography (IMAC) resin.

Cell lysis buffer : 50 mM Tris/HCl pH 8, 2 mM α-thioglycerol, 50 mM NaCl.

2.6.3.1 Protein purification with IMAC resin.

Use of immobilised metal affinity chromatography (IMAC) that uses nickel ions for purifying recombinant polyhistidine (His-) tagged proteins has been done for several years [70]. Two IMAC systems with different linkers namely Ni^{2+}-IDA (immuno diacetic acid) and Ni^{2+}-NTA (Nitrilotriacetic acid) were used for purification of the proteins.

2.6.3.1.1 Purification with Ni^{2+}-IDA.

The cell lysis supernatant was mixed well with 250 mM NaCl and 250 µl *Profinity* ^{TM} *IMAC* and incubated on ice for 1 hour with mild shaking. After the incubation time the mixture was centrifuged (1100Xg, 5 min, 4ºC) to pellet the protein bound affinity material. The pellet was mixed with 2 ml of the wash-buffer A and packed on a miniprep column (cleaned from Wizard plasmid purification kit) with the help of a syringe. The following wash steps were done :

- 2X with 2ml and 8 ml wash-buffer A
- 1X with 5ml wash-buffer B.

After washing out the unbound material the protein was eluted with 600 µl elution buffer. The column is then washed again with 100-200 µl of the elution buffer and collected separately. After checking the concentration of the protein, the protein was run on SDS-PAGE for checking the integrity. The proteins were further checked for cyclase activity and then stored at -20ºC with 35% glycerol until further use.

2.6.3.1.2 Purification with Ni^{2+}-NTA.

The cell lysis supernatant was mixed well with 250 µl of Ni2+-NTA pre-equilibriated with 1 ml of wash-buffer A and incubated on ice for 2 hours with mild shaking. After the incubation time the mixture was centrifuged (1100Xg, 5 min, 4ºC) to pellet the protein bound affinity material. After centrifugation and packing of the column the following wash steps were done:

- 2X with 2ml and 8 ml wash-buffer A
- 1X with 5ml wash-buffer B.

After washing out the unbound material the protein was eluted with 600 µl elution buffer. The column is then washed again with 100-200 µl of the elution buffer and collected separately. After checking the concentration of the protein, the protein was run on SDS-PAGE for checking the integrity. The proteins were further checked for cyclase activity and then stored at -20ºC with 35% glycerol until further use.

Solutions.

Wash-buffer A : 50 mM Tris/HCl pH 8, 250 mM NaCl, 5 mM $MgCl_2$, 15 mM imidazole, pH 8, 10% glycerol.

Wash-buffer B : 50 mM Tris/HCl pH 8, 0.16% α-thioglycerol, 5 mM $MgCl_2$, 15 mM imidazole, pH 8, 10% glycerol, 0.16% α-thioglycerol

Elution buffer : 50 mM Tris/HCl pH 8, 5 mM $MgCl_2$, 250 mM imidazole**,** 10% glycerol

2.6.4 Preparation of membrane fractions

Frozen cell pellets were thawed on ice (10-15 min), suspended in 20 ml of cell lysis buffer, passed twice through the French Press (1000 psi) and the homogenate was centrifuged (30 min, 5000 x g, 4°C) to remove the debris. The supernatant was ultracentrifuged (1 hr, 100,000 x g, 4°C). The supernatant was discarded and pellet was resuspended in 2-3 ml of membrane resuspension buffer and stored at -80°C.

Solutions.

Membrane resuspension buffer: 40 mM Tris/HCl buffer pH 8, 1.6 mM α-thioglycerol, (0.16%), 20% glycerol, 250 mM NaCl.

2.6.5 Bio-Rad Protein determination

A concentration of 1 mg/ml of BSA was used as a standard. 4-12 µg of protein were pipetted to 800 µl distilled water and vortexed. 200 µl of Dye reagent concentrate (5X) was added, vortexed and the absorbances at OD_{595} were measured and protein concentrations were calculated according to the calibration curve.

2.6.6 SDS-PAGE

The expression and molecular weight of the protein was determined by SDS PAGE [71]. Protein was mixed with 4X sample buffer. In case of membrane proteins the samples were left at room temperature and purified proteins were heated for 95°C for 5 min and loaded on the gel. Gels were run at a constant current: 20mA, 200V, 1 hr, stained with coomassie blue for 30 min with gentle agitation, decolourised for 20-25 min and washed with water until the bands are clearly detected. Usually, SDS-PAGE was carried out simultaneously with pellets and supernatant of *E. coli* containing an empty vector as a control. Protein marker components (10 µl containing 1µg of each protein) were from Peq Lab (Peq gold). (http://www.peqlab.de/wcms/en/pdf/27-1010.pdf).

Solutions.

Resolving Gel buffer	: 1.5 M Tris/HCl pH=8.8, 100 mM NaCl and 0.4% SDS.
Stacking Gel Buffer	: 500 mM Tris/HCl pH=6.8, 0.4% SDS.
4x sample buffer	: 130 mM Tris/HCl pH 6.8, 10% SDS, 20% Glycerol, 0.06% Bromophenol blue, 10% β-mercaptoethanol.
10x electrophoresis buffer	: 250 mM Tris, 1.92 M Glycine, 1% SDS.
Coomassie staining solution	: 0.2% Brilliant Blue G-250, 40% Methanol, 10% Acetic acid.
Destaining solution	: 10% Acetic acid, 30% Methanol.

2.6.7 Western Blot

For immunochemical detection, proteins were transferred after SDS-PAGE to PVDF-membrane through semi-Dry-Electrotransfer [72]. The blot membrane was successively soaked in methanol, water and Towbin buffer each for 2 min. Three Whatmann 3 MM papers were soaked in Towbin buffer and laid on the anode plate. The blot membrane was laid over them, the gel and finally three soaked Whatmann papers again on the side of the cathode plate. Protein transfer was carried out for 2-3 hr at 20V and 2.5 mA/cm^2. The gel was stained in coomassie brilliant blue to check transfer efficiency. The membrane was stained in ponceau S for about 5 min, then it was decolourized with deionized water until the protein bands were clear enough to mark the marker bands with a pencil. The membrane was blocked

with M-TBS buffer for at least 1 hr at RT or overnight at 4°C and washed with TBS-T buffer (2 x 10 sec, 2 x 5 min). It was then incubated with the primary antibody (mouse monoclonal RGS-His_6 antibody 1:2000, or Tetra-His antibody 1:1000 diluted in M-TBS) for 1 hr. After washing (TBS-T, 2 x 15 min) it was incubated with the secondary antibody (goat anti-mouse IgG-F_c or goat anti-rabbit IgG-F_c horseradish peroxidase conjugated antibodies 1:5000 diluted in M-TBS) for 1 hr and then washed as above with TBS-T. The chemiluminescent reaction with the ECL Plus Western Blotting Detection Kit (Amersham) was carried out according to the manufacturer's instructions and it was detected on hyperfilm-ECL after its exposure to the detection reaction (from 10 sec to 5 min).

Solutions.

TBS buffer (Tris Buffer Saline)	: 20 mM Tris/HCl pH 7.5, 150 mM NaCl.
Ponceau S staining solution	: 0.1% (w/v) Ponceau S, 5% Acetic acid.
TBS-T	: 0.1% Tween 20 in TBS buffer.
M-TBST	: 5% Milk powder in TBS buffer.
Towbin- Blot buffer	: 25 mM Tris/HCl, 192 mM Glycine and 20% Methanol

2.6.7.1 Densitometry for protein determination

Proteins were also quantified by densitometry. The ETAN DIGE Image has quantitative measurement software. A protein standard was taken which was the marker band 70kda from the marker protein. The standard was set as 100%. The membrane proteins which had to be estimated were run on the SDS PAGE along with the control and then the Western blot was carried out. The photographic film containing the protein bands after developing the blot was scanned by the photographic scanner. The band intensities of the proteins were calculated. Intensities were compared with the standard and the amount of the protein was calculated accordingly. This qualitative measure was done to compare whether there is a significant difference in the expression of the proteins.

2.7 Adenylyl cyclase assay

The AC activity was tested by measuring the amount of ^{32}P-cAMP formed from α^{32}P-ATP used as a substrate [73]. Assay volume was 100 µl which contained 40 µl of protein sample including ligands (serine, aspartate etc.) and 50 µl of AC test cocktail and 10 µl of ATP start solution. The final concentrations were: 50 mM Tris/HCl buffer pH 7.5, 22% glycerol, 6 mM $MnCl_2$ and 200 µM ATP. The reaction was terminated by addition of 150 µl stop buffer. 10 µl of [2,8-^{3}H]-cAMP were added as internal standard followed by 750 µl of water and the mixture was poured into a Dowex column (9 ×1 cm glass column with 1.2 g Dowex 50). After washing with 3.5 ml water, the samples were eluted with 5 ml water in Al_2O_3 columns (10 × 0.5 cm plastic column with 1 g active neutral Al_2O_3 90). Samples were immediately eluted with 4.5 ml 0.1 M Tris/HCl pH 7.5, mixed with 4 ml of Ultima Gold XR Scintillator solution and counted. Dowex columns were regenerated with 1×5 ml 2M HCl, 1×10 ml water and 1×5 ml water, Al_2O_3 columns with 2×5 ml 0.1 M Tris/HCl pH 7.5. Specific activity, (pmol/mg/min) was calculated with the following formula.

$$A = \frac{Substrate\,(\mu M) \times 100\,\mu l}{time\,(\text{min})} \times \frac{1000}{protein\,(\mu g)} \times \frac{cpm\left[^3H\right]_{total}}{cpm\left[^3H\right]_{sample} - 3\%\left[^{32}P\right]_{sample}} \times \frac{cpm\left[^{32}P\right]_{sample} - cpm\left[^{32}P\right]_{blank}}{cpm\left[^{32}P\right]_{total}}$$

3% of the phosphorous counts were subtracted from the tritium values because of the spill over of ^{32}P into the tritium channel. Activities lower than double background (in cpm) were considered zero.

Solutions.

ATP Stock Solution : 10 mM pH 7.5 (adjusted with NaOH)

10x AC Start solution : 0.75 to 10mM ATP stock solutions with 2.5-4x10^6 Bq/ml [α^{32}P]-ATP

2x AC-Cocktail : 100 mM Tris/HCl pH 7.5, 6 mM $MnCl_2$, 43.5% Glycerol, 4 mM cAMP with 2-4x10^3 Bq/ml (^{3}H-cAMP), 6 mM creatine phosphate (CP), 0.46 mg/2 ml creatine kinase (CK). (CP and CK only for membrane protein).

AC Stop buffer : 3 mM cAMP/Tris pH 7.5, 3 mM ATP, 1.5% SDS.

2.8 Bioinformatics

DNA sequences were analyzed by DNASTAR. Multiple alignments of protein sequences were done using the Megalign feature of DNASTAR followed by manual correction by the GENEDOC. Secondary structure prediction was done by using the program [COILS] [74]. Transmembrane regions in individual proteins were predicted using TMPRED, HMMTOP 2.0 and DAS programme with default parameters [75-77]. For documentation of the programmes see, (http://www.ch.embnet.org/software/TMPRED_form.html) and (http://www.enzim.hu/hmmtop/). The domain analysis was done by the SMART programme (Simple Modular Architecture Research Tool) and NCBI (National Center for Biotechnology Information) conserved domain search [78-80]. For documentation of the programmes see (http://smart.embl.de/) and (http://www.ncbi.nlm.nih. gov/Structure/cdd/wrpsb.cgi).

3 Map of all constructs

3.1 NpHAMP domains in test system.

The fusion PCR products were cloned into the BamHI and HindIII site of the pETDUET3 vector without the MCS2 (pETDUET3, -MCS2).

1) Tsr_{1-215}-$NpHAMP1_{84-136}$-$Rv3645_{331-549}$

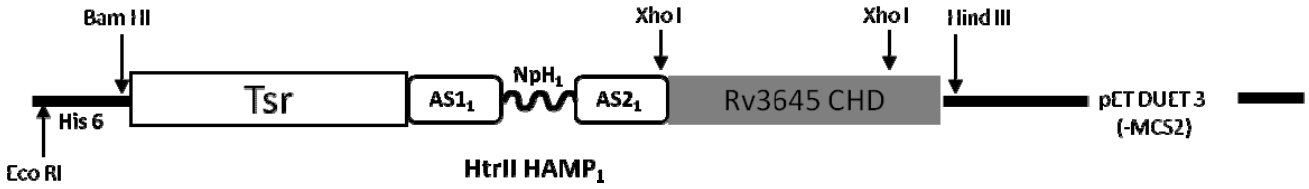

2) Tsr_{1-215}- $NpHAMP1_{84-136}$-$CyaG_{431-672}$

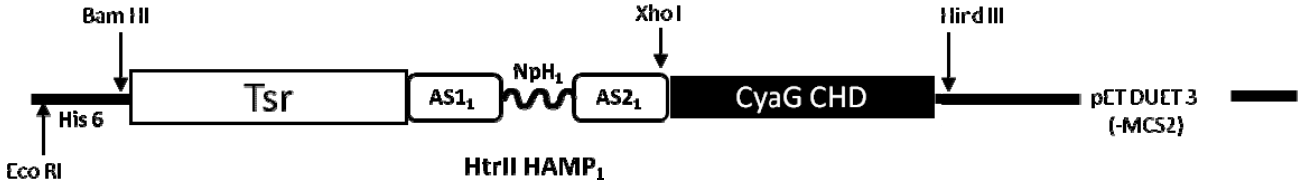

3) Tar_{1-213}- $NpHAMP1_{84-136}$-$CyaG_{431-672}$

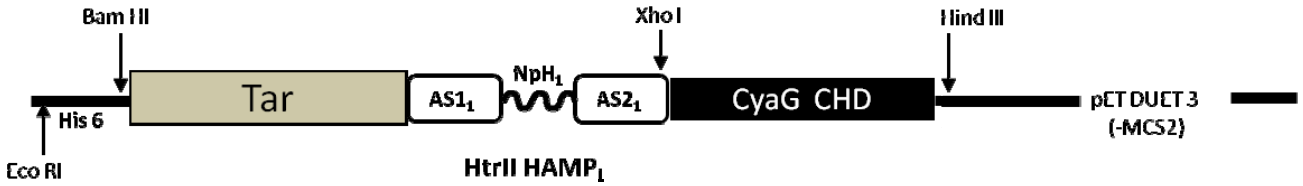

4) Tsr_{1-215}- $NpHAMP2_{157-210}$-$Rv3645_{331-549}$

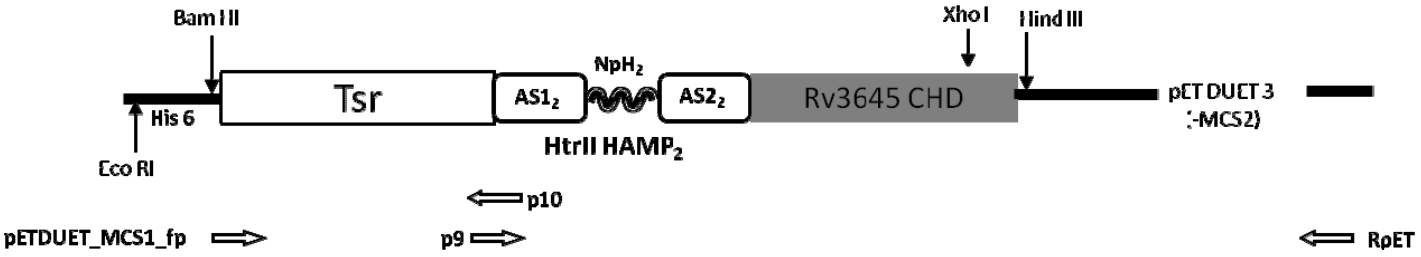

5) Tsr$_{1-215}$-NpHAMP tandem$_{84-210}$-Rv3645$_{331-549}$

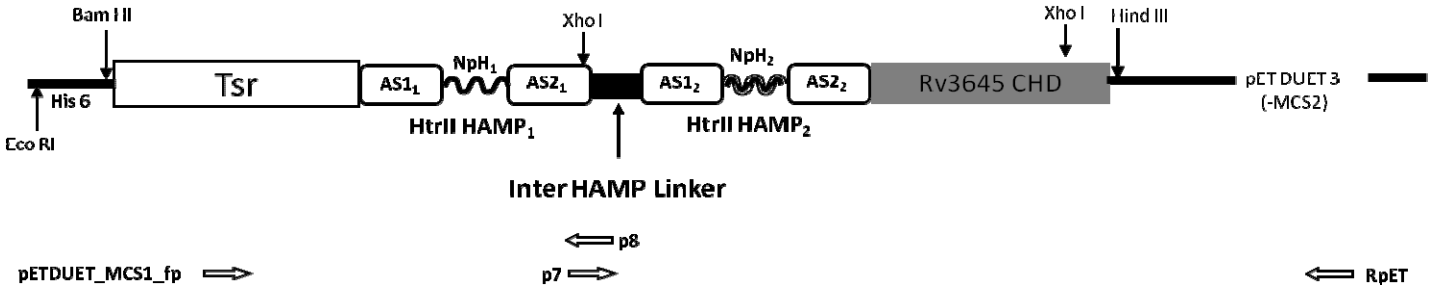

3.2 NpHAMP$_{1-mut5}$

1) Tsr$_{1-215}$-NpHAMP$_{1-mut5(84-136)}$-Rv3645$_{331-549}$

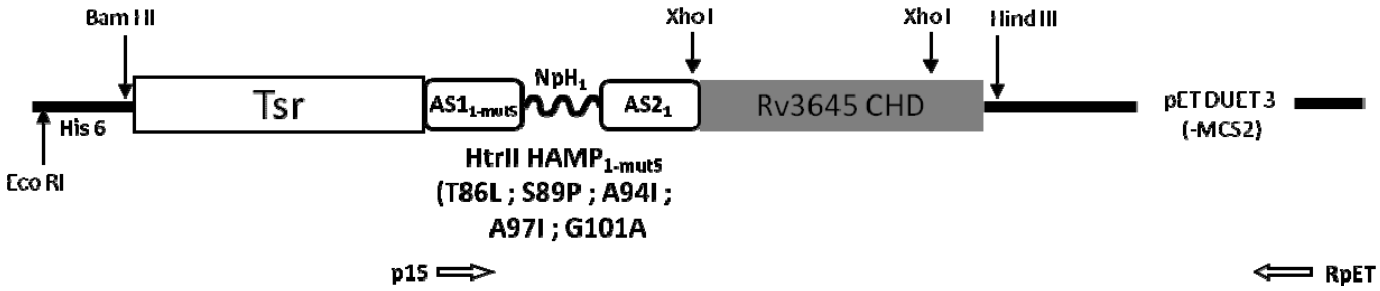

The primer p15 and template Tsr-NpHAMP$_1$-Rv3645 were used. The PCR product (HAMP+Rv3645) was cut with SmaI and HindIII and ligated to StuI and HindIII cut Tsr sensor in pETDUET3 (-MCS2).

2) Tsr$_{1-215}$-NpHAMP$_{1-mut5}$ tandem$_{84-210}$-Rv3645$_{331-549}$

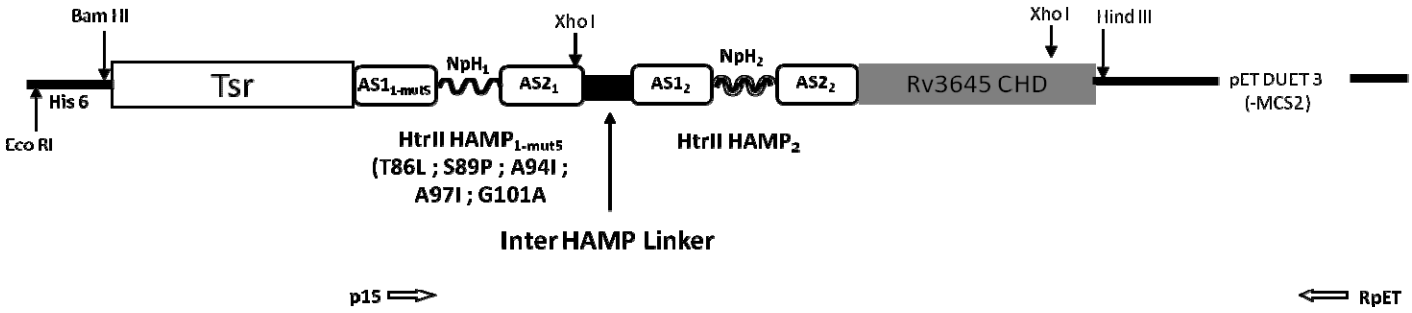

The primer p15 and template Tsr-NpHAMP tandem-Rv3645 were used. The PCR product was cut with SmaI and HindIII and ligated into StuI and HindIII cut Tsr sensor in pETDUET3 (-MCS2).

3) Mutational analysis of HAMP1 AS1.

The sequence of the AS1 of $HAMP_1$ of NpHAMP tandem is shown with the mutations in capitals. All chimeras were modifications of: Tsr_{1-215}-NpHAMP $tandem_{84-210}$-$Rv3645_{331-549}$. The primers and the corresponding templates are shown.

CHIMERA	Primer fp	Primer rp	Template
gdLaaPlstlIakasrmgd	p17		Hf
gdLaaPlstlIakIsrmgd	p97	p98	HfMI5
gdtaaPlstlIakIsrmgd	p16	p98	HfMI5
gdtaaslstlaakFsrmgd	p99	p100	Hf
gdLaaPlstlaakFsrmgd	p99	p100	HfMI5

3.3 Comparison of HAMP tandems.

1) Tsr_{1-215}-Tsr $HAMP_{216-268}$-$Rv3645_{331-549}$

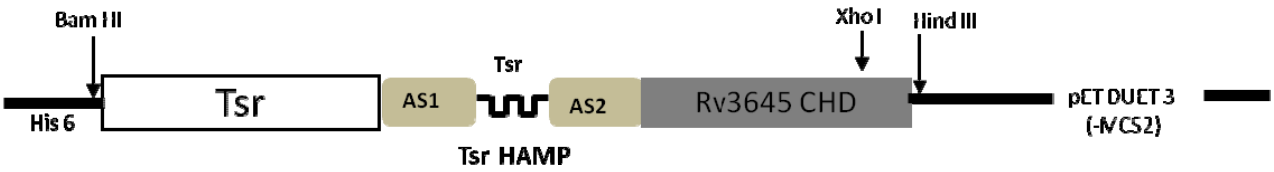

The construct Tsr-$HAMP_{Tsr}$-Rv3645 in pQE30 from Laura Garcia Mondéjar was cloned into BamHI and HindIII sites of pETDUET3 by A.Schultz.

2)Tsr$_{1\text{-}215}$ - HAMP tandem:H$_{1\text{-Tsr}_{216\text{-}268}}$ - H$_{2\text{-NpH 2}_{157\text{-}210}}$ - Rv3645$_{331\text{-}549}$

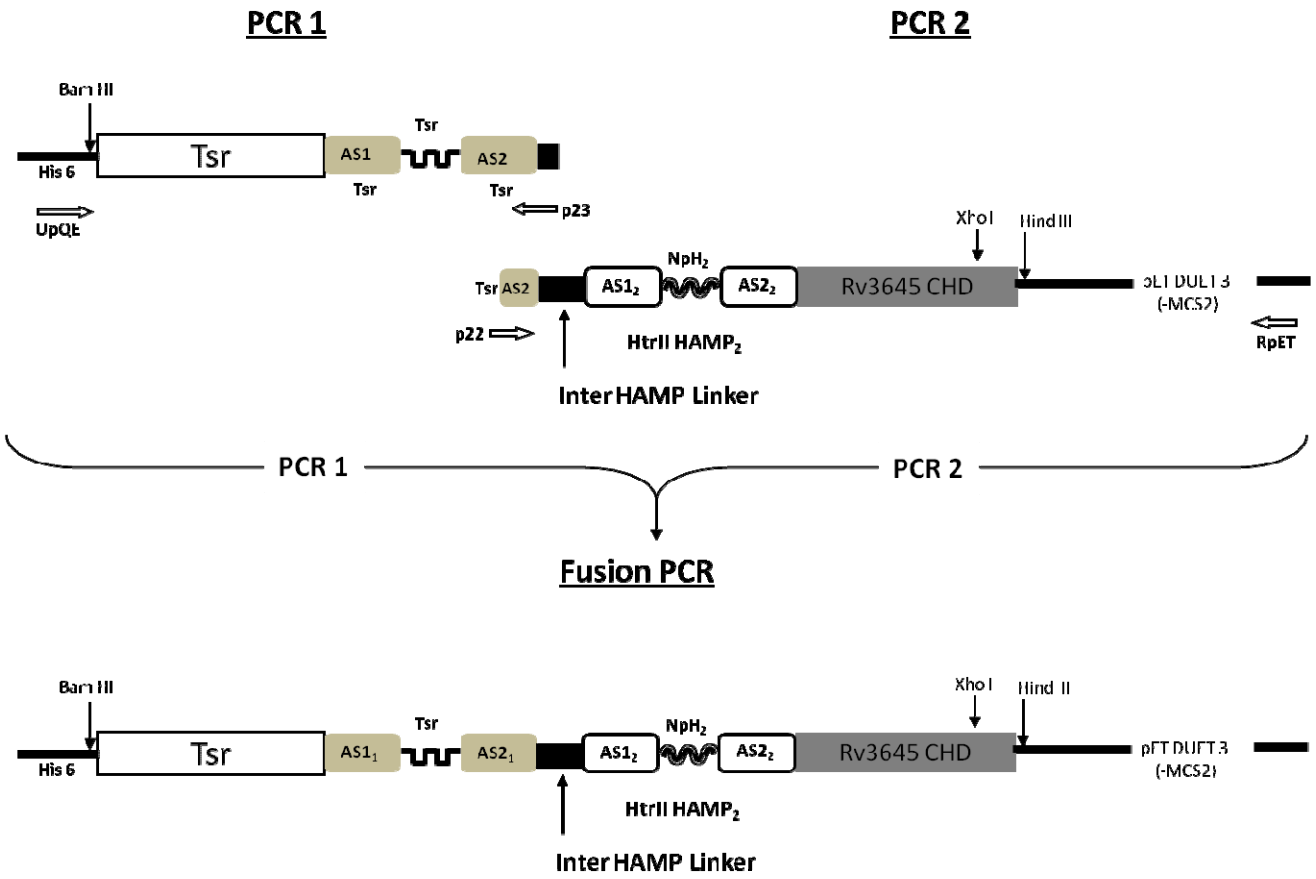

A fusion PCR was done to couple the Tsr HAMP to NpHAMP$_2$. The PCR fragments and the primers for the respective PCR reactions are indicated. The final product was cloned into the BamHI and HindIII sites of pETDUET3 (-MCS2).

3) Tsr$_{1\text{-}215}$-HAMP tandem:H$_{1\text{-Af1503}_{278\text{-}331}}$ - H$_{2\text{-NpH 2}_{157\text{-}210}}$ - Rv3645$_{331\text{-}549}$

A fusion PCR was done to couple the Af1503 HAMP to NpHAMP$_2$. The PCR fragments and the primers for the respective PCR reactions are indicated. The final product was cloned into the BamHI and HindIII sites of pETDUET3 (-MCS2).

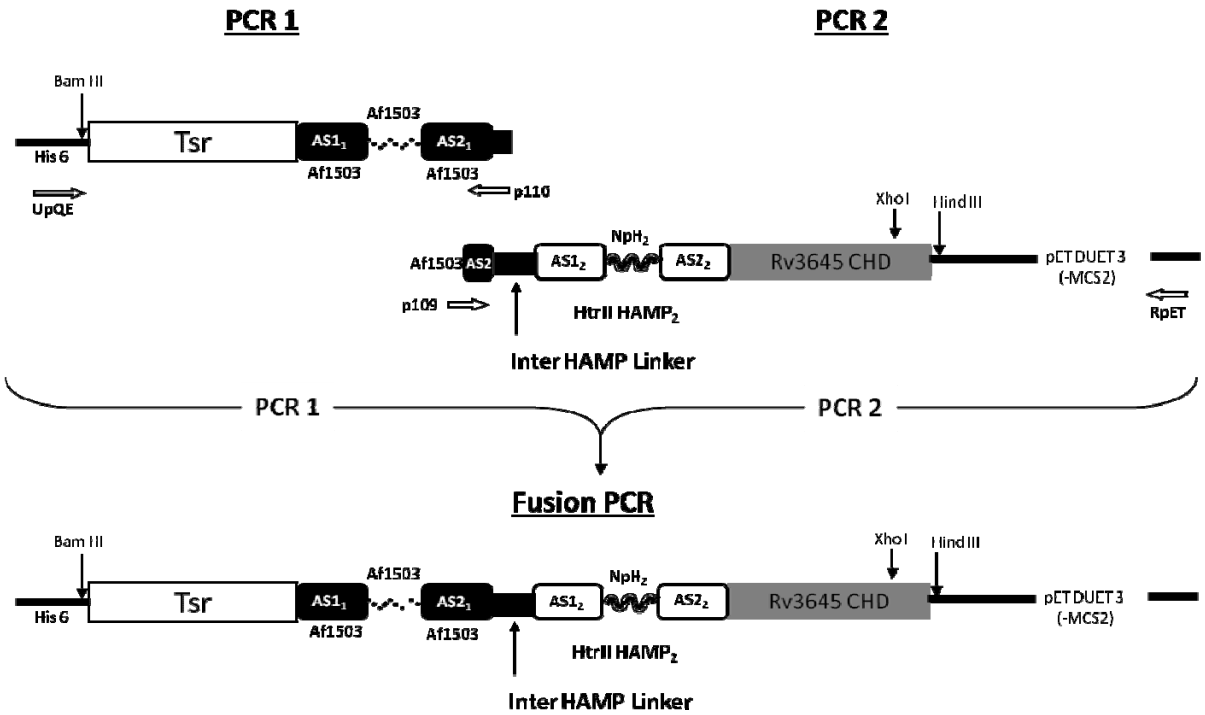

4) Tsr$_{1\text{-}215}$-HAMP tandem: H$_{1\text{-Af1503 (mut2)}}$$_{278\text{-}331}$ - H$_{2\text{-NpH2}}$$_{157\text{-}210}$ -Rv3645$_{331\text{-}549}$

A fusion PCR was done to couple Af1503 (mut2) HAMP to NpHAMP$_2$. The PCR fragments and the primers for the respective PCR reactions are indicated. The final product was cloned into the BamHI and HindIII sites of pETDUET3 (-MCS2).

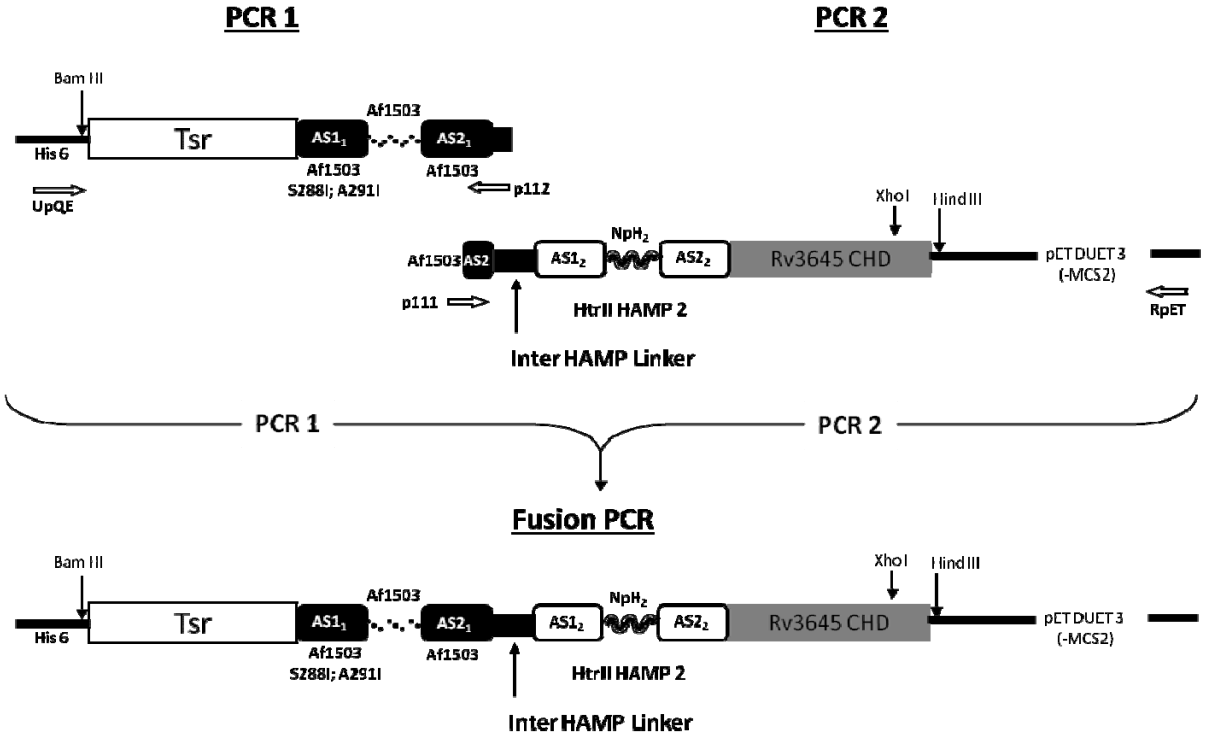

5) Tsr_{1-215}- HAMP tandem -$Rv3645_{331-549}$.
$HAMP_1$:AS1/AS2-NpH_1, connector-Tsr HAMP. $HAMP_2$: $NpHAMP_2$.

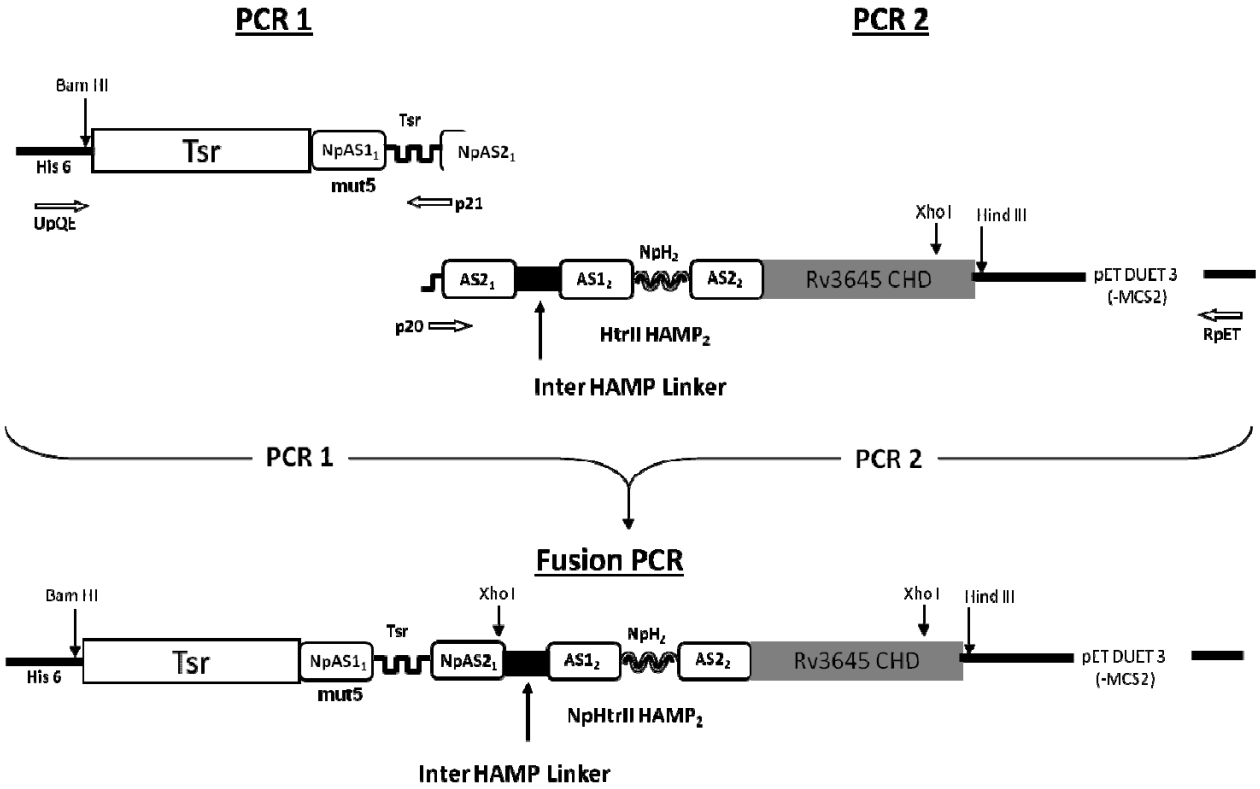

6) Tsr_{1-215}- HAMP tandem -$Rv3645_{331-549}$.

$HAMP_1$: AS1-Tsr, Connector/AS2-NpH_1. $HAMP_2$: $NpHAMP_2$.

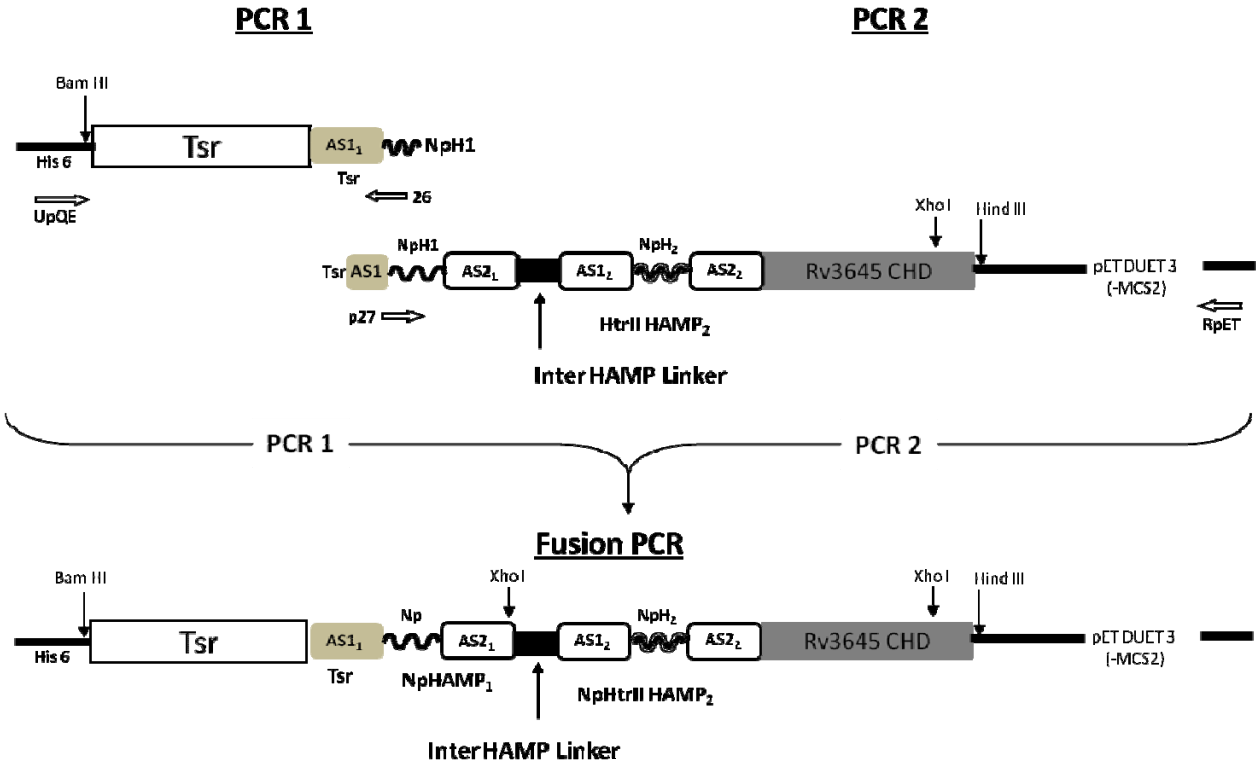

7) Tsr_{1-215}- HAMP tandem -$Rv3645_{331-549}$.
$HAMP_1$: AS1/ Connector -Tsr, AS2-NpH_1. $HAMP_2$: $NpHAMP_2$.

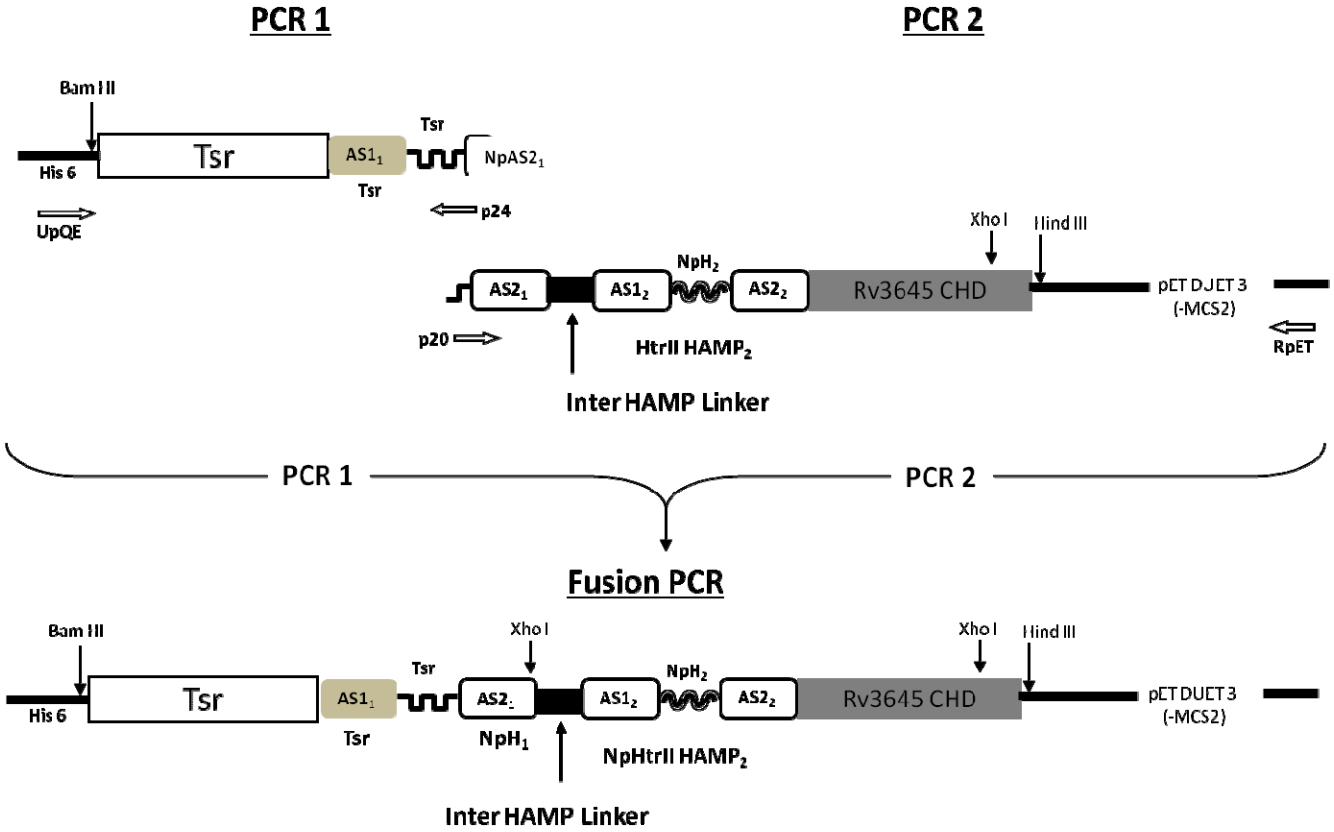

8) Tsr_{1-215}- HAMP tandem -$Rv3645_{331-549}$.
$HAMP_1$: AS1/ Connector -NpH_1, AS2-Tsr. $HAMP_2$: $NpHAMP_2$.

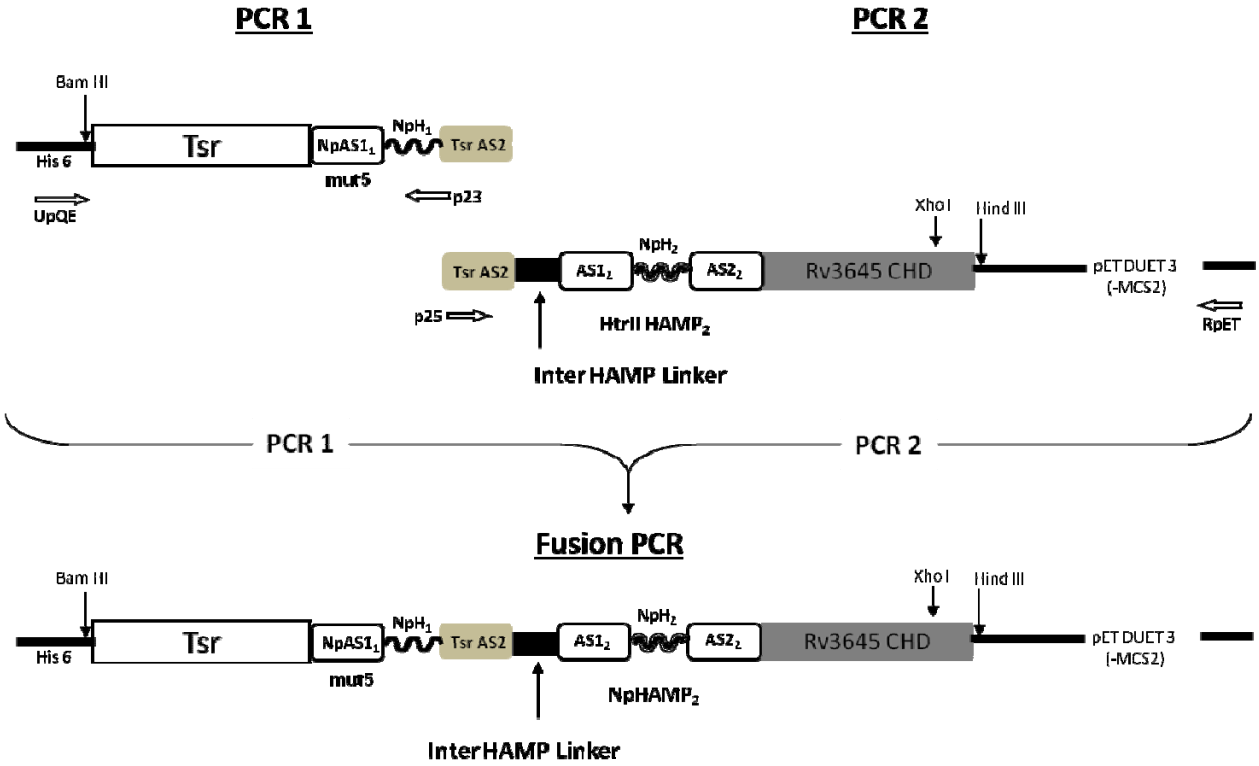

9) Tsr_{1-215}- HAMP tandem -$Rv3645_{331-549}$.
$HAMP_1$: AS1/AS2 -Tsr, Connector-NpH_1. $HAMP_2$: $NpHAMP_2$.

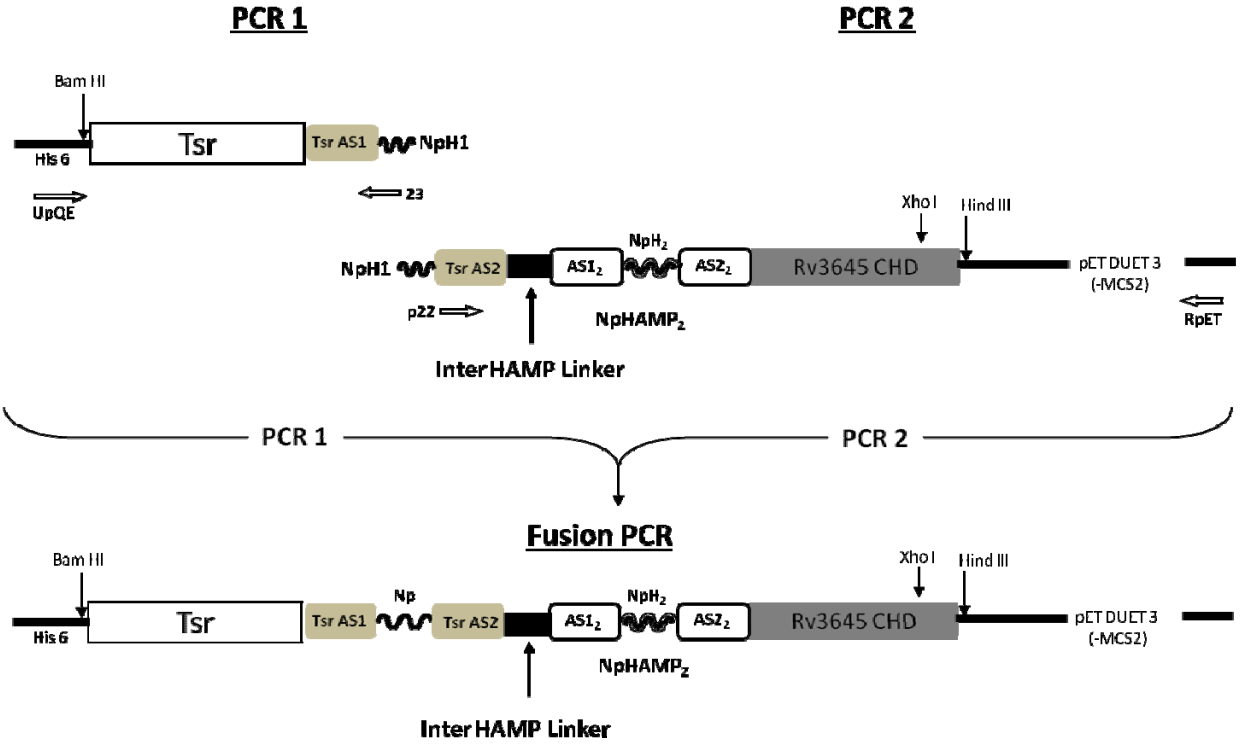

The chimeras 5-9 were cloned similarly. The PCR fragments and the primers for the respective PCR reactions are indicated. A fusion PCR was done to couple structural components of Tsr HAMP and $NpHAMP_1$. The final product was cloned into the BamHI and HindIII sites of pETDUET3 (-MCS2)

10) Tsr_{1-215}- HAMP tandem -$Rv3645_{331-549}$.
$HAMP_1$: AS1/connector -NpH_1, AS2 -Af1503. $HAMP_2$: $NpHAMP_2$.

Chimeras 10 and 11 had combinations of structural components of $Af1503_{mut2}$ HAMP and $NpHAMP_1$. The PCR fragments and the primers for the respective PCR reactions are indicated. The fusion PCR product was cloned into the BamHI and HindIII sites of pETDUET3 (-MCS2).

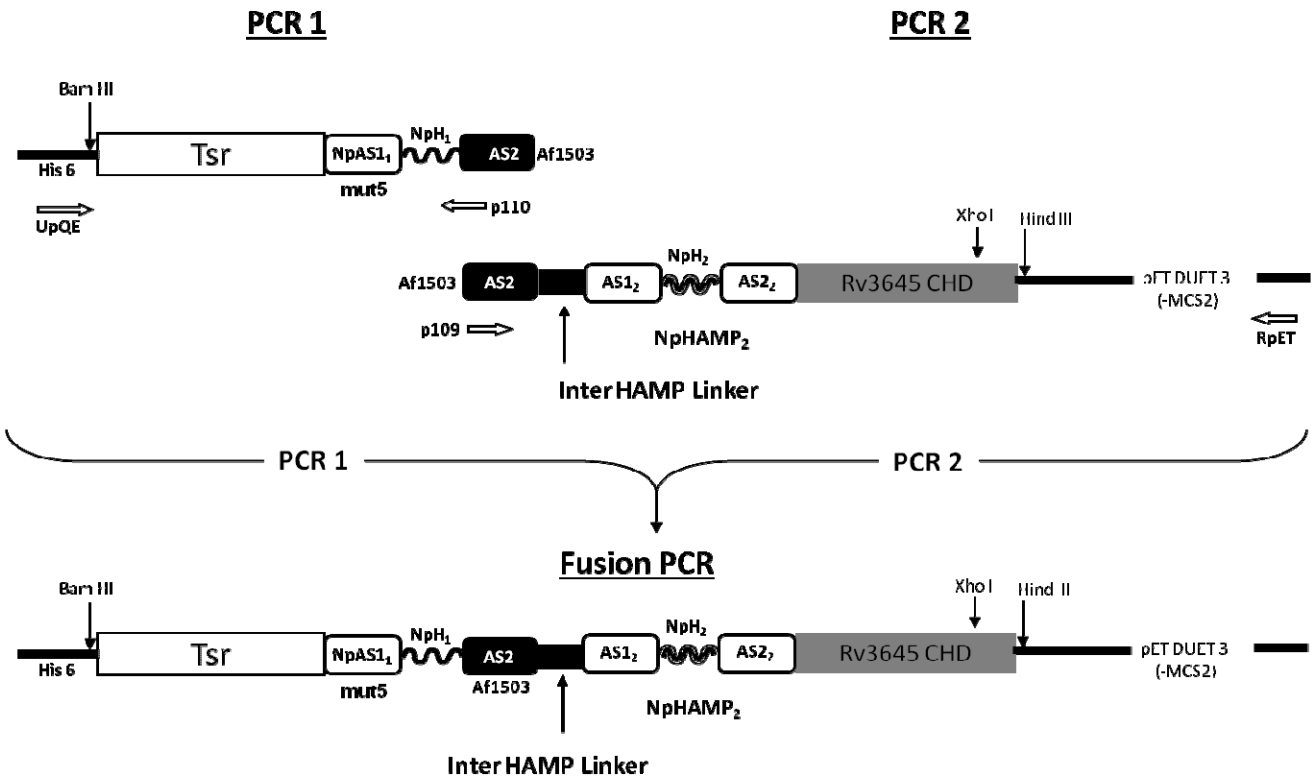

11) Tsr$_{1\text{-}215}$- HAMP tandem -Rv3645$_{331\text{-}549}$.

HAMP$_1$: AS1 - Af1503$_{mut2}$, Connector/AS2 -NpH$_1$. HAMP$_2$: NpHAMP$_2$.

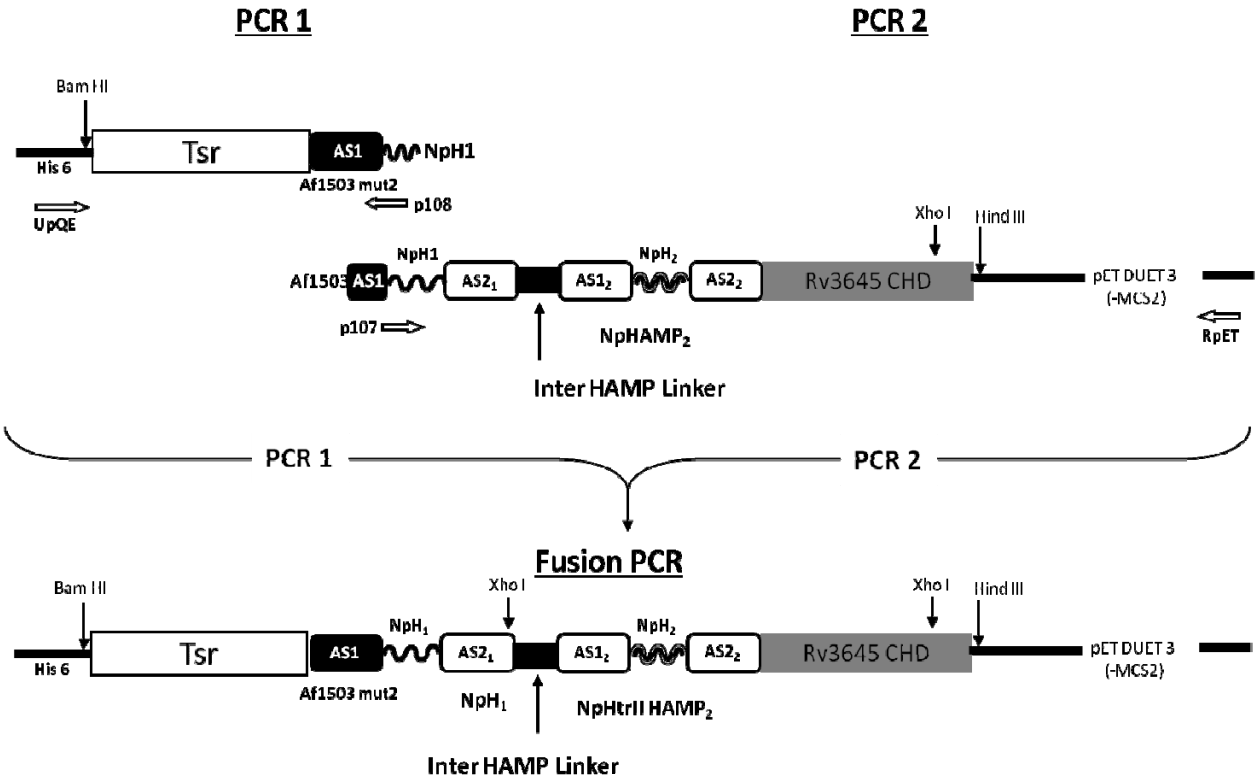

12) Tsr $_{1\text{-}215}$-HAMP (AS1- Tsr/NpH$_1$)-Rv3645$_{331\text{-}549}$.

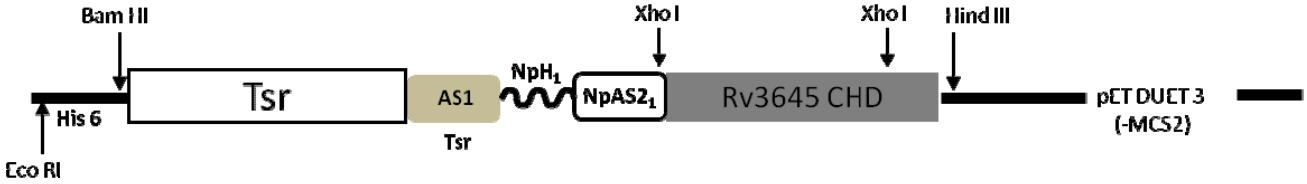

The primers p27 and p26 were used. The BamHI and HindIII cut fusion PCR product was ligated to BamHI and HindIII cut pETDUET3 (-MCS2).

13) Tsr $_{1\text{-}215}$-AS1 Tar/NpH1-Rv3645$_{331\text{-}549}$.

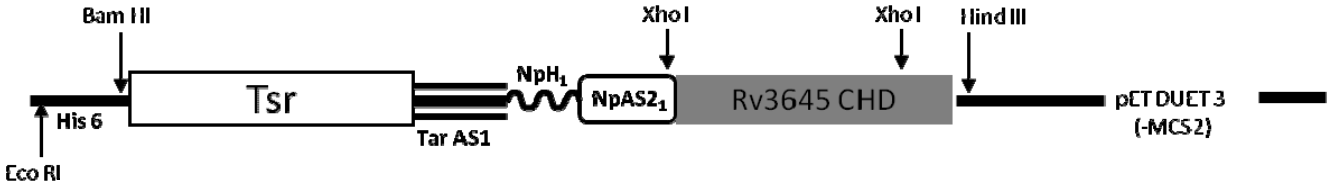

Primers p96 and p95 were used. The fusion PCR product ligated to BamHI and HindIII cut pETDUET3 (-MCS2).

14) Tsr$_{1\text{-}215}$- HAMP tandem -Rv3645$_{331\text{-}549}$.
HAMP$_1$: AS1-Tar, Connector/AS2-NpH$_1$. HAMP$_2$: NpHAMP$_2$.

A fusion PCR was done to couple structural components of Tar HAMP and NpHAMP$_1$. The PCR fragments and the primers for the respective PCR reactions are indicated. The final product was cloned into the BamHI and HindIII sites of pETDUET3 (-MCS2).

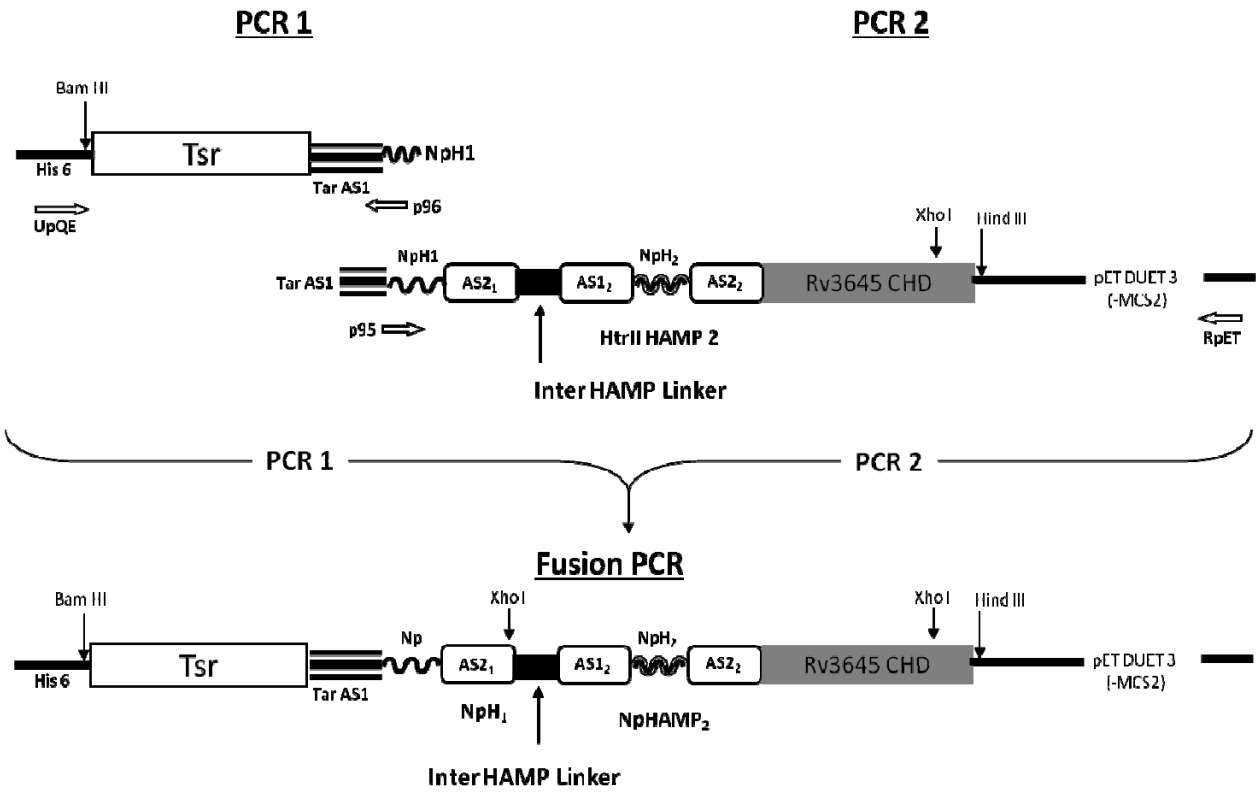

15) Tar $_{1\text{-}213}$-AS1 Tar/NpH1-Rv3645$_{331\text{-}549}$.

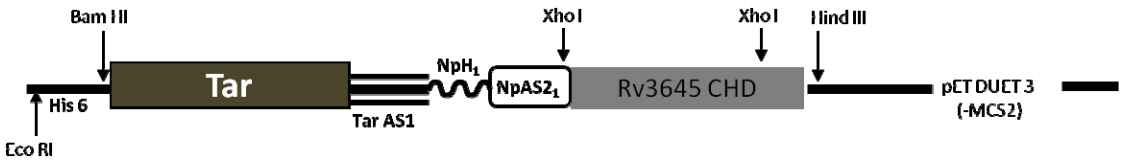

16) Tar$_{1\text{-}213}$- HAMP tandem -Rv3645$_{331\text{-}549}$.
HAMP1: AS1-Tar, Connector/AS2-NpH1. HAMP2: NpHAMP2.

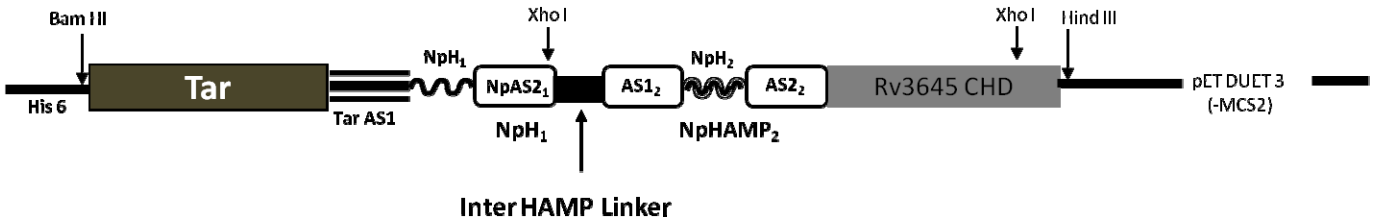

The cloning of the constructs 16 and 17 were similar. Primers p96 and p95 were used. The fusion PCR fragments were cloned into BamHI and HindIII cut pETDUET3 (-MCS2).

3.4 $AS1_1$ mutational analysis.

1) Five mutant chimera of $AS1_1$ of the tandem.

Final products were cloned into the BamHI and HindIII sites of pETDUET3.

$AS1_1$ (tandem)	Tandem chimera	Primer fp	Primer rp
GDlvapLnrlidsirhMaD	$AS1_{1\text{-}Tsr}$/NpH1 tandem	p125	p126
ASlaapMstliakisrIaG	$NpH_{1\text{-}mut5}$ tandem	p121	p122

2) Four mutant chimera of $AS1_1$ of the tandem.

Final products were cloned into the BamHI and HindIII sites of pETDUET3.

$AS1_1$ (tandem)	Tandem chimera	Primer fp	Primer rp
GDlvapLnrlidsirhMag	$AS1_{1\text{-}Tsr}$/NpH1 tandem	p159	p160
ASlaapMstliakisrIad	$NpH_{1\text{-}mut5}$ tandem	p157	p158

3) Functionally insignificant mutants of $AS1_1$ of the tandem.

Final products were cloned into the BamHI and HindIII sites of pETDUET3.

$AS1_{1\text{-}Tsr}$/NpH1 tandem	Primer fp	Primer rp
aslAapmnrlidsirhiag	p91	RpET
aslvapmnrlidsiShiag	p78	p79
aslvapmnrlidsisRiag	p127	p128
aslvapmnrlidKirhiaD	p80	p81
aslvapmnrliAKiShiag	p82	p85

$NpH_{1\text{-}mut5}$ tandem	Primer fp	Primer rp
gdlVaplstliakisrmaG		
gdlVaplNRliDSisrmad		
gSlaaplstliakisrmad	p147	p148

The first two $AS1_1$ of the $NpH_{1\text{-}mut5}$ tandem were unplanned. They were obtained as random mutations from PCR of other clones.

4) Functionally significant mutants of $AS1_1$ of the tandem.

$AS1_{1\text{-}Tsr}$/NpH1 tandem	Primer fp	Primer rp
aslvapmnrliAsirhiag	p76	p83
aslvapmnrlidKirhiag	p77	p83
aslvapmnrlidsirhiaD	p80	p81
aslvapmnrlidKiShiag	p78	p84
aslvapmnrliAKirhiag	p82	p83
aslAapmnrlidKirhiag	p91	RpET
aslAapmnrliAKirhiag	p91	RpET
aslAapLnrlidsirhiaD	p131	p132
aslAapmnrliAKiShiag	p91	RpET
aslAapmSTliAKiShiag	p117	p118
Gslvapmnrlidsirhiag	p149	p150
GslvapLnrlidsirhMag	p149	p150
aDlvapLnrlidsirhMag	p153	p154
aslvapLnrlidsirhMag	p135	p136
GDlvapLnrlidsirhiag	p165	p166

$NpH_{1\text{-}mut5}$ tandem	Primer fp	Primer rp
gdlVaplstliakisrmad	p106	RpET
gdlaaplstliaSisrmad	p101	p102
gdlaaplstliakisrmaG		
gdlaaplstliDSisrmad	p101	p102
gdlVapMstliakisrmaG	p137	p138
gdlaaplstliDSiRrmaG	p104	p105
gdlVaplstliDSiRrmaG	p106	RpET
gdlVaplNRliDSiRrmaG	p119	p120
Adlaaplstliakisrmad	p143	p144
gSlaapMstliakisrIad	p145	p146
ASlaaplstliakisrmad	p155	p156

Final products were cloned into the BamHI and HindIII sites of pETDUET3. The mutations in the $AS1_1$ are indicated with an increased font size.

5) Functionally significant mutants of $AS1_1$ of the tandem.

Final products were cloned into the BamHI and HindIII sites of pETDUET3 (-MCS2). The mutations in the $AS1_1$ are indicated with an increased font size.

$AS1_{1\text{-}Tsr}$/NpH1 tandem	Primer fp	Primer rp
aDlvapmnrlidsirhiag	p151	p152
GDlvapmnrlidsirhiag	p129	p130
GDlvapmnrlidsirhMag	p169	p170
aslAapmnrliAsirhiag	p91	RpET

$NpH_{1\text{-}mut5}$ tandem	Primer fp	Primer rp
gdlaapMstliakisrIad	p157	p158
ASlaapMstliakisrmad	p163	p164
ASlaaplstliakisrIad	p167	p168
gdlaaplstliakisHmad	p123	p124
gdlaaplstliaSisrmaG	p141	p142
gdlaaplstliDSiRrmad		

3.5 Connector mutants of NpHAMP tandem

1) $Tsr_{1\text{-}215}$- HAMP -$Rv3645_{331\text{-}549}$.
$HAMP_1$:AS1/AS2-NpH_1, connector-Tsr HAMP.

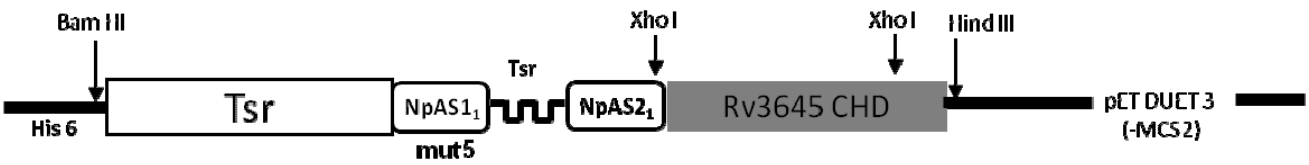

Primers p20 and p21 were used for cloning. The fusion PCR product was cloned into the BamHI/HindIII cut pETDURT3 (-MCS2).

2) Mutations in the $NpHAMP_1$ connector

All mutants were generated by fusion PCR. The PCR product was ligated into BamHI/HindIII cut pETDUET3.

$NpH_{1\text{-}mut5}$ tandem connector mutants	Primer fp	Primer rp
---V--------	p44	p45
----K-------	p42	p43
-----P------	p48	p49
--------V---	p50	p51
---------D--	p52	p53
----------G-	p54	p55
----------S	p40	p41
---VK-------	p42	p43
---V-P------	p48	p49
---------D-S	p36	p37
----------GS	p38	p39
---VKP------	p30	p31
---------DGS	p34	p35
--------VDGS	p28	p29

3) $NpHAMP_2$ connector

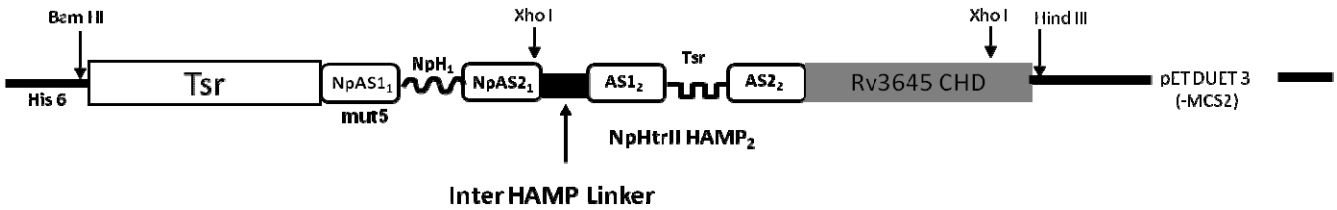

Primers p63 and p64 were used for fusion PCR. The final product was ligated into BamHI/HindIII cut pETDUET3 (-MCS2).

3.6 NpHtrII inter-HAMP linker mutants

The linker mutants were cloned by fusion PCR. The final PCR products were cloned into BamHI/HindIII sites of pETDUET3 (-MCS2). The linker (3X) mutant was unplanned. It was obtained as a mutant during linker (2X) cloning.

Inter-HAMP linker mutants	Primer fp	Primer rp
D-------AEQAQKRAEEIN	p56	p57
DAKNARED-------AEEIN	P60	p59
D----------AEEIN	p61	p62
DAAKNAREDAEQAQKRAEEIN	p66	p67
DAAAKNAREDAEQAQKRAEEIN	p68	p67
DAAAAKNAREDAEQAQKRAEEIN	p72	p71
DAAAAAKNAREDAEQAQKRAEEIN	p75	p74
DAKNAREDAEQAQKRAEEINTDAKNAREDAEQAQKRAEEIN	p113	p114
DAKNAREDAEQAQKRAEEINTDAKNAREDAEQAQKREEINTDAKNAREDAEQAQKRAEEIN		
DAERATARAEDAREDAEQQRADAEAAREDAEAARKDAQETA	p115	p116

3.7 Structural analysis of the tandems.

The following HAMP-cyclases were cloned to study the structural properties of the HAMPs. All the constructs were cloned into BamHI and HindIII of pETDUET3 (-MCS2).

1) NpHAMP tandem -Rv3645$_{331-549}$.

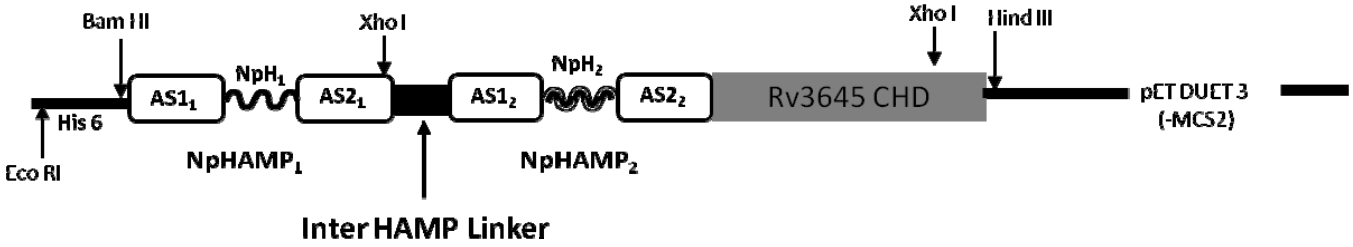

2) NpH-1mut5 tandem -Rv3645$_{331-549}$.

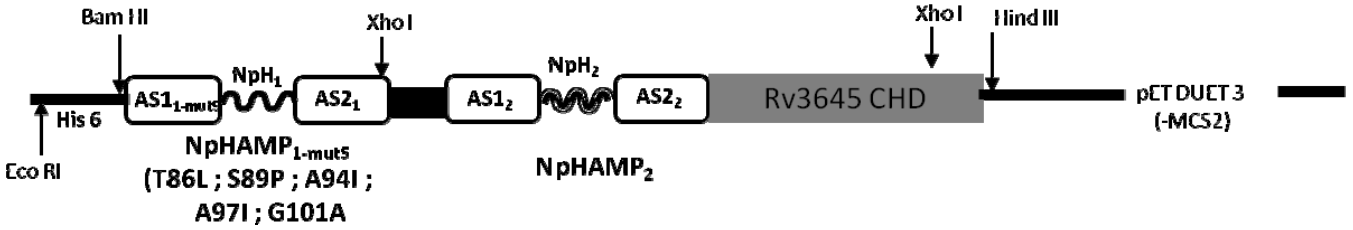

3) HAMP tandem -Rv3645$_{331-549}$.
HAMP$_1$: AS1-Tsr, Connector/AS2-NpH$_1$. HAMP$_2$: NpHAMP$_2$.

3.8 Oligonucleotides

The sequencing primers used in the study are:

s= sense primer
as= anti sense primer

No	Name	Sequence (5'- 3')	Comment
1	T7 s	TAA TAC GAC TCA CTA TAG GG	p-Bluescript II SK (-)
2	T3 as	AAT TAA CCC TCA CTA AAG GG	p-Bluescript II SK(-)
3	U-PQE s	GAA TTC ATT AAA GAG GAG AAA	Universal for PQE30
4	R-PQE as	CAT TAC TGG ATC TAT CAA CAG G	Reverse for PQE30
5	Switch oligo XmnI s	GCT CAT CAT TGG AAA ACG TTC TTC GGG	
6	pETDUET3_ MCS1_s	ATG CGT CCG GCG TAG A	Sense primer for pETDUET3 (MCS1-pQE30)
7	RpET	ACC CCT CAA GAC CCG TTT AGA	Reverse for MCS2 in pETDUET

Primers used for cloning:

The sequence of primers used for the cloning of all the chimeras is shown below. The abbreviations fp and rp mean sense and antisense primer respectively. The wobble primers were used to generate a combination of mutations in several positions. The universal codes for specifying a wobble are: R=A/G, Y=C/T, M=A/C, K=G/T, S=C/G, W=A/T, B=C/G/T, D=A/G/T, H=A/C/T, V=A/C/G, and N=A/C/G/T.

No	PRIMER SEQUENCE	NAME	MODIFICATIONS
p1	ttcggtattaaaggtgacaccgccgcc	#04_Tsr-HtrII(H1)_fp	
p2	ggcggtgtcacctttaataccgaacaa	#04_Tsr-HtrII(H1)_rp	
p3	tacggcattcggggtgacaccgccgcc	#04b_Tar-HtrII(H1)_fp	
p4	ggcggtgtcaccccgaatgccgtacca	#04b_Tar-HtrII(H1)_rp	
p5	ctggccaaact**T**gaggatggccac	#04_Rv3545c_δXhoI_fp	Removing Xho I restriction site from the cyclase.
p6	gtggccatcctc**A**agtttggccag	#04_Rv3545c_δXhoI_rp	
p7	acatcgctcgaggatgccaaaaatgcccgt	#06_HtrII_H1H2_fp	
p8	atttttggcatcctcgagcgatgtccg	#06_HtrII_H1H2_fp	
p9	ttcggtattaagaccgaactgcaagcggaa	#07_Tsr_HtrIIH2(TEL_fp	
p10	ttgcagttcggttttaataccgaaccagac	#07_Tsr_HtrIIH2(TEL_rp	
p11	ttcggtattaaaaccgaactgcaggcggaa	#07_Tsr_HtrIIH2(TEL_fp2	Silent mutations in the codon was corrected
p12	aaactgcagttcggttttaataccgaacca	#07_Tsr_HtrIIH2(TEL_rp2	
p13	ttcggtattaaggcggaagcggaacgc	#07b_Tsr_HtrII(H2-L)_fp	This clone was done to check boundaries for HAMP 2.
p14	ttccgcttccgccttaataccgaacca	#07b_Tsr_HtrII(H2-L)_rp	
p15	aaa**CCCGGG**acctcgccgccccgctttc aacgctgatcgcgaagatctcgcggatggccg acggcgac	#08_HtrII H1_Mut I_fp	**Sma I**. A2MI5. (five point mutations in NpHtrII HAMP 1 AS1)
p16	aaa**CCCGGG**acaYcgccgccYcgcttt caacgctg	#08_HtrII H1_Mut II_fp	**Sma I** . Wobble for NpHAMP1 position 86(T/L) and 89(P/S)
p17	aaa**CCCGGG**acaccgccgcctcgctttc aacgctgRYcgcgaagrYctcgcggatgg Scgacggc	#08_HtrII H1_Mut II_fp	**Sma I** . Wobble for NpHAMP1 position 94(A/I), 97(A/I) and 101(A/G).
p18	acatcgctcgaggatgccaaaaatgcccgt	#09_HtrII_H1H2_fp	Fusion PCR primers for combining HAMP 1 & 2.
p19	atttttggcatcctcgagcgatgtccg	#09_HtrII_H1H2_fp	
p20	gaaaccgattgaggtggatggctctgacgaaa tcggc	#12_A2MI5_connector exchange_fp	
p21	ccatccacctcaatcggtttcacgaggtcgccg tcg	#12_A2MI5_connector exchange_rp	
p22	gatgccaaaaatgcccgggaggatg	#13_TsrH+NpHAMP2_fp	
p23	gcatcctcccgggcatttttggcatcaccgacg gtacgcatcagc	#13_TsrH+NpHAMP2_fp	
p24	gaggtcgccgatttcgtcagagccatccacctc	#15_T(+H) tune 2_rp	
p25	gagcttgagacccgtcgcgagaatgagatgg ggcaactg	#16_T(+H) tune 3_fp	
p26	ctcgcgacgggtctcaagctcgacatcgaggt cgccgcctgc	#16_T(+H) tune 3_rp	
p27	catattgcaggcggcgacctcgatgtcgag	#17_T(+H) tune 4_fp	
p28	gatgtcgagcttgaggtggatggctct	#18_C-Mut I_fp	

No	PRIMER SEQUENCE	NAME	MODIFICATIONS
p29	cacctcaagctcgacatcgaggtcgcc	#18_C-Mut I_rp	
p30	gagacccgtcgcgaggacgaaatcggc	#19_C-Mut 2_fp	
p31	gtcctcgcgacgggtctcaagcggtttcac	#19_C-Mut 2_rp	
p32	gttgctgccacgctgggcggggacctcgccg ccccgc	#20_BE1_HfMI5_fp	
p33	ggcggcgaggtccccgcccagcgtggcagc	#20_BE1_HfMI5_rp	
p34	gtcgagcttgagACCgatSggtctgacg	#21+22_C_Mut 3+4_fp	Wobble for NpHAMP1 position 113(G/R) .
p35	gccgatttcgtcagaggSatcGGTctcaagc tc	#21+22_C_Mut 3+4_fp	
p36	gagcttgagaccgatcggtctgacgaaatcgg cgacctc	#22_C_Mut 4_fp	
p37	gatttcgtcagaccgatcggtctcaagctcgac atcgag	#22_C_Mut 4_rp	
p38	gtcgagcttgagACCCGGSggtctgacg	#23+24_C_Mut 5-6_fp	Wobble for NpHAMP1 position 113(G/R)
p39	gccgatttcgtcagaggSCCGGGTctcaa gctc	#23+24_C_Mut 5-6_rp	
p40	acccggcggtctgacgaaatcggcgacctc	#24_C_Mut 6_fp	
p41	gatttcgtcagaccgccgggtctcaagctc	#24_C_Mut 6_rp	
p42	gccgacggcgacctcgWcAAAgagcttg ag	#25+26_C_Mut 7-8_fp	Wobble for NpHAMP1 position 106(D/V)
p43	acgggtctcaagctcTTTgWcgaggtcgc c	#25+26_C_Mut 7-8_rp	
p44	gccgacggcgacctcgtggtggagcttgag	#27_C_Mut 9_fp	
p45	acgggtctcaagctccaccacgaggtcgcc	#27_C_Mut 9_rp	
p46	ggcgacctcgtggtggagcttgagacccgt	#27n_C_Mut 9_fp	
p47	aagctccaccacgaggtcgccgtcggc	#27n_C_Mut 9_rp	
p48	gccgacggcgacctcgWcgtgccgcttgag	#28+29_C_Mut 10-11_fp	Wobble for NpHAMP1 position 106(D/V)
p49	acgggtctcaagcggcacgWcgaggtcgcc	#28+29_C_Mut 10-11_rp	
p50	gagcttgaggtgcgtcgcgaggacgaaatc	#30_C Mut 12_fp	
p51	ctcgcgacgcacctcaagctcgacatcgag	#30_C Mut 12_rp	
p52	cttgagaccgaccgcgaggacgaaatcggc	#31_C Mut 13_fp	
p53	gtcctcgcggtcggtctcaagctcgacatc	#31_C Mut 13_rp	
p54	gagacccgtggcgaggacgaaatcggcgac	#32_C Mut 14_fp	
p55	ttcgtcctcgccacgggtctcaagctcgac	#32_C Mut 14_rp	
p56	acatcgctcgaggatgctgaacaagcccaaaa a	#33_HfMI5_Lin mut 1 _fp	
p57	ttgttcagcatcctcgagcgatgtccgcaccga	#33_HfMI5_Lin mut 1 _rp	
p58	acatcgctcgaggatgccaaaaatgcccgtga g	#34_HfMI5_Lin mut 2 _fp	
p59	atttttggcatcctcgagcgatgtccgcaccga	#34_HfMI5_Lin mut 2 _rp	
p60	gccaaaaatgcccgtgaggatgccgaagaga tcaatacc	#34n_HfMI5_Lin mut 2 _fp	
p61	acatcgctcgaggatgccgaagagatcaatac c	#35_HfMI5_Lin mut 3 _fp	
p62	ctcttcggcatcctcgagcgatgtccgcaccga	#35_HfMI5_Lin mut 3 _rp	
p63	aaaccgattgaggtggatggctctaatgaggc catgcaatca	#36_H2_C_Mut 1_fp	

No	PRIMER SEQUENCE	NAME	MODIFICATIONS
p64	aaaccgattgaggtggatggctctaatgaggc catgcaatca	#36_H2_C_Mut 1_rp	
p65	cggacatcgctcgaggatgccgccaaaaatgc ccgt	#37_fp	
p66	aaaaaactcgaggatgccgccaaaaatgcccg t	#37o_137A138_fp	
p67	ggcatcctcgagcgatgtccgcac	#37+38_rp	
p68	cggacatcgctcgaggatgccgccgccaaaa atgcccgt	#38_fp	
p69	aaaaaactcgaggatgccgccgccaaaaatgc ccgt	#38o_137AA138_fp	
p70	gatgccgccgccgccaaaaatgcccgtgag	#39_fp	
p71	tttggcggcggcggcatcctcgagcgatgtcc g	#39_rp	
p72	aaaaaactcgaggatgccgccgccgccaaaa atgcccgt	#39_137AAA138_fp	
p73	gatgccgccgccgccgccaaaaatgcccgtg	#40_fp	
p74	ggcggcggcggcggcatcctcgagcgatgtc	#40_rp	
p75	aaaaaactcgaggatgccgccgccgccgcca aaaatgcccgt	#40o_137AAAA138_fp	
p76	cgcctgattgccagcattcgtcatattgca	#41_fp	
p77	ctgattgacaagattcgtcatattgcaggc	#42_fp	
p78	gacagcattagccatattgcaggcggcgac	#43_fp	
p79	tgcaatatggctaatgctgtcaatcaggcg	#43_rp	
p80	catattgcagacggcgacctcgatgtcgag	#44_fp	
p81	gaggtcgccgtctgcaatatgacgaatgctgtc	#44_rp	
p82	cgcctgattgccaagattcgtcatattgcaggc	#45_fp	
p83	atgacgaatcttggcaatcaggcgattcattgg	#45_rp	
p84	tgcaatatggctaatcttgtcaatcaggcgatt	#46_rp	
p85	tgcaatatggctaatcttggcaatcaggcgattc attgg	#47_rp	
p86	aaaaaa**GGATCC**atgtcgctgaacgtatc acgg	#54_Bam HI start_fp	**Bam HI**
p87	gaggtaaccctttacaactgacatcaggc	#54_TM1_ser loop_fp	
p88	ttgtaaaagggttacctcaccgtatgcg	#54_TM1_ser loop_rp	
p89	gcctcctacagcgtatcggccattctcggg	#54_TM2_ser loop_fp	
p90	tggccgatacgctgtaggaggcattgttatcgc	#54_TM2_ser loop_rp	
p91	cggtattaaggcctcgctggcagcgccaatga atcgc	#56_fp	
p92	tttaagcttttaaccaaccagtgcttcgattcc	#61+62_rp	
p93	aaggagatcgccgcacagaccgagc**R**cgtc gccaacggcgacctcgatgtcgagctt	#63_fp	Wobble primer for constructs #63 -66
p94	tgcggcgatctccttgatgctggcgacggtct**S** ggctttaataccgaaccagacggc	#63_rp	
p95	cgcgaaatcgccggtggcgacctcgatgtc	#67_fp	
p96	gacatcgaggtcgccaccggcgatttcgcg	#67_rp	
p97	ctttcaacgctgatcgcgaagatctcgcgg	#70_fp	
p98	gcgatcagcgttgaaagcggggcggcggtg	#70_rp	

No	PRIMER SEQUENCE	NAME	MODIFICATIONS
p99	tcaacgctggccgcgaagttctcgcgg	#71+72_fp	
p100	cgcggccagcgttgaaagcgRggcggcggt	#71+72_rp	Wobble at NpHAMP1 position 89 (S/P)
p101	acgctgatcgMcagcatctcgcggatggccgac	#76+77_fp	Wobble at NpHAMP1 position 95(A/D)
p102	ccgcgagatgctgKcgatcagcgttgaaagcgg	#76+77_rp	
p103	aaaaaa**CCCGGG**gacctcgccgccccgctttcaacgctgatcgccagcatctcgcgg	#76n_fp	**Sma I**
p104	atcgacagcatcaggcggatggccgacggc	#78_fp	
p105	atcgaggtcgcccccggccatccgcctgat	#78_rp	
p106	attaaaggggacctcgtcgccccgctttcaacg	#79_fp	
p107	gacaagattgccgaaggcgacctcgatgtc	#82_fp	
p108	atcgaggtcgccttcggcaatcttgtcgat	#82_rp	
p109	atcgaaaggctgagaaggagcctcaaggtcgccatggaggatgccaaaaatg	#83_fp	
p110	ggctccttctcagcctttcgatactctttgcaagaataccgatttcatc	#83_rp	
p111	aaggtcgccatggaggatgccaaaaatgcc	#84_fp	
p112	atttttggcatcctccatggcgaccttgag	#84_rp	
p113	gcccgtgaggatgctgaacaagcccaaaaacgtgccgaagagatcaataccgaactgcaagcg	#85_fp	
p114	ttcagcatcctcacgggcatttttggcatcggtattgatctcttcg	#85_rp	
p115	cagcagcgcgccgacgccgaagccgcccgcgaagacgccgaagccgcccgcaaggacgccccaagaaacggctaccgaactgcaagcg	#86_fp	
p116	ttcggcgtcggcgcgctgctgttcggcgtcctcacgggcgtcctcggcgcgtgccgtcgcgcgttcggcgtcctcgagcgatg	#86_rp	
p117	tcgctggcagcgccaatgagtaccctgattgccaagattagc	#87_fp	
p118	gctaatcttggcaatcagggtactcattggcgctgccagcga	#87_rp	
p119	gacctcgtcgccccgcttaaccggctgatcgacagcatcagg	#88_fp	
p120	cctgatgctgtcgatcagccggttaagcggggcgacgaggtc	#88_rp	
p121	atcgacagcatcaggcatatggccggcggcgac	#100_fp	
p122	gtcgccgccggccatatgcctgatgctgtcgat	#100_rp	
p123	atcgcgaagatctcgcatatggccgacggcgac	#101_fp	
p124	gtcgccgtcggccatatgcgagatcttcgcgat	#101_rp	
p125	attgccaagattagccggattgcaggcggcgac	#102_fp	

No	PRIMER SEQUENCE	NAME	MODIFICATIONS
p126	gtcgccgcctgcaatccggctaatcttggcaat	#102_rp	
p127	attgacagcattcgtcggattgcaggcggcga c	#103_fp	
p128	gtcgccgcctgcaatccgacgaatgctgtcaat	#103_rp	
p129	tggttcggtattaaaggtgacctggtagcgcca atg	#105_fp	
p130	cattggcgctaccaggtcacctttaataccgaac ca	#105_rp	
p131	attaaagcctcgctggccgcgccacttaatcgc ctgattgac	#107_fp	
p132	gtcaatcaggcgattaagtggcgcggccagcg aggctttaat	#107_rp	
p133	gacctggccgcgccacttaatcgcctgattgac	#108_fp	
p134	tggcgcggccaggtccccttttaataccgaacc a	#108_rp	
p135	tggttcggtattaaagcctcgctcgccgccccg ctt	#109_fp	
p136	aagcggggcggcgagcgaggctttaataccg aacca	#109_rp	
p137	attaaaggggacctcgtagccccgatgtcaac gctgatcgcg	#111_fp	
p138	cgcgatcagcgttgacatcggggctacgaggt ccccttttaat	#111_rp	
p139	ctcgtagccccgatgtcaacgctgatcgcgag c	#112_fp	
p140	catcggggctacgagcgaggctttaataccga acca	#112_rp	
p141	tcaacgctgatcgccagcatctcgcggatggc c	#113_fp	
p142	ggccatccgcgagatgctggcgatcagcgttg a	#113_rp	
p143	tggttcggtattaaagccgacctcgccgcc	#114_fp	
p144	ggcggcgaggtcggctttaataccgaacca	#114_rp	
p145	ttcggtattaaaggttcgctcgccgccccgctt	#115_fp	
p146	aagcggggcggcgagcgaacctttaataccg aa	#115_rp	
p147	aaatacgtagcctcgccgccccgctttc	#115n2_fp	
p148	aagcggggcggcgagcgaacctttaataccg aaaccagacggc	#115n_rp	
p149	tggttcggtattaaaggttcgctggtagcgcca	#116_fp	
p150	tggcgctaccagcgaacctttaataccgaacca	#116_rp	
p151	ttcggtattaaagccgacctggtagcgccaatg	#117_fp	
p152	cattggcgctaccaggtcggctttaataccgaa	#117_rp	
p153	ctgacctggtagcgccaatgaat	#117n2_fp	
p154	cattggcgctaccaggtcggctttaataccgaa ccagacggc	#117n_rp	
p155	tggttcggtattaaagcctcgaccgccgcctcg ctt	#118_fp	

No	PRIMER SEQUENCE	NAME	MODIFICATIONS
p156	aagcgaggcggcggtcgaggctttaataccgaacca	#118_rp	
p157	acgctgatcgcgaagatctcgcggatcgccgacggcgacctc	#119_fp	
p158	cttcgcgatcagcgttgacatcggggcggcgagg	#119_rp	
p159	ctgattgacagcattcgtcatatggcaggcggcgacctc	#122_fp	
p160	aatgctgtcaatcaggcgattcagtggcgctaccagg	#122_rp	
p161	atctcgcggatcgccgacggcgacctcgatgtc	#125_fp	
p162	gacatcgaggtcgccgtcggcgatccgcgagat	#125_rp	
p163	gcgaagatctcgcggatggccgacggcgacctcgatgtc	#126_fp	
p164	gacatcgaggtcgccgtcggccatccgcgagatcttcgc	#126_rp	
p165	gacagcattcgtcatattgcaggcggcgacctc	#127_fp	
p166	gaggtcgccgcctgcaatatgacgaatgctgtc	#127_rp	
p167	gctggcagcgccacttagtaccctgattgcc	#128_fp	
p168	ggcaatcagggtactaagtggcgctgccagc	#128_rp	
p169	cctcgtcgccccgatgaaccggctgatcgac	#129_fp	
p170	gtcgatcagccggttcatcggggcgacgagg	#129_rp	

4 RESULTS

4.1 Biochemical analysis of tandem HAMP from *Natronomonas pharaonis*.

This work involves biochemical characterization of the tandem HAMP domains from *N. pharaonis.*

4.1.1 Tandem HAMP from *N. pharaonis*.

The phototaxis transducer of *N. pharaonis* HtrII has a HAMP tandem connecting the two transmembrane spans to the kinase control module. The $HAMP_1$ and $HAMP_2$ are interconnected by a linker. The necessity for a tandem HAMP domain as a signal transducer in a transmembrane signaling protein is not obvious. Compared to signal transduction via a single HAMP domain the predicted outcome via a tandem HAMP is inversion of the signal sign [42, 48].

The $NpHAMP_1$ and $HAMP_2$ were grouped into different groups of HAMPs [42]. The sequences of the NpHtrII HAMPs were aligned to the previously analyzed HAMP sequences (Fig. 4-1) to identify the boundaries for NpHAMP domains. The boundary of the HAMP included two residues in the N-terminal which were present in the initial NMR structure and are now disputed to be part of control cable [43, 81].

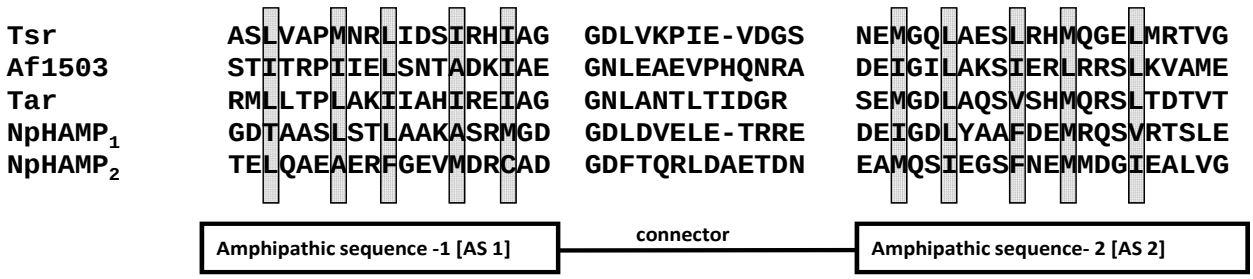

Figure 4-1. Sequence alignment of NpHAMP tandem with Tsr, Tar and Af1503 HAMP. The grey bars indicate the 'a' and 'd' positions in AS1 and AS2.

To examine signal transduction through the NpHAMP tandem we employed chimeras analogous to constructs consisting of the *E. coli* serine receptor Tsr, a single HAMP domain, and the catalytic domain of the mycobacterial AC Rv3645 [68, 69].

4.1.2 Triple chimera generation.

To biochemically characterize the NpHAMP tandem domains we initially combined $NpHAMP_1$ with various domains to check which is functional. We attached N-terminally sensors for serine, Tsr, or for aspartate, Tar, and C-terminally two different adenylyl cyclases Rv3645 and CyaG. Three different constructs were generated: Tsr-$NpHAMP_1$-Rv3645, Tsr-$NpHAMP_1$-CyaG and Tar-$NpHAMP_1$-CyaG. The Tar-$NpHAMP_1$-CyaG chimera was inactive. The two chimeras with Tsr receptor were active although not affected by serine. The Tsr-$NpHAMP_1$-CyaG and Tsr-NpHAMP1-Rv3645 had basal activities of 0.5 ± 0.1 and 1.7 ± 0.3 nmol/mg/min, respectively. The Western blots indicated protein expression (Fig. 4-2). The $NpHAMP_1$ possibly cannot function as a monomer as in the native state it works in tandem.

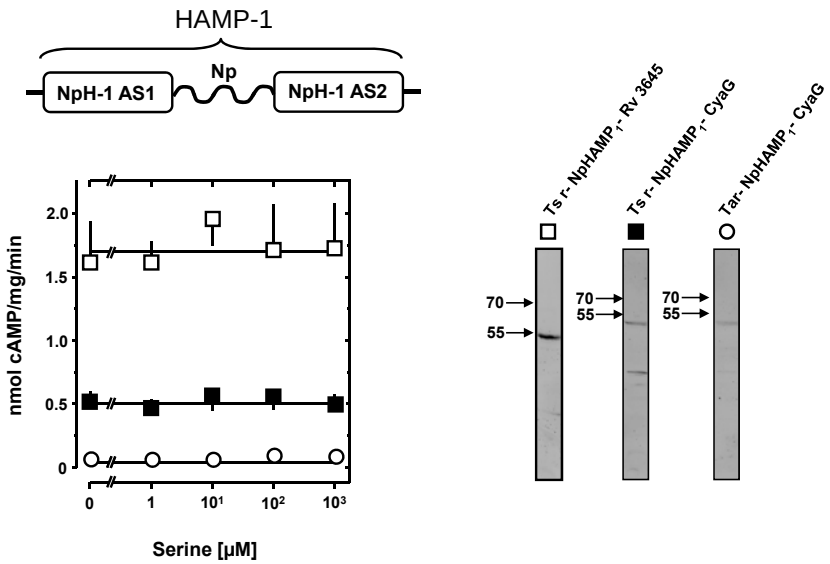

Figure 4-2. Left, activity of the $NpHAMP_1$ constructs in combination with the various input and output domains. Right, Western blots of the expressed proteins (5 µg protein/lane). The 70 and 55 kDa MW markers are indicated. (n=4).

The $NpHAMP_1$, $NpHAMP_2$ and the NpHAMP tandem were tested along with Tsr and Rv3645. The NpHAMP tandem and $NpHAMP_2$ in the chimera had a higher activity compared to $NpHAMP_1$ in the system. Both the mono-HAMPs were unaffected by serine although active. Basal activities of $NpHAMP_1$, $NpHAMP_2$ and NpHAMP tandem chimeras were 0.5 ± 0.1, 3.2 ± 0.2 and 6.2 ± 0.7 nmol/mg/min, respectively (Fig. 4-3). The NpHAMP tandem showed a tendency to be inhibited by serine at 3mM serine although the inhibition was insignificant (*, $p>0.05$; n=4). The Western blots confirmed similar expression levels.

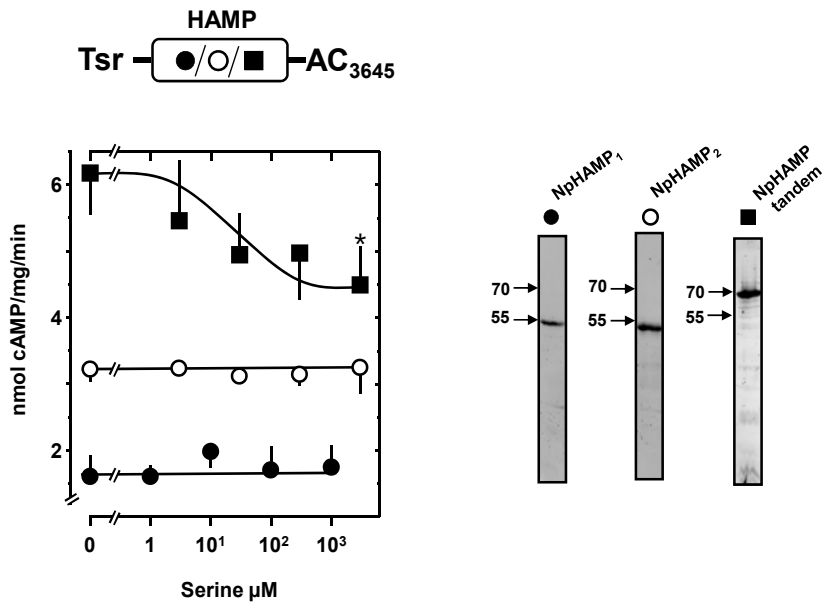

Figure 4-3. Left, response of the chimeras with $NpHAMP_1$ (filled circles), $NpHAMP_2$ (open circles) or NpHAMP tandem (filled squares) in the chimera. *, serine inhibition not significant (p>0.05). Right, Western blots of the expressed protein (5 µg protein/lane). The 70 and 55 kDa MW markers are indicated. (n=4-6).

The NpHAMP domains seemed to work best with the Tsr receptor and Rv3645 AC as input and output sensors, respectively. All further chimeras described have the same sensor domains.

4.1.2.1 Mutation of AS1 of $NpHAMP_1$

A sequence comparison of $NpHAMP_1$ with $HAMP_{Tsr}$, demonstrated that $NpHAMP_1$ AS1 lacked specific conserved residues that are supposed to be involved in the uptake of the signal from the transmembrane (Fig. 4-4). These residues have been designated as the green network based on a exhaustive bioinformatic analysis of HAMP domains [42]. Accordingly we replaced five positions in $NpAS1_1$ by their positional equivalents in $HAMP_{Tsr}$ generating $NpHAMP_{1\text{-}mut5}$: T86L – replaced a hydrophilic core residue by a hydrophobic one; S89P – serine was replaced by proline, the most conserved residue at this position in canonical HAMP domains which together with DExG in $NpAS2_1$ constitute a capping motif supposedly associated with transmembrane signaling; A94I – change of a critical flanking residue in the coiled coil; A97I – this core position was replaced by a large hydrophobic residue; G101A – introduction of a highly conserved alanine (Fig. 4-4).

	AS1	connector	AS2
	84 86 88 90 92 94 96 98 100 102	103 105 107 109 111 113	115 117 119 121 123 125 127 129 131 133 135
$NpHAMP_1/NpH_1$	gdtaaslstlaakasrmgd	gdldveletrre	deigdlyaafdemrqsvrtsle
TsrHAMP	aslvapmnrlidsirhiag	gdlvkpievdgs	nemgqlaeslrhmqgelmrtvg
	216 218 220 222 224 226 228 230 232 234	235 237 239 241 243 245	247 249 251 253 255 257 259 261 263 265 267
$NpH_{1\text{-}mut5}$	gdLaaPlstlIakIsrmAd	gdldveletrre	deigdlyaafdemrqsvrtsle
	86 89 94 97 101		

Figure 4-4. The sequence comparison between Tsr and $NpHAMP_1$. The bottom sequence shows the mutations in $NpHAMP_1$ AS1.

$NpHAMP_{1\text{-}mut5}$ was tested for signal transduction either alone or in tandem with $NpHAMP_2$ (Fig. 4-5). AC activity of the chimera with the $NpHAMP_{1\text{-}mut5}$ monomer was not affected by serine. However, in tandem with $NpHAMP_2$ the chimera was significantly inhibited by L-serine (IC_{50}=30 µM; n=4; *, $p<0.05$; Fig. 4-5). Basal activities of $NpHAMP_{1\text{-}mut5}$ monomer and tandem were 0.6 ± 0.1 and 0.8 ± 0.1 nmol/mg/min, respectively. 1 mM aspartate had no effect on both the chimeras (Fig. 4-5).

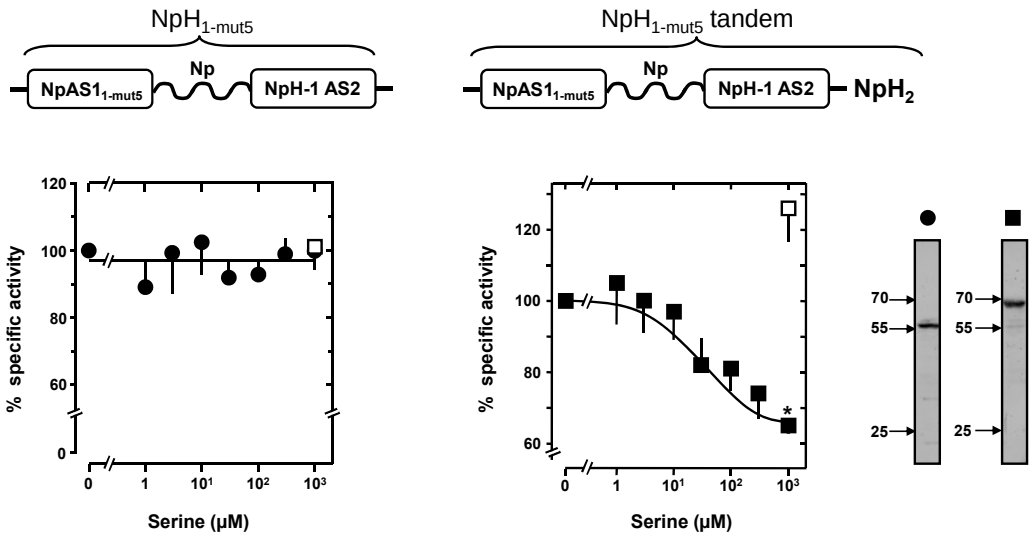

Figure 4-5. The response to serine (filled circles and squares) and aspartate (open squares) by $NpH_{1\text{-}mut5}$ monomer and tandem in the test system. Serine inhibited the $NpH_{1\text{-}mut5}$ tandem by 40 % (*, $p<0.05$). Western blots at right, indicate absence of proteolysis. (n=4).

The $NpHAMP_{1\text{-}mut5}$ which as a HAMP monomer did not effectively transduce a signal was in fact a signal transducing module in combination with $NpHAMP_2$, i.e. in conjunction with another inactive monomer. The inhibition of AC activity by serine in the construct with the NpHAMP tandem appeared to contradict the predicted signal inversion because serine also inhibited AC activity in chimeras with the $HAMP_{Tsr}$ monomer as reported earlier [68, 69].

To find out if all five mutations were required to establish signal transduction constructs with variable combinations of 3 or 4 point mutations were generated (Table 4-1).

	AS1	connector	AS2
$NpH_{1\text{-}mut5}$	gdLaaPlstlIakIsrmAd	gdldveletrre	deigdlyaafdemrqsvrtsle

	NpHAMP tandem: $AS1_1$ mutations	Basal activity (nmol cAMP/mg/min)	1mM serine
1)	gdLaaPlstlIakasrmgd	0.3 ± 0.1	n.r.
2)	gdLaaPlstlIakIsrmgd	inactive	
3)	gdtaaPlstlIakIsrmgd	inactive	
4)	gdtaaslstlaakFsrmgd	inactive	
5)	gdLaaPlstlaakFsrmgd	inactive	

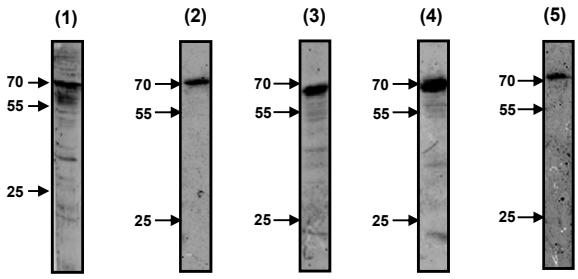

Table 4-1. Above, mutations generated in $NpHAMP_1$ AS1. Below, Western blots of the respective chimeras. (n=4).

The T86L/S89P/A94I triple mutant of NpHAMP tandem lost the response to serine but was active. All other mutants were inactive (Table 4-1). The A97F mutation was generated to mimic similar mutation in Af1503 HAMP which rendered the HAMP functional [68]. It was obvious that all 5 mutations were necessary for the $HAMP_1$ to be functional in the tandem.

4.1.2.2 Effect of salt on $NpH_{1\text{-}mut5}$ tandem.

N. pharaonis is an extremely haloalkaliphilic archaeon, living in salt-saturated lakes and grows optimally at 3.5 M NaCl [82]. It has reversed sodium to potassium ratio [83]. Due to effects of salt on electrostatic and hydrophobic interactions [84] the structure and dynamic properties of the HAMP domain are expected to be influenced by salt as well. It has been reported that the NpHtrII is affected by salt concentration for its function [82]. Several other studies reported that salt had only minimal effects on the function of HtrII in physiological assays [85]. To check the effect of salt in our test system, four conditions with/-out salt in the

lysis (50 mM NaCl) and membrane resuspension (250 mM NaCl) buffers were generated. The effect of 1mM serine at each condition was also tested. The basal activity of the tandem chimera (0.8 ± 0.1 nmol/mg/min) which had salt in both buffers was set as 100%. All other activities are in comparison to this basal activity.

	No NaCl in lysis and Membrane buffer	NaCl in lysis (50 mM)	NaCl in membrane buffer (250 mM)	NaCl in lysis (50 mM) and membrane buffer (250 mM)
Basal activity	22[b]	51[b]	31[b]	100[a]
1mM serine	14[b]	39[b]	12[b]	58[b]

[a.] Basal activity with NaCl in both buffers (0.8 ± 0.1 nmol/mg/min) is set as 100%.
[b.] All remaining activities are in comparison to this activity (a)

Table 4-2. The effect of salt on the activity of the $NpH_{1\text{-}mut5}$ tandem. (n=2).

With no salt in buffers the chimera completely failed to form a functional protein (Table 4-2). The activity of the chimera was below the cut off for an active enzyme. The presence of salt either in lysis or membrane resuspension buffers improved the chimeric cyclase activity indicating more stabilized protein. On comparison of chimeras with salt in membrane buffer and lysis buffer, the activity with salt in lysis buffer was better indicating that the need of salt to aid in proper folding of the protein.

Salt was included in lysis and membrane resuspension buffers with all NpHAMP chimeras. It is not surprising as apart from the presence of high salt in cytoplasm, the HAMP domains from NpHtrII have a higher amount of charged amino acids on a comparison with Tsr HAMP. The charges probably need the salt for stabilizing the structure. This is a classical example of the adaptation of the archaea to its harsh habitat.

4.1.2.3 Kinetics of NpH_{1mut5} tandem

4.1.2.3.1 Protein dependence

The protein dependence of the tandem protein was examined (20 to 120 µg). The activity in nmol cAMP/min was linear (Fig. 4-6). In all assays 20-25µg of membrane protein was used.

4.1.2.3.2 Time dependence

The assays are usually carried out at 37ºC for 10 mins. To see if this was within the linear range of cyclase activity, 20 µg of protein was assayed at a time range from 0 to 16 minutes. The activity in nmol cAMP/mg of the protein was linear (Fig. 4-6).

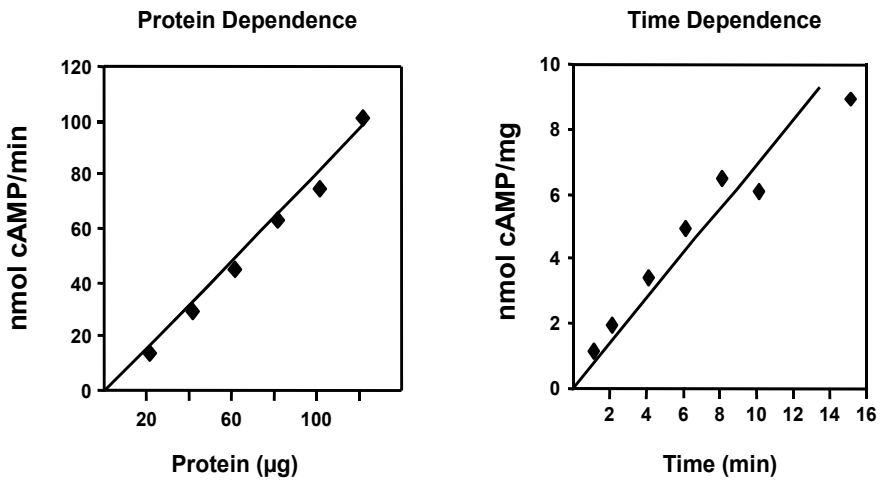

Figure 4-6. Protein and time dependence for the $NpH_{1\text{-}mut5}$ tandem. Assay conditions: 200 µM ATP, Tris/HCl pH 7.5, n=2.

4.1.2.3.3 pH dependence

The Rv3645 cyclase works optimally at pH 7.5. To see if the chimeric cyclase had the same pH optimum we tested activity from pH 4 to 10. Buffers used: Acetate, pH-4.5; Pyridine, pH-4.7,5.4; MES/Tris, pH- 5.5,6.5; MOPS/Tris, pH- 6.5,7; Tris/HCl, pH-7,7.5,8,8.5; HEPES, pH-8,8.5; Glycine, pH-8.5,9 and Glycine/NaOH, pH-9,10.
The optimal pH was 7.5 (Fig. 4-7).

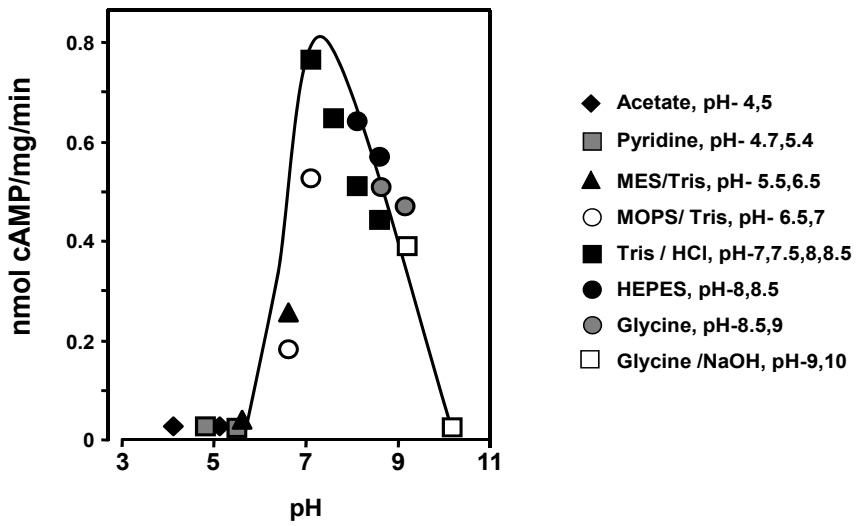

Figure 4-7. The pH dependence of $NpH_{1\text{-}mut5}$ tandem. Assay conditions: 200 µM ATP, 20 µg of protein, 37ºC, 10 minutes, n=2.

4.1.2.3.4 Temperature dependence.

25 µg of the protein was assayed at temperatures from 0º to 60ºC. On increasing the temperature there was a continuous increase in specific activity up to 40°C after which there was a decrease in specific activity. The temperature optimum was 37ºC (Fig. 4-8). The activation energy derived from an Arrhenius plot was 79.8 KJ/mol, i.e., identical to Rv3645 cyclase alone.

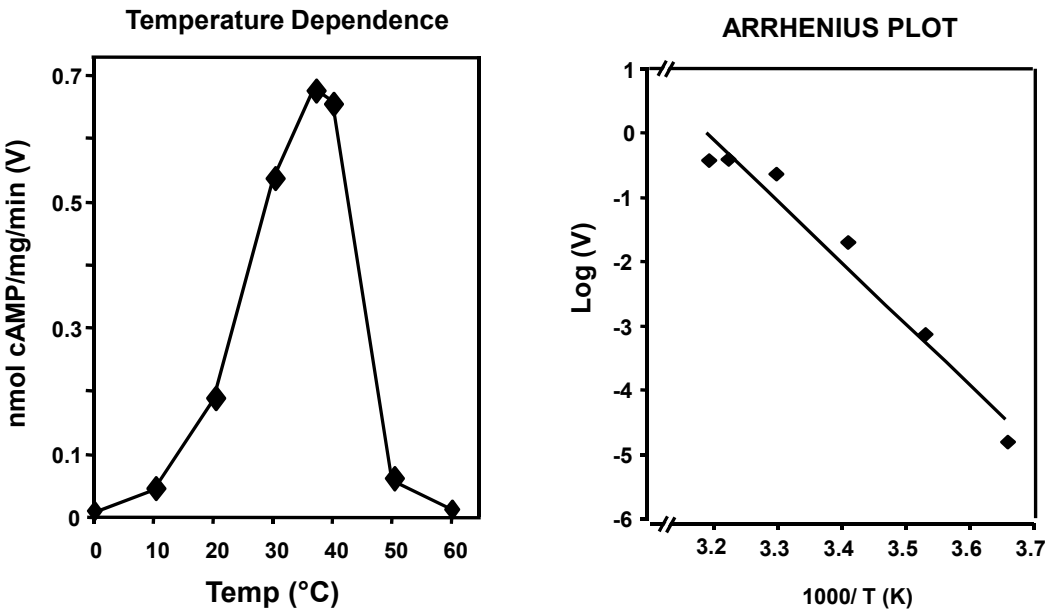

Figure 4-8. Left, temperature dependence of $NpH_{1\text{-}mut5}$ tandem. Right. Arrhenius plot. Activation energy is 79.8 KJ/mol. Assay conditions: 200 µM ATP, 0.1 mM Tris/HCl pH 7.5, 10 min, n=2 and 25 µg of protein.

4.1.2.3.5 ATP dependence

With the increase in the ATP concentration, there was hyperbolic increase in specific activity giving an ideal Michaelis-Menten curve. ATP concentrations from 20 to 2000 µM with and without serine were tested (Fig. 4-9). Lineweaver-Burk plot showed that in the absence and presence of serine the chimera had a Vmax of 3.4 and 3.8 nmol/mg/min, respectively; while the Km was 649 and 1428 µM respectively (Fig. 4-9). The Hill coefficient as calculated from the Hill plot was 0.89 (R^2 = 0.99) for the reaction without serine and 0.85 (R^2 = 0.98) for the reaction with serine. Since the chimera had a Hill coefficient slightly lower than one, it can be classified as non-cooperative.

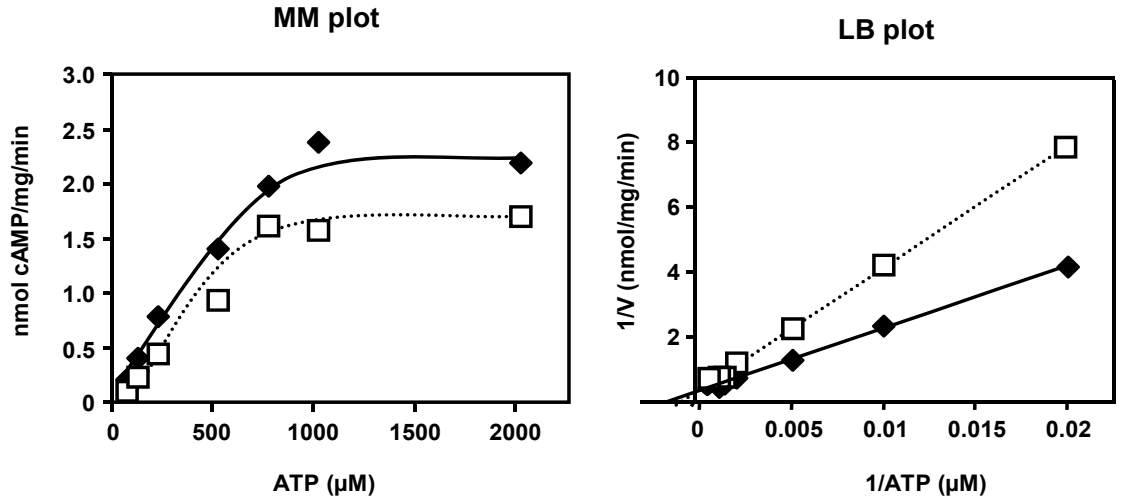

Figure 4-9. The substrate kinetics of $NpH_{1\text{-}mut5}$ tandem. Left, Michaelis-Menten plot (MM plot); Right, Lineweaver-Burk plot (LB plot); without serine (filled diamonds) and with 1mM serine (open squares). Assay conditions: 0.1 mM Tris/HCl pH 7.5, 10 min, 37°C, n=4.

4.2 Comparison of tandem HAMP domains

The $NpHAMP_1$, Tsr, and Af1503 are canonical HAMPs and may be replaced without loss of function [42, 62, 68, 69]. To check if Tsr and Af1503 could couple to $NpHAMP_2$, chimeric tandems with Tsr or Af1503 as $HAMP_1$ and $NpHAMP_2$ were generated.

4.2.1 Tsr HAMP-$NpHAMP_2$ tandem

$HAMP_{Tsr}$ was tested as a monomer and in tandem with $NpHAMP_2$ in the chimera. The $HAMP_{Tsr}$ chimera was inhibited by serine as reported earlier [68, 69]. Basal activity was 45 ±

5 nmol/mg/min and was inhibited by 3 mM serine by about 75% (n=4; IC_{50}=10 µM; *, p<0.001; Fig. 4-10). The $HAMP_{Tsr}$ in tandem to $NpHAMP_2$ was unaffected by serine (Fig. 4-10). Basal activity was 1.4 ± 0.2 nmol/mg/min. 1 mM aspartate no effect on both chimeras (Fig. 4-10).

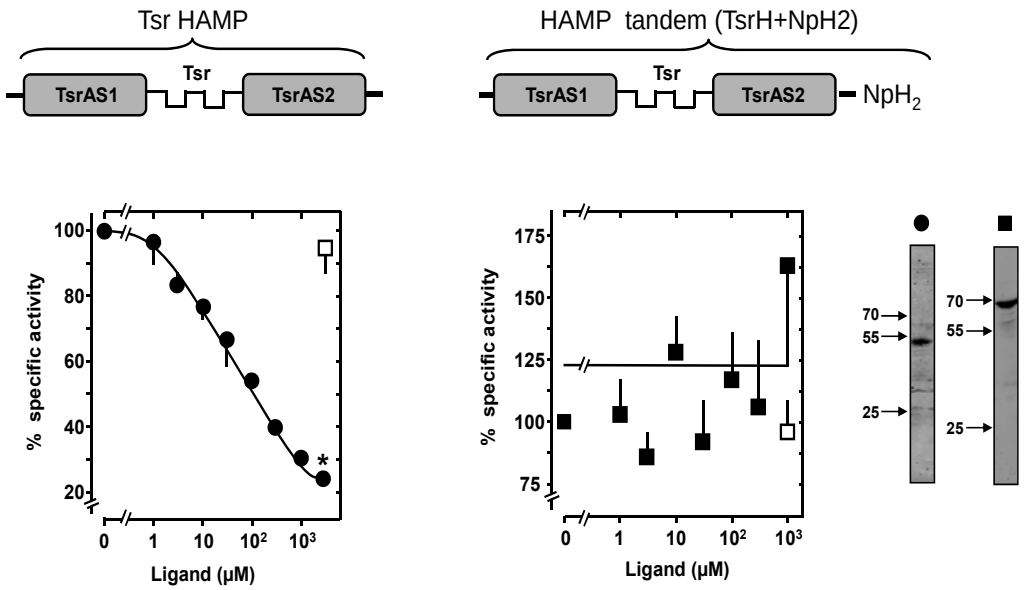

Figure 4-10. Left, response of the Tsr HAMP monomer and in tandem with $NpHAMP_2$ (middle). Serine inhibited $HAMP_{Tsr}$ monomer significantly (*, p<0.001, filled circles) but not in tandem (filled squares). Aspartate had no effect on the chimeras (open squares). Right, Western blots of 5 µg protein/lane. (n=4).

4.2.2 Af1503 HAMP - $NpHAMP_2$ tandem

In a similar approach Af1503 HAMP, another archaeal HAMP, was coupled to $NpHAMP_2$ to examine whether they functionally couple. Two HAMP tandem chimeras with Af1503 and $NpHAMP_2$ were generated: $HAMP_{Af1503mut2}$ in tandem to $NpHAMP_2$ and $HAMP_{Af1503}$ in tandem with $NpHAMP_2$. Two targeted point mutations in Af1503 AS1 were required and sufficient for signal transduction ($Af1503_{mut2}$, [68]). The $Af1503_{mut2}$ in tandem with $NpHAMP_2$ had a basal activity of 4.2 ± 0.3 nmol/mg/min. It was activated to about 22% at 1mM serine. (EC_{50}=300; n=4; *, p<0.05; Fig. 4-11). This was surprising as there was a reversal of signal sign in tandem when compared to the output from the mono HAMP [68]. The $HAMP_{Af1503}$ in tandem with $NpHAMP_2$ was unaffected by serine although it was active (basal activity = 2.4 ± 0.1 nmol/mg/min, Fig. 4-11). This was not surprising as Af1503 HAMP alone does not transduce a serine signal [43].

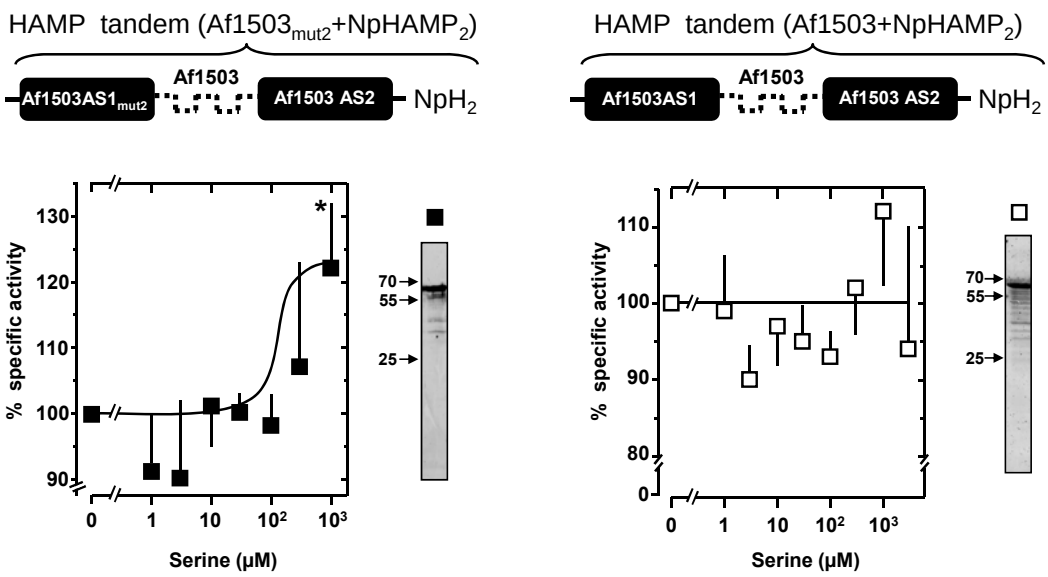

Figure 4-11. Left, serine activates the chimera with $Af1503_{mut2}$ in tandem with $NpHAMP_2$ (*, $p<0.05$, filled squares) but not the chimera with Af1503 in tandem with $NpHAMP_2$ (open squares), right. Western blots are shown next to the respective chimera. (n=4-6).

The $Af1503_{mut2}$ HAMP monomer and in tandem with $NpHAMP_2$ had reversed the signal sign from inhibition to activation by serine. This was opposite compared to the inhibitory output by the $NpH_{1\text{-}mut5}$ tandem. These data indicate that in $HAMP_1$ structural components exist which may determine the signal sign. To analyze the structural mechanisms in $HAMP_1$ influencing the signal sign a series of tandem HAMP combinations was generated.

4.2.3 $HAMP_1$ chimeras $HAMP_{Tsr}$-$NpHAMP_1$.

In order to find out why $HAMP_{Tsr}$ was unable to couple whereas the $Af1503_{mut2}$ was functional in the chimera, a chimeric $HAMP_1$ was generated by combining its different structural components. A HAMP domain consists of three structural elements: amphipathic helix 1 (AS1), a flexible connector and amphipathic helix 2 (AS2). Five chimeric tandems with various combinations were generated (Table 4-3).

The first tandem chimera had the connector exchanged with that of Tsr but the $AS1_{1\text{-}mut5}$ and AS2 was retained from $NpHAMP_1$. This chimera was unaffected by serine. The basal activity was lower compared to the parent $NpHAMP_{1\text{-}mut5}$ tandem chimera (Table 4-3). In the second chimera $AS1_{1\text{-}mut5}$ of $NpHAMP_1$ was replaced with Tsr AS1. This chimera, $AS1_{1\text{-}Tsr}/NpH_1$ tandem surprisingly was activated by serine to 129% at 1mM serine (EC_{50}=10 µM; n=4; *, $p<0.05$). Compared to the $NpH_{1\text{-}mut5}$ tandem this tandem had an opposite signal to serine. In the third chimeric tandem the AS1 and connector were exchanged with that of Tsr (Table 4-

3). This chimera was inactive although it was well expressed. In the fourth chimera AS2 of $NpH_{1\text{-}mut5}$ was exchanged with that of Tsr. This chimera was well expressed but inactive. The fifth chimeric tandem had the AS1 and AS2 from Tsr and the connector of $NpHAMP_1$. This chimera was active but was unregulated.

Chimeric $HAMP_1$ in NpHAMP tandem		Basal activity (nmol cAMP/mg/min)	1mM serine	EC_{50} µM
$NpAS1_{1\text{-}mut5}$ – Tsr – $NpAS2_1$		0.2 ± 0.02	n.r.	
TsrAS1 – Np – $NpAS2_1$		2.5 ± 0.5	+129%*	10
TsrAS1 – Tsr – $NpAS2_1$		inactive		
$NpAS1_{1\text{-}mut5}$ – Np – TsrAS2		inactive		
TsrAS1 – Np – TsrAS2		0.3 ± 0.02	n.r.	

Table 4-3. The model representation of the chimeric $HAMP_1$ along with its basal activity and response to serine. The $AS1_{1\text{-}Tsr}/NpH_1$ tandem was significantly activated by serine (*, $p<0.05$). (n=4-6).

4.2.4 $HAMP_1$ chimeras $HAMP_{Af1503}$ -$NpHAMP_1$

Swapping of $AS1_1$ in NpHAMP tandem had a profound effect on the signal sign (Table 4-3). To check if $Af1503_{mut2}$ would have the same effect on the signal sign two chimeric $HAMP_1$ tandems with combinations of $Af1503_{mut2}$ and $NpH_{1\text{-}mut5}$ tandem were generated (Table 4-4). The first chimera had the $HAMP_1$ AS2 exchanged to that of Af1503 (Table 4-4). This chimera was inactive. The expression of the protein was confirmed by Western blotting. In the second chimera AS1 was exchanged with that of Af1503 $AS1_{mut2}$ (Table 4-4). The Af1503 $AS1_{mut2}$ was used as the unmutated Af1503 was non-functional [68]. This chimeric tandem, although active and expressed, was unaffected by serine.

Chimeric $HAMP_1$ in NpHAMP tandem		Basal activity (nmol cAMP/mg/min)	1mM serine
$NpAS1_{1\text{-}mut5}$ — Np — Af1503 AS2		inactive	
Af1503$AS1_{mut2}$ — Np — $NpAS2_1$		1.7 ± 0.1	n.r.

Table 4-4. Model representation of the chimeric $HAMP_1$ between Af1503 and $NpHAMP_1$ with the respective Western blot, basal activity and response to serine. (n=4).

Replacement of the complete $HAMP_1$ with $Af1503_{mut2}$ was functional (Fig. 4-11) whereas none of the structural combination chimeras worked (Table 4-4). It has been reported that the Af1503 HAMP forms salt bridges between the α-helices and the connector to stabilize the HAMP [68]. The inability of the Af1503 $AS1_{mut2}$ or AS2 to functionally combine with $NpHAMP_1$ may be due to rupture of the salt bridges.

4.2.5 Effect of $HAMP_1$ AS1 on signal sign.

4.2.5.1 Effect of Tsr AS1 on NpHAMP tandem.

The chimeric tandem with AS1 of $NpHAMP_1$ replaced by the corresponding α-helix from $HAMP_{Tsr}$ in tandem with $NpHAMP_2$ was activated by serine. The chimera with the $AS1_{1\text{-}Tsr}/NpH_1$ monomer was significantly inhibited by serine by 47% (IC_{50}=10 μM; n=6; †, $p<0.001$). Basal activity was 2.5 ± 0.2 nmol/mg/min. This finding emphasized the importance of $AS1_1$ for signaling as already apparent from the above experiments with $NpHAMP_{1\text{-}mut5}$ (Fig. 4-5). $AS1_{1\text{-}Tsr}/NpH_1$ in tandem with $NpHAMP_2$ transduced an activating serine signal to the AC output domain (Table 4-3). Serine sensitivity was identical for the HAMP monomer and HAMP tandem constructs (EC_{50}/IC_{50} = 10μM). The inversion of the signal sign observed in the tandem HAMP construct was in agreement with the earlier proposal based on HAMP rotation in signal transduction [42, 48]. Yet, the data were in contrast to the data with the comparable $NpHAMP_{1\text{-}mut5}$ constructs reported above. According to the gearbox model the sign of the output signal should flip in a poly-HAMP unit with each additional HAMP domain because $AS2_1$ and $AS1_2$ are predicted to rotate in the same direction. The above experiments demonstrated that the sign of the output signal in HAMP tandems appeared to be determined by peculiar properties of $HAMP_1$ as $NpHAMP_2$ was identical in all chimeras.

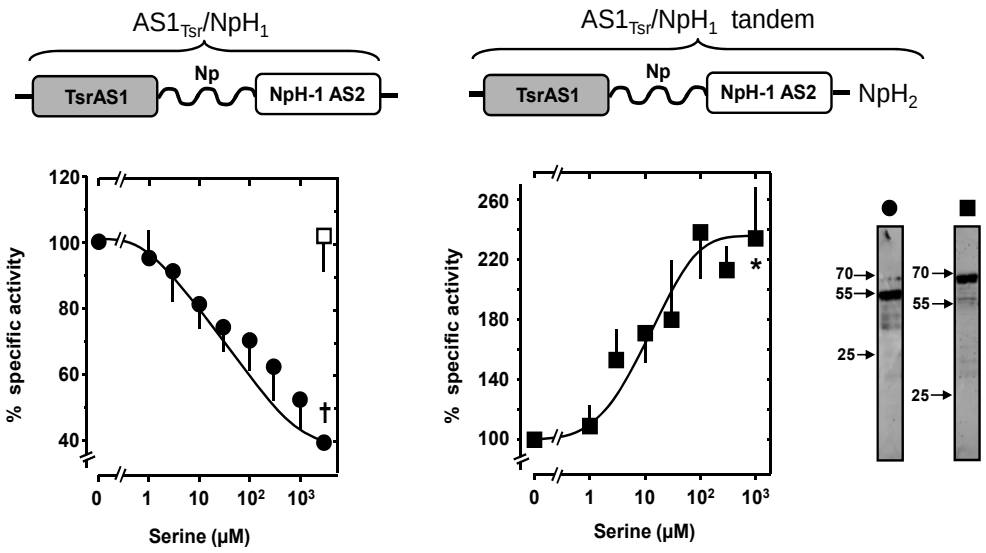

Figure 4-12. Serine had a significant effect on the $AS1_{1\text{-}Tsr}/NpHAMP_1$ monomer (†, p<0.001, filled circles) and in tandem with $NpHAMP_2$ (*, p<0.05, filled squares). Aspartate (open squares) had no effect on both proteins. Right, Western blots (5 µg protein/lane) indicated no proteolysis. (n=4-6).

4.2.5.2 Effect of varied ligands on $AS1_{1\text{-}Tsr}/NpHAMP_1$ tandem HAMP

The tandem constructs with either $NpHAMP_{1\text{-}mut5}$ or $AS1_{1\text{-}Tsr}/NpH_1$ in the first HAMP domain transduced the same serine signal from Tsr to an invariant C-terminal AC output reporter, yet with opposite outcomes. An opposite response to the same ligand would imply two different conformations of the HAMP tandems as the input sensor and the output domain remain the same. Tsr mediates attractant and repellant responses to different stimuli. The ligand serine is an attractant whereas sodium benzoate, leucine, and indole are reported to be repellants [11, 86, 87] . To check whether the exchange of ligands would then reverse the sign of signal again, we checked the effect of these ligands on the sensitivity of $AS1_{1\text{-}Tsr}/NpHAMP_1$ tandem (Fig. 4-13). Basal activity of 2.5 ± 0.2 nmol/mg/min was set as 100 % for better comparison. L-serine, an attractant of MCP Tsr, activates the adenylyl cyclase. To check the specificity of the response aspartate was tested at the highest concentration of L-serine. Aspartate has no effect on the cyclase. The response to L-serine was further verified by checking the response to D-serine. D-serine at 300 and 3000 µM did not have a significant effect on the chimera.

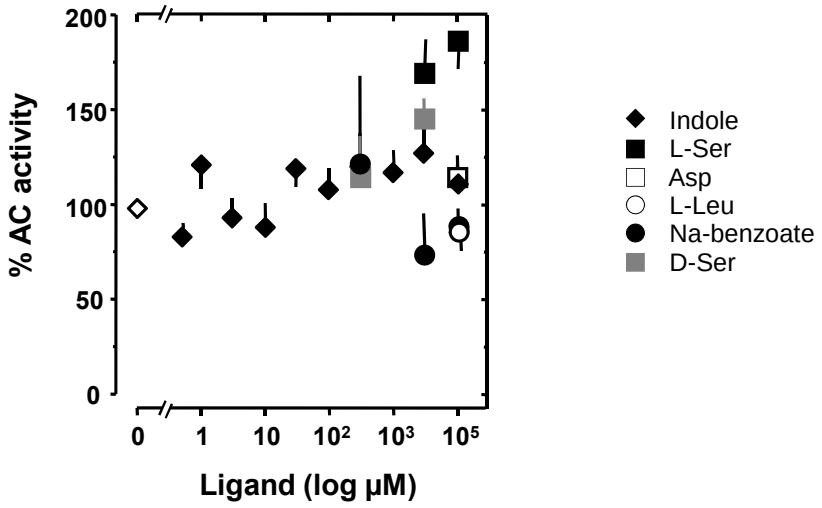

Figure 4-13. The response of $AS1_{1\text{-}Tsr}$/$NpHAMP_1$ tandem chimera to various ligands. (n=4).

Next the repellants were tested. L-Leucine at millimolar concenrations was reported to have an effect on the Tsr sensor [86, 88]. The ligand had no effect on the chimeric cyclase. Similarly sodium benzoate was proposed to have an effect on the Tsr sensor at higher concentrations [86]. Benzoate also had no significant effect. Indole has been reported to have a strong effect on the Tsr [86, 87]. But on the chimeric cyclase, indole also had no effect.
It is possible that all these ligands do not act directly on the sensor but have either a binding protein or cause changes in membrane fluidity. Since only the crude membrane fractions are used in the assays the inability of the ligands to affect the chimera might be due to this. Some ligands are reported to be effective only at millimolar concentrations which are questionable.

4.2.5.3 Effect of Tar AS1 on NpHAMP tandem

Tar and Tsr HAMP domains are placed in the same canonical group yet cannot be swapped without loss of function [42, 69]. The Tar HAMP was able to functionally couple to Tsr sensor and Rv3645 [69]. So, to check if the Tar HAMP had a similar effect on signal sign as the Tsr HAMP the AS1 of $NpHAMP_1$ was replaced with the AS1 of Tar.
The $AS1_{1\text{-}Tar}$/NpH_1 monomer was inhibited by serine by 52% (IC_{50}= 10 µM; n=4; *, $p<0.05$). Basal activity was 12.4 ± 6.7 nmol/mg/min (Fig. 4-14). Aspartate at 3 mM concentration did not have an effect on the monomer (Fig. 4-14). $AS1_{1\text{-}Tar}$/NpH_1 in tandem with $NpHAMP_2$ was unresponsive to serine. Basal activity was 0.6 ± 0.1 nmol/mg/min (Fig. 4-14). This was surprising as in a mono HAMP the chimera was functional.

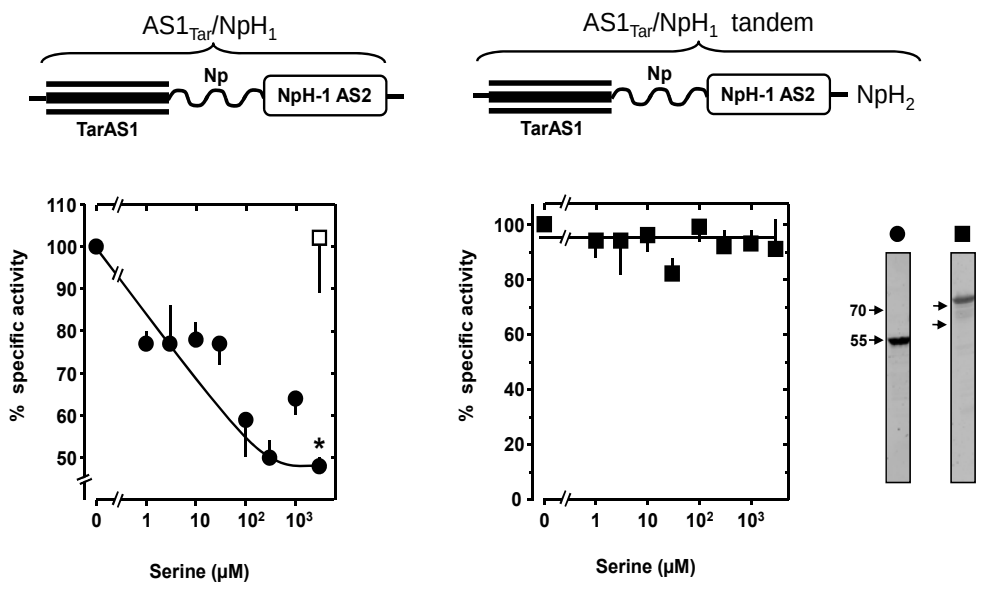

Figure 4-14. Left, serine inhibited $AS1_{1\text{-}Tar}/NpH_1$ monomer (*, p<0.05, filled circles) but had no effect on the tandem chimera (filled squares). 3 mM aspartate (open square) has no effect on the monomer. Right, Western blots of 5 µg protein/lane. (n=4).

4.2.5.4 Effect of Tar on $AS1_{1\text{-}Tar}/NpH_1$ tandem

The Tar HAMP coupled to the Rv3645 cyclase only with the Tsr receptor but not with the Tar receptor [69]. Also the $AS1_{1\text{-}Tar}/NpHAMP_1$ tandem did not couple functionally with the Tsr receptor (Fig. 4-14, filled squares). The HAMP chimeras were attached to the Tar receptor to check whether with the exchange of the signal input the tandem would become functional. Both the monomer and the tandem was unaffected by serine although active and well expressed (Table 4-5).

Chimeric $HAMP_1$	Basal activity (nmol cAMP/mg/min)	1mM serine	
Tar — TarAS1 — Np — $NpAS2_1$	1.5 ± 0.3	n.r.	
Tar — TarAS1 — Np — $NpAS2_1$ — NpH_2	2.8 ± 0.1	n.r.	

Table 4-5. Model representation of the chimeric $HAMP_1$ is indicated along with its Western blot (5 µg protein/lane), basal activity and serine response. (n=4-6).

Since the chimeras with the Tar receptor did not work as well it can be assumed that somehow the signal input from the Tar receptor entity did not couple properly to the NpHAMP tandem.

4.3 $AS1_1$ and signal sign

The tandem constructs with either $NpHAMP_{1\text{-}mut5}$ or $AS1_{1\text{-}Tsr}/NpH_1$ as $HAMP_1$ transduced the same serine signal from Tsr to an invariant C-terminal AC output reporter, yet with opposite outcome. The differences in the sign of signal output were independent of $NpHAMP_2$ which together with its adjoining linker was never changed in the HAMP tandem. Obviously the sign of the output signal was dependent on the structural fine-print of AS1 in $NpHAMP_1$, i.e. the α-helix which directly receives the signal from the second transmembrane span of the Tsr receptor. A comparison of $NpAS1_{1\text{-}mut5}$ and $AS1_{1\text{-}Tsr}$ sequences showed that 7/19 residues are identical. In these chimeras the inserted HAMP domains included two N-terminal residues which were a part of the initial NMR structure of the Af1503 HAMP domain and now they are debated to be part of a poorly delimited sequence of five residues termed control cable [43, 46, 81, 89]. It conjoins the exit of the last transmembrane span of the Tsr sensor domain, probably Trp211 or Phe212, with the actual start of the four helix bundle coiled coil of the HAMP domain [43].

What then are the parameters of $NpAS1_1$ in a HAMP tandem which affect the sign of the signal output? In an attempt to identify by exhaustive mutational analysis the most significant residues in the $AS1_1$ of the tandems a total of 48 mutations were generated in both $AS1_{1\text{-}Tsr}$ tandem HAMP and $NpH_{1\text{-}mut5}$ tandem. The mutational analysis identified 5 positions that were responsible for the control of the signal sign. The mutants are classified as critical (inversion of sign of signal), insignificant (same sign of signal), significant (no serine response) and lethal (no AC activity).

4.3.1 Critical mutations

Analysis of a total of 26 $AS1_{1\text{-}Tsr}$ and 22 $NpHAMP_{1\text{-}mut5}$ tandem mutants in all former and present constructs indicated that the sign of the signal output is determined by five positions; A216/S217/M222/I232/D234 in $AS1_{1\text{-}Tsr}$ tandem and G84/D85/I90/M100/G102 in $NpHAMP_{1\text{-}mut5}$ tandem respectively. The amino acids in these positions were swapped between the two tandems and two mutants were generated. The A216G/S217D/M222I/I232M/G234D mutant of $AS1_{1\text{-}Tsr}$ tandem HAMP was inhibited 42% by serine (IC_{50}= 60 µM; n=6; *, $p<0.05$; Fig. 4-16). Basal activity of the chimera was 2.3 ± 0.4 nmol/mg/min. Compared to the parent $AS1_{1\text{-}Tsr}/NpH_1$ tandem chimera the sign of the signal was inversed (Fig. 4-12). When the identical positions were mutated in the $NpH_{1\text{-}mut5}$

tandem, the G84A/D85S/I90M/M100I/D102G mutant was activated by serine by 42% (EC_{50}= 10µM; n=6; *, p<0.05, Fig. 4-16). Basal activity of the chimera was 0.6 ± 0.4 nmol/mg/min. Basal activities in both constructs were comparable to their respective templates. Yet, the sign of the output signal was inversed in both constructs compared to the appropriate parent chimeras (Fig. 4-5, 4-12). It can be concluded that the sign of signal output transduced by a HAMP tandem can be changed simply by manipulation of certain positions in the first α-helix of the first HAMP of the tandem.

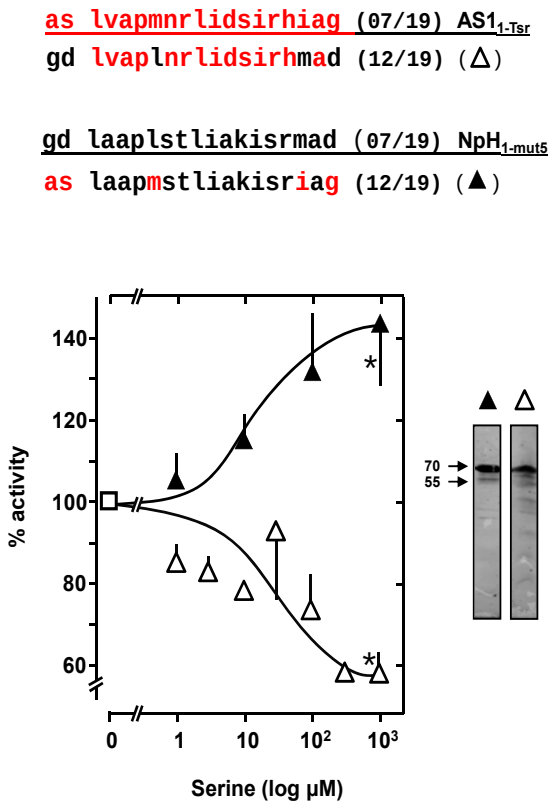

Figure 4-16. Five amino acid mutations inverse the sign of signal output in the tandem. Serine inhibits the $AS1_{1\text{-}Tsr}/NpH_1$ tandem mutant by 42% (*, p<0.05, open triangles) and activates the $NpHAMP_{1\text{-}mut5}$ tandem by 42% (*, p<0.05, filled triangles). Right, Western blot of 5 µg protein/lane. (n=6).

4.3.1.1 Activation vs. inhibition as signal sign

G234 and D102 are located at the end of the AS1 in $AS1_{1\text{-}Tsr}$ tandem and $NpH_{1\text{-}mut5}$ tandem, respectively. It has been reported in previous studies that these residues are not important/critical for the function of the domain [46, 90]. This position was also mutated in the 5 mutant tandem chimeras which inversed the sign of signal again (Fig. 4-16). The amino acids in these positions A216/S217/M222/I232 in $AS1_{1\text{-}Tsr}/NpH_1$ tandem and G84/D85/I90/M100 in $NpHAMP_{1\text{-}mut5}$ tandem were swapped between the two tandems and

two mutants were generated. The A216G/S217D/M222I/I232M mutant of $AS1_{1\text{-}Tsr}/NpH_1$ tandem HAMP was inhibited to about 20% by serine (IC_{50}=300 µM; n=12; *, $p<0.05$; Fig. 4-16). Compared to the parent tandem chimera, $AS1_{1\text{-}Tsr}/NpH_1$ tandem the sign of the signal was inversed again (Fig. 4-12). When the identical positions, G84A/D85S/I90M/M100I were mutated in the $NpH_{1\text{-}mut5}$ tandem, serine had no effect (Fig. 4-16). Aspartate has no effect on both the chimeras (Fig. 4-16).

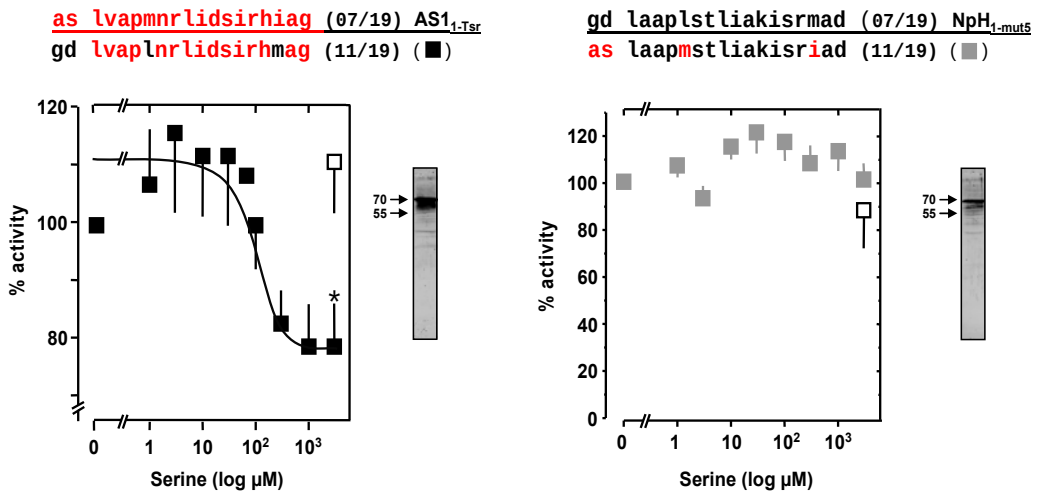

Figure 4-16. Four mutations invert the sign of signal output in $AS1_{1\text{-}Tsr}/NpH_1$ tandem. Serine inhibited the cyclase (*, $p<0.05$, black squares) while in $NpHAMP_{1\text{-}mut5}$ tandem with the same mutations, serine had no effect on cyclase activity (grey squares). Aspartate did not affect both chimeras (open squares). The Western blots are in the right of the respective chimeras. (n=4-12).

For inhibition, it is enough to have a ``ASLM`` motif in AS1, but for activation, it is necessary to have a ``GDMIG`` motif. Glycine had a significant effect in maintaining the signal. This is contrary to the effect of this position on mono-HAMPs. It's possible that in tandem prerequisites of HAMP domain differ from those of the mono-HAMP.

4.3.2 Insignificant mutants

4.3.2.1 Insignificant mutants of $AS1_{1\text{-}Tsr}/NpH_1$ tandem HAMP

Five mutations in $AS1_1$ of the $AS1_{1\text{-}Tsr}/NpH_1$ tandem had no effect on the sign of the output signal, i.e., chimeras were activated by serine.

aslvapmnrlidsirhiag	
216 218 220 222 224 226 228 230 232 234	
TsrAS1 analysis	
(1) as lAapmnrlidsirhiag	(10)
(2) as lvapmnrlidsiShiag	(10)
(3) as lvapmnrlidsisRiag	(10)
(4) as lvapmnrlidKirhiaD	(11)
(5) as lvapmnrliAKiShiag	(12)

Table 4-6. Above, Tsr AS1 sequence with the numbering below. Bottom, $AS1_1$ sequence of functionally insignificant mutants of $AS1_{1\text{-}Tsr/}NpH_1$ tandem chimera. The number of identical positions between the two tandems is indicated in brackets after the sequence.

The single mutant V219A was activated to about 30% at 1mM serine (EC_{50}=300 µM; n=4; *, p<0.05, Fig. 4-17/Table 4-6). Basal activity was 2.2 ± 0.2 nmol cAMP/mg/min. The single mutant R230S was activated to about 70% at 1mM serine (EC_{50}=200 µM; n=4; *, p<0.05; Fig. 4-17/Table 4-6). Basal activity, 0.2 ± 0.02 nmol cAMP/mg/min, was lower compared to the V219A mutant. The H231R mutant was activated to 85% at 1mM serine (EC_{50}=40 µM; n=4; *, p<0.05; Fig. 4-17/Table 4-6). Basal activity was 2.4 ± 0.2 nmol cAMP/mg/min. The double mutant S228K/G234D was activated to 68% by 1mM serine (EC_{50}=150 µM; n=4; *, p<0.05; Fig. 4-17/Table 4-6). Basal activity was 1.1 ± 0.1 nmol cAMP/mg/min. The triple mutant D227A/S228K/R230S was activated to about 95% at 1mM serine (EC_{50}=300 µM; n=4; *, p<0.05; Fig. 4-17/Table 4-6). Basal activity was 0.4 ± 0.02 nmol cAMP/mg/min. In all mutants aspartate had no effect on the cyclase activity (Fig. 4-17).

Two of the constructs which had the mutation R230S had a lower activity when compared to the others (constructs 2 and 5 in 4-17/Table 4-6). The EC_{50} concentrations and the percentage of activation followed no specific pattern.

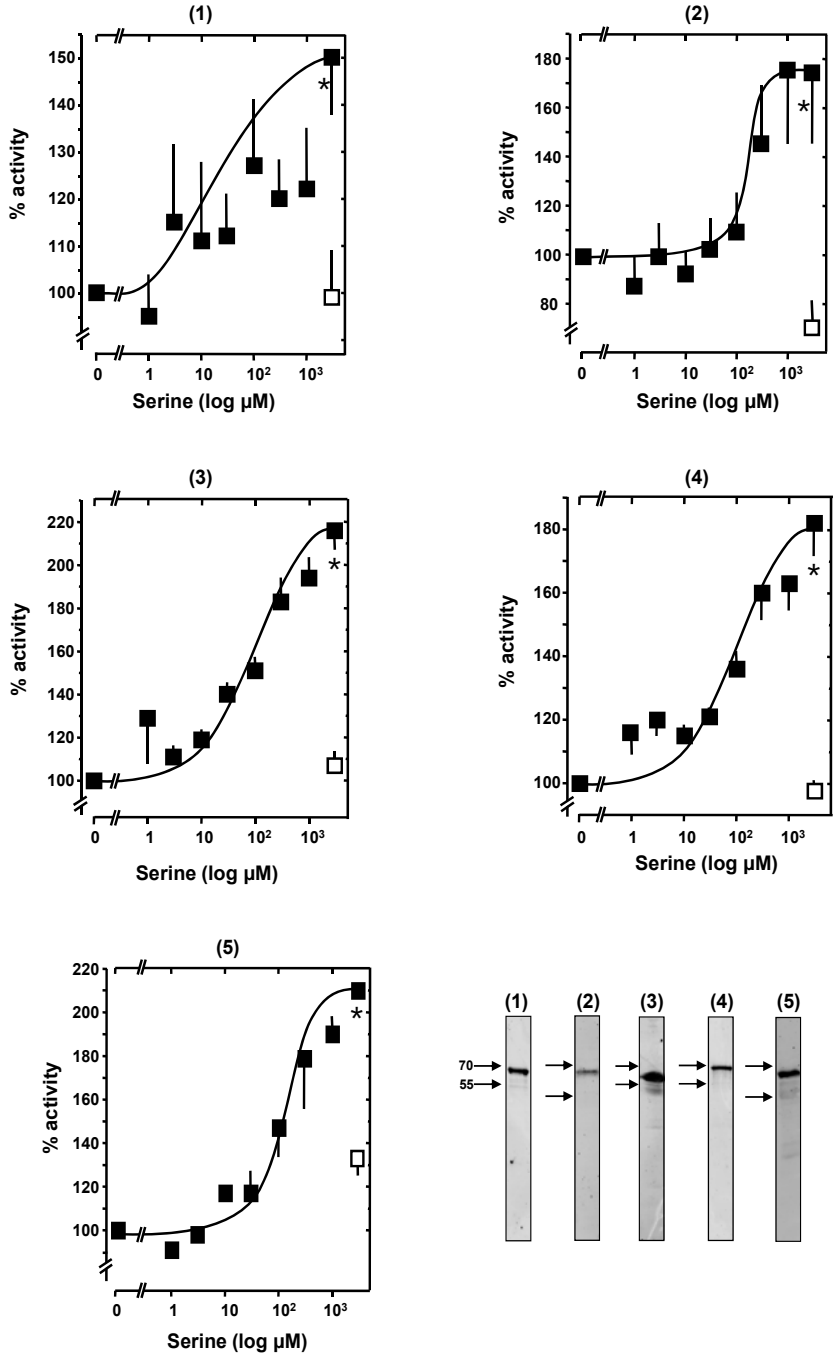

Figure 4-17. Serine activated all mutants to different extents (*, p<0.05). Aspartate had no effect (open squares). Western blots on the right of respective chimera showed no proteolysis. (n=4).

4.3.2.2 Functionally insignificant mutants of $NpH_{1\text{-}mut5}$ tandem

In the $NpH_{1\text{-}mut5}$ tandem three mutants had no significant effect on the sign of the signal output (Table 4-7).

```
gdLaaPlstlIakIsrmAd
  86  89    94  97  101
```

$NpAS1_{1mut5}$ analysis
(1) gd lVaplstliakisrmaG (11)
(2) gd lVaplNRliDSisrmad (14)
(3) gS laaplstliakisrmad (10)

Table 4-7. Above, $AS1_{mut5}$ sequence of $NpH_{1\text{-}mut5}$ tandem with its respective numbering. Bottom, $AS1_1$ sequence of functionally insignificant mutants of $NpH_{1\text{-}mut5}$ tandem chimera. The number of identical positions between the two tandems is indicated in brackets after the sequence.

The first chimera a A87V/D102G double mutant was inhibited by serine by 44% at 1mM (IC_{50}=30 µM; n=4; *, $p<0.05$; Table 4-7/Fig. 4-18). Basal activity was 1.2 ± 0.2 nmol cAMP/mg/min. The second chimera A87V/S91N/T92R/A95D/K96S mutant was inhibited by serine by 50% at 1mM (IC_{50}=10 µM; n=4; *, $p<0.05$; Table 4-7/Fig. 4-18). Basal activity was 1.3 ± 0.1 nmol cAMP/mg/min.

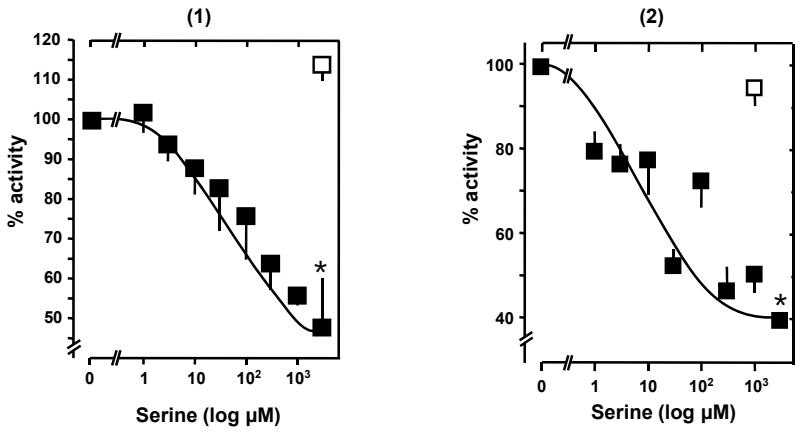

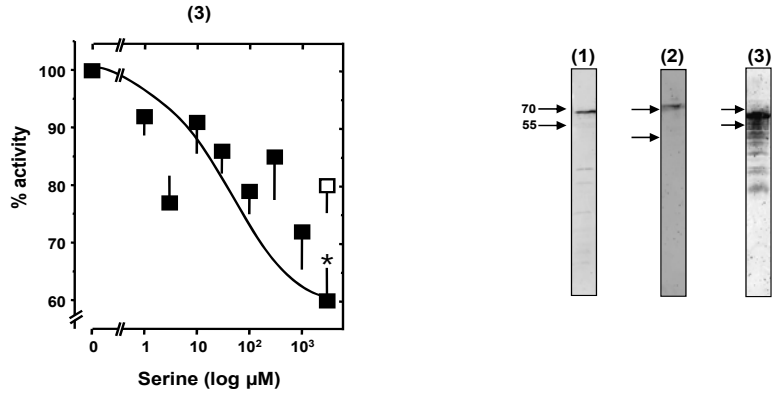

Figure 4-18. Serine significantly inhibited the mutants to different extents (*, p<0.05). Aspartate had no effect on the activity of the mutants (open squares). Western blots of the mutants showed absence of proteolysis. (n=4).

The third mutant, D85S chimera was inhibited by serine by 33% at 1mM (IC_{50}= 90 µM; n=4; *, p<0.05; Table 4-7/Fig. 4-18). Basal activity was 13 ± 0.8 nmol cAMP/mg/min. This mutant had a 14 fold higher basal activity compared to the $NpH_{1\text{-}mut5}$ tandem. In none of the mutant chimeras, aspartate had an effect on cyclase activity.

The data from insignificant mutations from $AS1_{1\text{-}Tsr/}NpH_1$ and $NpHAMP_{1\text{-}mut5}$ tandem mutants point out these mutations do not strongly impact potential inter-helical bonds and/or affect structural orientations of $AS1_1$ in the tandem.

4.3.3 Significant mutations

4.3.3.1 Significant mutants of the $AS1_{1\text{-}Tsr/}NpH_1$ tandem HAMP

In $AS1_{1\text{-}Tsr}$ tandem HAMP a total of 15 mutants were generated involving 11 positions (A216/S217/V219/M222/N223/R224/D227/S228/R230/I232/G234). Basal activities ranged from 5.4 to 0.3 nmol/mg/min. All proteins were well expressed as visualized by Western blotting (Table 4-8).

Most of the mutations which involved the positions D227, S228 and R230 resulted in loss of response to serine. The D227A substitution resulted in loss of charge at this position. S228K substitution resulted in introduction of a charged residue and the R230S resulted in loss of charge and bulkiness at this position. The stark changes in the properties at this position might be the reason for loss of functionality.

aslvapmnrlidsirhiag

216 218 220 222 224 226 228 230 232 234

TsrAS1 analysis	Basal Activity (nmol cAMP/mg/min)	
as lvapmnrliAsirhiag	1.5 ± 0.2	
as lvapmnrlidKirhiag	5.4 ± 0.3	
as lvapmnrlidsirhiaD	1.4 ± 0.1	
as lvapmnrlidKiShiag	4.1 ± 0.5	
as lvapmnrliAKirhiag	2.9 ± 0.6	
as lAapmnrlidKirhiag	0.3 ± 0.2	
as lAapmnrliAKirhiag	0.3 ± 0.03	
as lAapLnrlidsirhiaD	0.7 ± 0.2	
as lAapmnrliAKiShiag	0.4 ± 0.1	
as lAapmSTliAKiShiag	1.0 ± 0.1	
Gs lvapmnrlidsirhiag	2.5 ± 0.7	
Gs lvapLnrlidsirhMag	2.3 ± 0.2	
aD lvapLnrlidsirhMag	3.2 ± 0.4	
as lvapLnrlidsirhMag	3.9 ± 0.7	
GD lvapLnrlidsirhiag	0.3 ± 0.03	

Table 4-8. Above, sequence of the Tsr AS1 with its respective numbering. Below, mutations in the $AS1_{1\text{-}Tsr}$/NpH_1 tandem that resulted in loss of regulation. Western blots of the respective mutant is at right. (n=4).

4.3.3.2 Significant mutants of $NpH_{1\text{-}mut5}$ tandem

In $NpH_{1\text{-}mut5}$ tandem, the same 11 positions as above (G84/D85/A87/I90/S91/T92/A95/K96/S98/M100/D102) were mutated and analyzed with 11 mutants. Basal activities ranged from 5.4 to 0.2 nmol/mg/min (Table 4-9). All proteins were well expressed as visualized by Western blotting.

In $NpH_{1\text{-}mut5}$ tandem the mutations of positions A95, K96 and S98 had a significant effect on the response to serine like the identical positions in the $AS1_{1\text{-}Tsr}$ tandem. The loss of functionality at these positions is thought to be due to the following reasons; the A95D substitution resulted in introduction of charge at this position. K96S substitution results in

loss of a charged residue and the S98R resulted in introduction of charge and bulkiness at this position.

gdLaaPlstlIakIsrmAd
86 89 94 97 101

NpAS1$_{1mut5}$ analysis	Basal Activity (nmol cAMP/mg/min)	
gd lVaplstliakisrmad	0.3 ± 0.1	
gd laaplstliaSisrmad	0.5 ± 0.1	
gd laaplstliakisrmaG	0.2 ± 0.1	
gd laaplstliDSisrmad	0.3 ± 0.02	
gd lVapMstliakisrmaG	0.3 ± 0.02	
gd laaplstliDSiRrmaG	2.4 ± 0.6	
gd lVaplstliDSiRrmaG	1.0 ± 0.2	
gd lVaplNRliDSiRrmaG	5.3 ± 0.1	
Ad laaplstliakisrmad	0.5 ± 0.1	
gS laapMstliakisrIad	0.5 ± 0.04	
AS laaplstliakisrmad	1.3 ± 0.1	

Table 4-9. Above, AS1$_{mut5}$ sequence of NpH$_{1\text{-}mut5}$ tandem with its respective numbering. Below, mutations in the NpH$_{1\text{-}mut5}$ tandem that resulted in loss of regulation. Western blots of the respective mutant indicate well expressed proteins. (n=4-6).

4.3.4 Lethal mutations.

These mutations completely killed the enzyme i.e., the proteins were inactive. The expressions of the proteins were confirmed by Western blotting. A total of 10 mutants, 4 of AS1$_{1\text{-}Tsr}$ tandem HAMP and 6 of NpH$_{1\text{-}mut5}$ tandem were inactive. The combination of these positions; A216,S217,V219,D227 and I232 in AS1$_{1\text{-}Tsr}$ tandem HAMP and G84,D85, I90, A95, K96, S98, R99, M100 and D102 NpH$_{1\text{-}mut5}$ tandem seemed to have a critical effect on the functional folding of the proteins.

aslvapmnrlidsirhiag

216 218 220 222 224 226 228 230 232 234

gdLaaPlstlIakIsrmAd

86 89 94 97 101

AS1$_{1\text{-}Tsr}$ tandem	NpAS1$_{1\text{-}mut5}$ tandem
aD lvapmnrlidsirhiag	gd laapMstliakisrIad
GD lvapmnrlidsirhiag	AS laapMstliakisrmad
GD lvapmnrlidsirhMag	AS laaplstliakisrIad
as lAapmnrliAsirhiag	gd laaplstliakisHmad
	gd laaplstliaSisrmaG
	gd laaplstliDSiRrmad

Table 4-10. Above, sequence of AS1 of Tsr (red) and NpH$_{1\text{-}mut5}$ (black) with their respective numbering. All mutations resulted in loss of AC activity. Western blots are shown next to the respective sequence. (n=4-6).

In both AS1$_{1\text{-}Tsr}$ tandem and NpH$_{1\text{-}mut5}$ tandem HAMP chimeras the mutation of the first two residues of the HAMP results in loss of regulation or inactivity. This indicates that the first two amino acids cannot be exchanged or mutated. The R99H mutation seems lethal only in NpH$_{1\text{-}mut5}$ tandem HAMP as mutation of the same position in AS1$_{1\text{-}Tsr}$ tandem had no effect, neither on the activity nor on the response to serine.

The mutations that make the tandem inactive seem to differ for the tandems indicating an effect of a specific amino acid rather than a position in AS1$_1$ being critical for function. Replacements at the beginning of the AS1$_1$ had a lethal effect on the AS1$_{1\text{-}Tsr}$ tandem HAMP whereas replacements at the end of AS1$_1$ seem to be more critical in NpH$_{1\text{-}mut5}$ tandem HAMP. The lethality indicates the importance of uptake of signal in the AS1$_{1\text{-}Tsr}$ tandem and the transmission of signal in the NpH$_{1\text{-}mut5}$ tandem HAMP, respectively.

4.4 Connector in NpHAMP

4.4.1 $NpHAMP_1$ connector

The connector is the least conserved element in the HAMP domain. A motif with three conserved positions ``G-x-HR1-x-x-x-HR2´ was identified by an extensive bioinformatic and mutational analysis (boxed in the Fig. 4-19, [42, 43, 90]). This motif is conserved in the $NpHAMP_1$ connector as well (Fig. 4-19). The connector has been shown to form salt bridges which help in stabilizing the HAMP domain [43, 68]. The connector in $NpHAMP_1$ is highly charged in comparison to the Tsr connector. The presence of charges in the connector raises questions on the interactions between the helices.

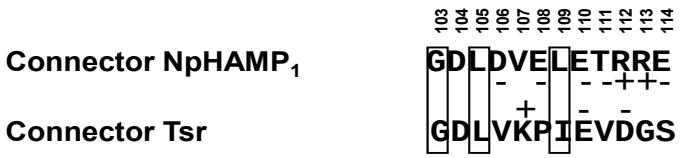

Figure 4-19. The connector of NpHAMP1 is highly charged. The boxed positions indicate the conserved motif. The numbering on top is $NpHAMP_1$.

The number of amino acids is exactly the same in $HAMP_{Tsr}$ and $NpHAMP_1$. The connector in $NpHAMP_1$ was replaced with that from Tsr in $NpH_{1\text{-}mut5}$. The connector exchange was tested as a monomer and in tandem with $NpHAMP_2$.

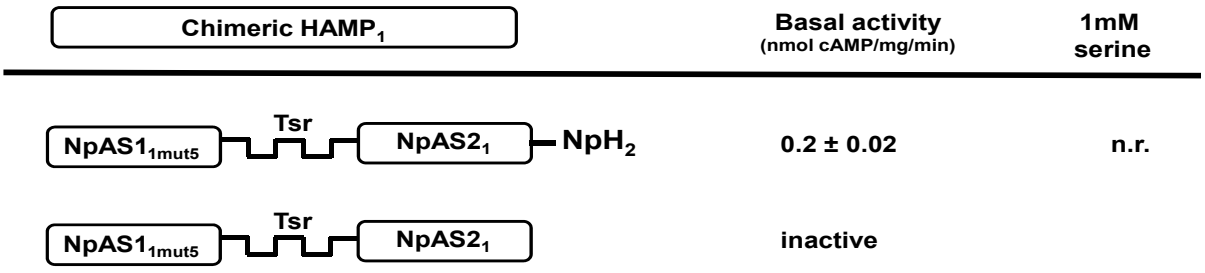

Table 4-11. Swapping the connector between $NpHAMP_1$ and Tsr resulted in loss of regulation in tandem and an inactive protein as a mono-HAMP. (n=4).

The connector exchange mutant $NpH_{1\text{-}mut5}$ monomer was inactive. The connector exchange mutant $NpH_{1\text{-}mut5}$ in tandem with $NpHAMP_2$ was unaffected by serine. The chimera was active but with a drop in activity when compared to the parent chimera, $NpH_{1\text{-}mut5}$ tandem. The charges seem to be indispensable for the functionality of the tandem.

4.4.1.1 Importance of the charges in the connector.

The $NpHAMP_1$ and $HAMP_{Tsr}$ connector differ by seven residues (D106, V107, E108, T111, R112, R113 and E114; NpH_1 numbering). To identify the connector residues necessary for a functional coupling of AS1 and -2, each residue which differed from its positional equivalent in Tsr HAMP was exchanged individually and in combination (Table 4-12).

	NpHAMP tandem H_1-connector mutants	Basal Activity (nmol cAMP/mg/min)	1mM Serine	IC_{50} µM
	---V--------	2.0 ± 0.2	n.r.	
	----K-------	1.0 ± 0.2	n.r.	
	-----P------	1.4 ± 0.3	n.r.	
	--------V---	2.4 ± 0.3	-43%*	10
	---------D--	1.7 ± 0.5	n.r.	
	----------G-	0.3 ± 0.03	n.r.	
	----------S	6.1 ± 1.2	n.r.	
	---VK-------	1.9 ± 0.2	n.r.	
	---V-P------	1.0 ± 0.1	n.r.	
	---------D-S	2.2 ± 0.2	n.r.	
	----------GS	inactive		
	---VKP------	0.5 ± 0.04	n.r.	
	---------DGS	2.2 ± 0.4	n.r.	
	--------VDGS	1.6 ± 0.2	n.r.	

Table 4-12. Mutations in the connector of $NpH_{1\text{-}mut5}$ tandem. Only the T111V mutant retained the response to serine (*, $p<0.05$). (n=4).

Of the 7 single mutants, only an unsuspicious T111V exchange ($NpHAMP_1$ numbering) was tolerated. 3mM serine inhibited the cyclase by 43 % (IC_{50}=10 µM; n=4; *, $p<0.05$). Not a single charged amino residue could be replaced by an uncharged one without loss of regulation. Because all point mutations were well expressed as membrane delimited proteins and had reasonable AC activity folding of the proteins obviously was not the problem. This was extended by a further seven connector mutants comprising double, triple and quadruple exchanges. It appeared that each charged amino acid was required for a functional interaction most probably with AS2 in NpHAMP1 which itself is highly charged (7/22 compared to 4/22 in Tsr HAMP AS2). This accumulation of charges in the connector - AS2 segment of NpHAMP1 may mirror peculiar structural and functional requirements in the hypersaline

cytoplasm of this archaeon. On the other hand, because the connector appears to preferably interact with AS2 a replacement of AS1 of $NpHAMP_1$ with that from Tsr HAMP was tolerated without detrimental structural or functional consequences.

4.4.2 $NpHAMP_2$ connector

The highly charged connector in NpHAMP2 has 13 amino acids, similar to the $HAMP_{Af1503}$ but one amino acid more compared to the $HAMP_{Tsr}$ connector. The connector in $NpHAMP_2$ was also exchanged with $HAMP_{Tsr}$ connector in $NpH_{1\text{-}mut5}$ tandem (Table 4-13).

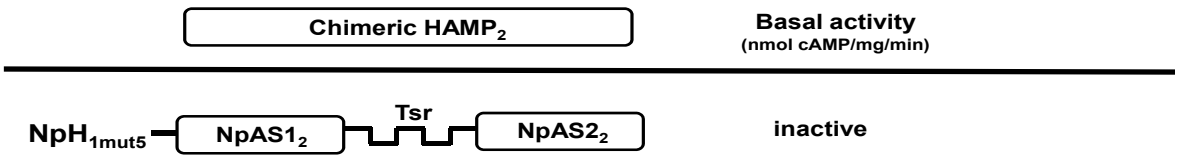

Table 4-13. Replacement of the connector in $NpHAMP_2$ results in a dead protein. (n=4).

The mutant protein was inactive (Table 4-13). The expression of the protein was visualized by Western blotting. This result was not surprising as the $HAMP_2$ connector is also highly charged. There is a possibility of inter-helical interactions in $NpHAMP_2$ as well. Also the $NpHAMP_2$ is in a different classification compared to the Tsr and $NpHAMP_1$ [42]. The inability to form functional chimeras might be also due to a lack of specific structural constraints not met by the combination of $NpHAMP_2$ and Tsr.

4.5 Inter-HAMP linker in NpHAMP tandem.

In NpHtrII the second helix of $HAMP_1$ (amphipathic sequence 2; $AS2_1$) is connected to the first amphipathic sequence of $HAMP_2$ ($AS1_2$) via a continuous α-helix of 20 amino acids. The NpHtrII and HsHtrII both have a tandem HAMP except for the size of inter-HAMP linker. Both the *N. pharaonis* (20 aa) and in *H. salinarium* (42 aa) linkers are predicted to be α-helical [91, 92].

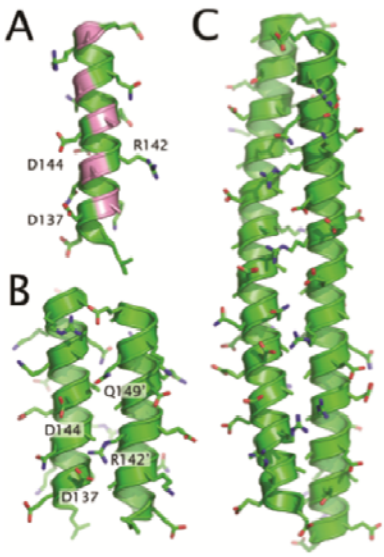

Figure 4-20. Proposed models for the inter-HAMP region from [91]. (A) The structure presented in panel A was determined by NMR [PDB entry 2RM8 [93]]. Alanines within the linker residues (135-153) are highlighted in pink. (B) Structure of a homodimer of the two NpHtrII inter-HAMP regions of residues 135-153. (C) Structure of a homodimer of the two HsHtrII inter-HAMP regions of residues 356-400.

The linker is a unique coiled coil as most of the hydrophobic core positions are occupied by alanine. Usually in a coiled coil, the core positions are occupied by larger hydrophobic residues. The presence of alanine residues in the core raises questions as to the stability and interaction between two α-helices wherein the linker forms a coiled coil with two α-helices. To understand the specificity of the linker, several deletions and insertions were done.

4.5.1 Significance of the length of the linker.

As the linker is a coiled coil continuous from the AS2 of $HAMP_1$, two heptads were identified within the sequence (Fig. 4-21). These were deleted separately and together to check their effect on the function.

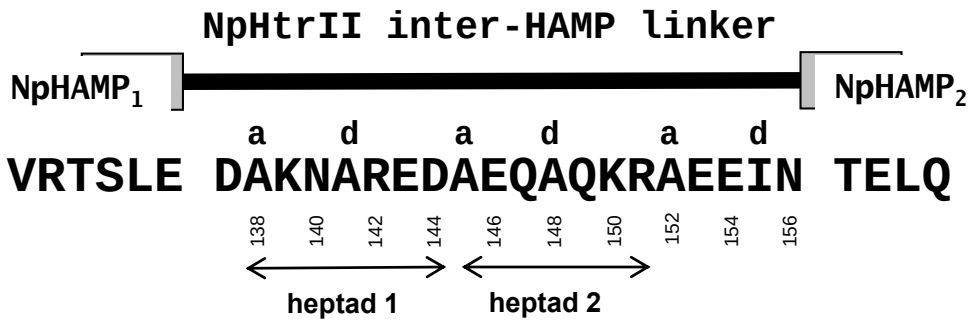

NpHAMP tandem H_1-connector mutants	Basal Activity (nmol cAMP/mg/min)	1mM Serine	IC_{50} µM
VRTSLEDAKNAREDAEQAQKRAEEINTELQ	NpH1mut5 tandem		
(1) VRTSLED-------AEQAQKRAEEINTELQ	0.2	-36%*	30
(2) VRTSLEDAKNARED-------AEEINTELQ	0.2	n.r.	
(3) VRTSLED----------AEEINTELQ	inactive		
a d a d a d a d a			

Figure 4-21. Above, NpHtrII linker with its respective numbering. The 'a' and 'd' residues in the heptad are indicated above the sequence. The two identified heptads within the linker are marked. Below, effect of the removal of the heptad residues in the linker and their response to serine. Removal of the first heptad had no effect on function ((1); *, p<0.05) but not with second heptad or the double heptad deletion. The grey columns indicate the 'a' and 'd' positions in the linker which is mostly an alanine residue. (n=4-6).

The deletion of first heptad from (AKNARED) in the linker lead to a drop in activity compared to parent chimera, $NpH_{1\text{-}mut5}$ tandem but serine significantly inhibited the cyclase (Fig. 4-21; IC_{50}=30 µM; n=4; *, p<0.05). Whereas, the deletion of second heptad (AEQAQKR) was unaffected by serine and also a drop in activity compared to parent tandem (Fig. 4-21). When both the heptads were deleted the protein was dead (Fig. 4-21).

4.5.1.1 Inter-HAMP linker addition mutations.

The linker is predicted to form a coiled coil with two α-helices [91, 92]. Since the deletion of the first heptad still retained functionality (Fig. 4-21), a series of alanine insertions were done before the beginning of the heptad A138 to check their effect on function. One to four alanine residues were inserted after D137 to check if a proper helical register is required for communicating the serine signal (Table 4-14).

NpHAMP tandem H_1-connector mutants	Basal Activity (nmol cAMP/mg/min)
(1) VRTSLEDAAKNAREDAEQAQKRAEEINTELQ	inactive
(2) VRTSLEDAAAKNAREDAEQAQKRAEEINTELQ	inactive
(3) VRTSLEDAAAAKNAREDAEQAQKRAEEINTELQ	inactive
(4) VRTSLEDAAAAAKNAREDAEQAQKRAEEINTELQ	inactive
a d a d a d a d a	

Table 4-14. Insertion of alanine residues in the inter-HAMP linker renders all chimeric proteins inactive. (n=4).

None of the four mutants generated with variable alanine residues were active (Table 4-14). The protein probably falls apart structurally due to instability of the linker because of these insertions.

4.5.2 The function of all HtrII inter-helical linkers.

Repellent phototaxis in *H. salinarum* is mediated by NpHtrII which also has a tandem HAMP. The inter-HAMP linker in *H. salinarum* is exactly twice the size of *N. pharaonis* linker. *H. salinarum* HtrII linker also has alanine as the predominant core residue similar to *N. pharaonis* linker whose structure has been determined. If the inter-HAMP linker is only a signal transducer then swapping of the linkers between the archaea would be possible. A chimera was generated wherein the linkers were exchanged (Table 4-15).

To check if the length of the linker had an impact on the tandem, doubling and tripling of the NpHtrII inter-HAMP linker was done. These constructs had 42 and 62 amino acids, respectively, as the NpHtrII linker. Both mutants were inactive (Fig. 4-22). When the linker between the archaea was swapped, the mutant had an inter-HAMP linker of 42 amino acids. This mutant was significantly inhibited by serine to about 35% (IC_{50}= 100 µM; n=12; *, $p<0.05$; Fig. 4-22). Basal activity was 2.4 ± 0.4 nmol cAMP/mg/min. The inhibition to serine by this chimera indicates a similar function of these two linkers.

Swapping the entire linker did not affect the signal sign but a mere doubling or even tripling of the linker chimera with the same residues from N. pharaonis linker was lethal as the chimeras were inactive. The doubled linker chimera had exactly the same number of amino

acids as the HsHtrII linker. This indicates a possible interaction in the linker region which is similar in the NpHtrII and HsHtrII.

NpHAMP tandem H_1-connector mutants	Inter-HAMP linker
(1) VRTSLEDAKNAREDAEQAQKRAEEINTDAKNAREDAEQAQKRAEEINTELQ	NpHtrII-2X
(2) VRTSLEDAKNAREDAEQAQKRAEEINTDAKNAREDAEQAQKREEINTDAKNAREDAEQAQKRAEEINTELQ	NpHtrII-3X
(3) VRTSLEDAERATARAEDAREDAEQQRADAEAAREDAEAARKDAQETATELQ	*Hs*HtrII
a d a d a d a d a d a d a d a d a d a d a d	

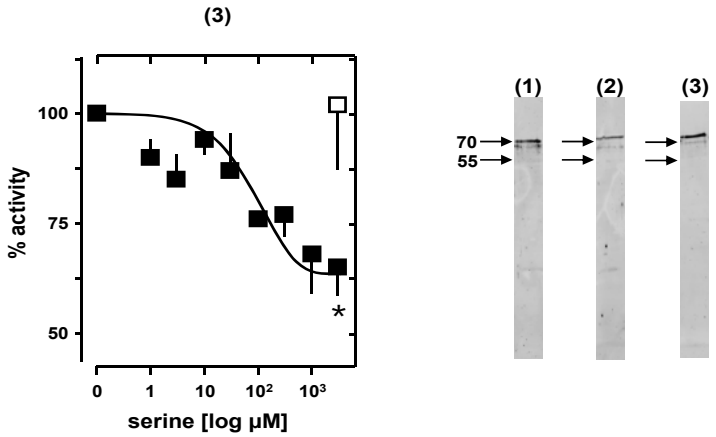

Figure 4-22. Above, sequence of the linker residues tested in the chimera. Below, Swapping of the linkers between NpHtrII and HsHtrII does not affect serine function (*; p<0.05, filled squares). Aspartate has no effect on the chimera (open squares). Western blots (5 µg protein/lane) of the mutants shown at right. (n=4-12).

4.6 Structural analysis of the tandems.

Three constructs, with a tandem HAMP and cyclase were generated for structural analysis. These constructs were purified for CD spectrum analysis to check if the mutations in the NpHAMP tandem affected its stability.

4.6.1 CD spectrum of tandem HAMP domains.

Circular dichroism (CD) spectroscopy is one of the most widely used techniques for the characterization of proteins and peptides in solution. Far-UV spectra of proteins can be used to predit their secondary structure. Isolated α-helices, β-sheets, and random coils possess distinctly different signatures (Fig. 4-23) and this is used in determining structural characteristics of a protein in solution.

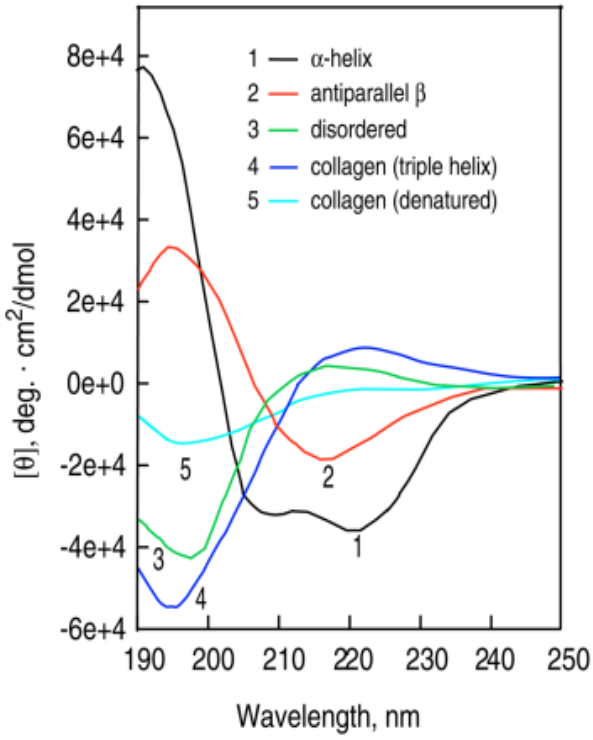

Figure 4-23. Characteristic CD spectra of proteins with representative secondary structures [94].

The NpHAMP tandem, $NpH_{1\text{-}mut5}$ tandem and $AS1_{1\text{-}Tsr}/NpH_1$ tandem which are unresponsive, inhibited and activated by serine respectively, were generated with only the output domain to make them soluble. The proteins were purified with Ni^{2+}-IDA as the specificity of purification was higher with it than Ni^{2+}-NTA. The basal activity of the purified chimeras was tested. A Western blot confirmed the molecular weight (40 kDa) of these chimeras.

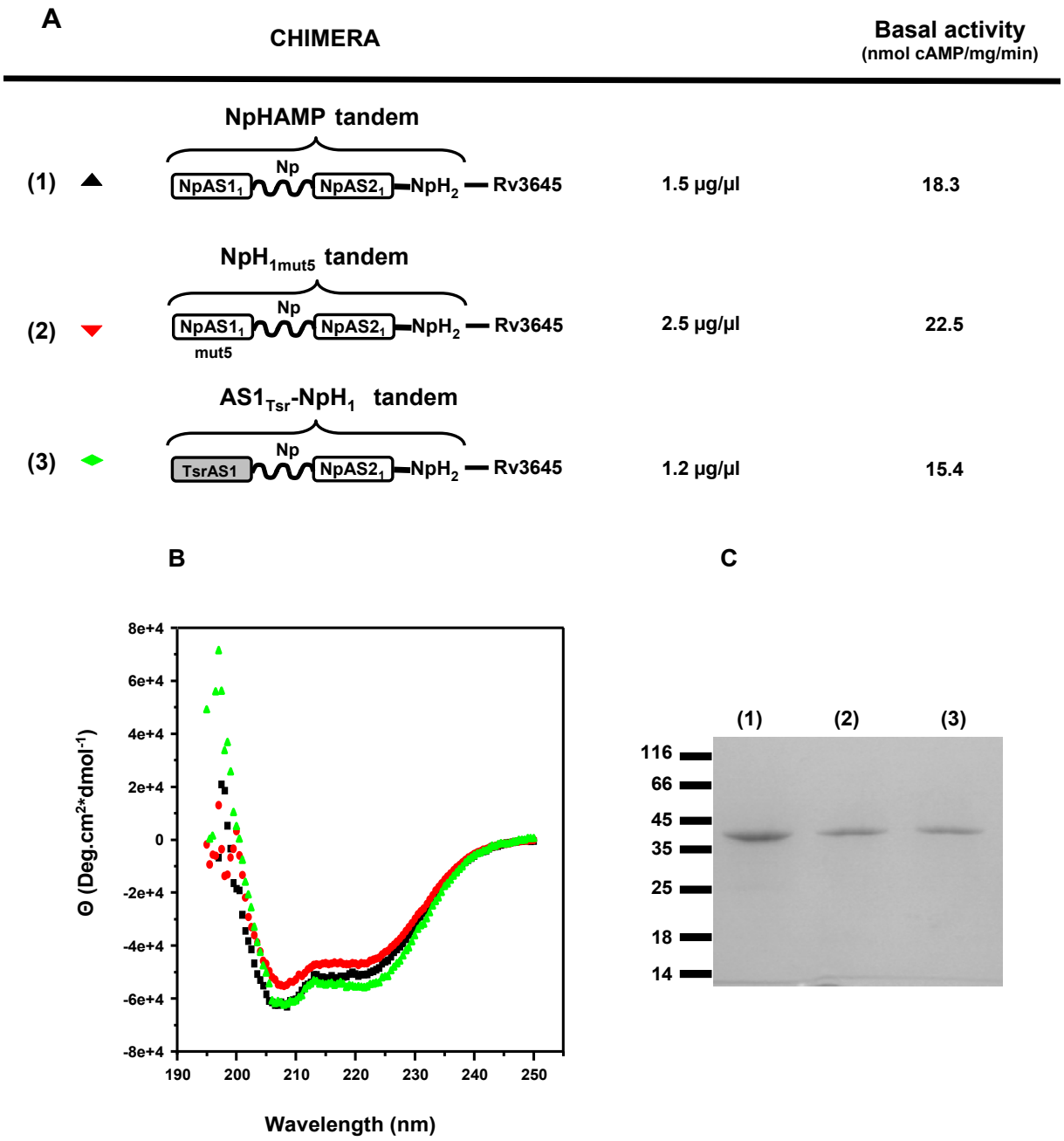

Figure 4-24. A, the HAMP chimeras purified for CD spectrum with their respective concentration and basal activities. B, CD spectrum of the HAMP domains indicates a high α helical content for all chimeras. C, Western blot of 2µg protein/lane. (n=2). Buffer: 10 mM HEPES; pH 7.5; 100 mM NaCl; 3 mM $MgCl_2$ and 2 mM DTT.

The CD spectra indicated strongly a propensity to form an alpha helix (Fig. 4-24).

4.6.2 Homology model of the tandem HAMPs

Homology modeling is a hypothetical structure prediction of protein sequences. The tri-HAMP structure of Aer2 protein is known [48]. Using the Aer2 structure, a homology model of $NpH_{1\text{-}mut5}$ tandem and $AS1_{1\text{-}Tsr}$/ $NpHAMP_1$ tandem was generated. The $HAMP_{1/2}$ in Aer2 like the NpHAMP tandem has a helical inter-HAMP linker connecting the HAMP domains. The length of this linker is shorter (only 5 amino acids compared to 20 in NpHAMP tandem). The predicted structure from different modeling programs were superimposed to see obvious differences in structure using Accelrys discovery studio software.

Using Swiss-Prot alignment mode, the sequence of the tandem proteins are threaded over the template tri-HAMP Aer2 structure (3LNR). The sequence was aligned according to the Aer2 sequence to adjust to the shorter linker stretch of Aer2 (Fig. 4-25).

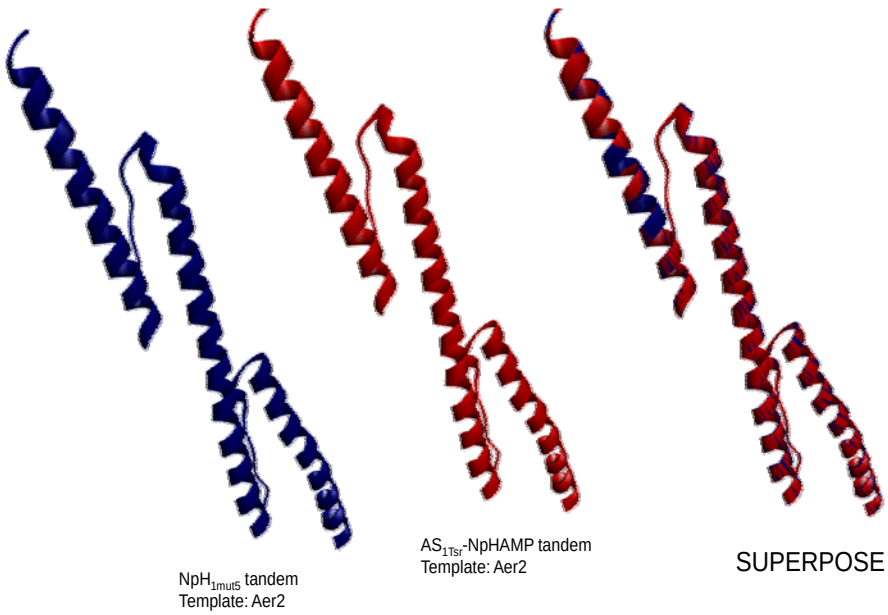

Figure 4-25. Shows the model predicted for the $NpH_{1\text{-}mut5}$ tandem (blue) and $AS1_{1\text{-}Tsr}$/$NpHAMP_1$ tandem (red). The extreme right model is the superposed structure of both models. The structure is the same for both tandems.

In a different approach only the $HAMP_1$ of both tandems was modeled using the software 3D-JIGSAW in alignment mode with Aer2 $HAMP_1$ structure (3LNR). However, no differences in the models were seen (Fig. 4-26).

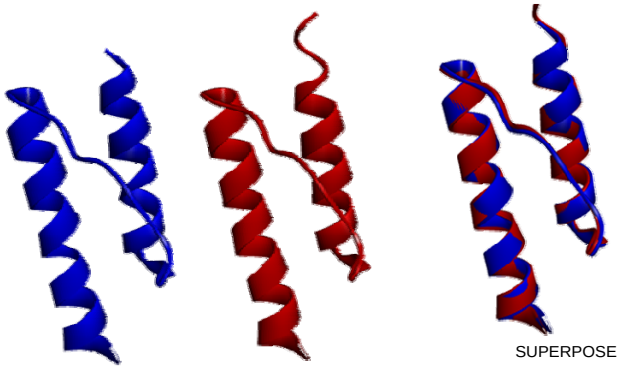

Figure 4-26. Shows the model predicted for the $NpH_{1\text{-}mut5}$ tandem (blue) and $AS1_{1\text{-}Tsr}$/$NpHAMP_1$ tandem (red). The extreme right model is the superposed structure of both models.

The inter-HAMP linker in Aer2 is only 5 amino acids. Four different shortening of the $NpH_{1\text{-}mut5}$ tandem linker was made and then modeled using the Aer2 structure (3LNR) using Swiss-Prot alignment mode (Fig. 4-27).

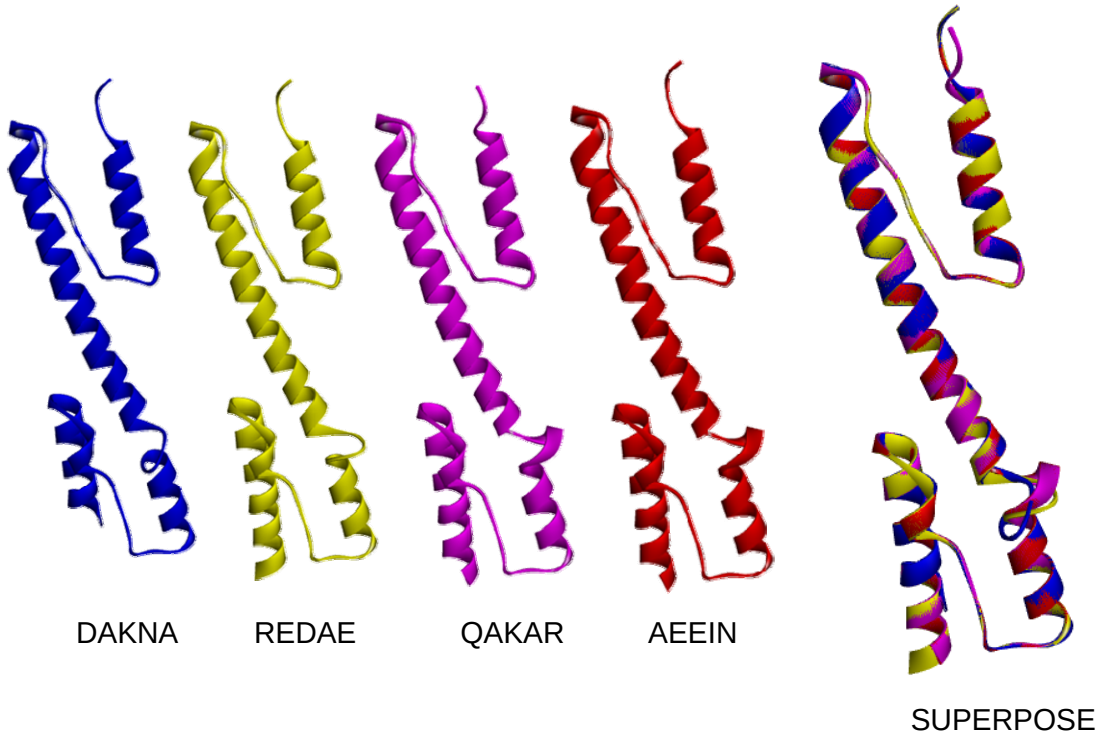

Figure 4-27. Shows the model predicted for the inter-HAMP linker in $NpH_{1\text{-}mut5}$ tandem. The extreme right model is the superposed structure of both models.

Since both tandems modeled differ only in their $AS1_1$ and given the highly identical core positions, the homology modeling did not show a difference in the structure. This does not rule out the fact that these AS1 may have an effect on the conformational alignment of the helices downstream.

5 DISCUSSION

HAMP domains are present in various modular proteins wherein they function as signal transducing modules. Tsr is a bi-functional receptor mediating attractant and repellant responses while NpHtrII is uni-functional (repellant). In a poly-HAMP module it is predicted that the sign of signal is reversed with each additional HAMP domain. So, the sign of signal from any tandem HAMP with the same stimulus should be identical. Two tandem HAMP domains were identified in this work that with the reporter system have opposite responses to the same ligand contrary to the predictions. The data from the mutants clearly point out that the sign of the signal transmitted to the output is determined by a specific sequence of the first alpha helix of the tandem that receives the input signal. The work illustrates the importance of the HAMP domains in determining the sign of signal. These chimeric tandems generated with opposite responses give a new insight into the functionality of these domains. Although it is arguable that these are chimeric domains one cannot rule out the possibility of the existence of these combinations in the native state as well.

5.1 Tandem HAMP domains.

HAMP modules up to 31 in a single protein have been identified [42]. The most frequent of poly-HAMP modules are tandem HAMP domains. Recent bioinformatic analysis pointed out that in many poly-HAMP modules the $NpHAMP_1$ belongs to the "canonical group" and $NpHAMP_2$ is in the "divergent group" [42]. In poly HAMPs each additional HAMP is predicted to reverse the sign of output signal [42, 48]. In an odd numbered poly-HAMP module the sign of signal output is predicted to be the same as a mono-HAMP whereas in an even numbered poly-HAMP module the sign of signal is reversed.

To study signal transduction via HAMP domains we used an *in vitro* biochemical system in which the signal output is affected exclusively by the HAMP domain that is inserted between the Tsr receptor as the input and the Rv3645 adenylyl cyclase as output domain [68, 69]. This setup differs from the swarm plate assays which have been employed to genetically characterize HAMP-mediated signal transduction [46, 90]. Consequently, partially competing proposals concerning the mechanisms of HAMP-mediated signal transduction emerged, each supported by carefully tailored experiments [43, 46]. In *P. aeruginosa* the sensor Aer2 has a PAS sensor sandwiched between three N-terminal and two C-terminal HAMP domains [48]. The structure of the Aer2 tri-HAMP suggested that each additional HAMP must invert the sign of signal output but physiological assays identified that the proximal $HAMP_{2/3}$ and distal

$HAMP_{4/5}$ tandems affect Aer2 signaling in *E. coli* in opposite ways i.e., $HAMP_{2/3}$ and $HAMP_{4/5}$ work as one unit contrary to prediction [48, 95]. Thus, presently a simple general mechanism of HAMP signaling which satisfactorily accounts for all experimental data cannot be presented.

5.2 NpHtrII HAMP tandem does not inverse the signal sign

The NpHtrII HAMP tandem did not functionally combine with the test system. Neither did NpHAMP1 and $NpHAMP_2$ as monomers. The inability of the monomers or the tandem to combine functionally can be speculated to be due to the differences in the input signal. The Tsr HAMP receives the signal from the conformational changes in the transmembrane region due to the ligand serine binding at the periplasmic receptor. The NpHtrII receives the input signal from conformational changes in the associated protein, SRII upon retinal excitation. In NpHtrII the second transmembrane rotates counter clockwise in addition to the downward piston movement but in Tsr there is only a piston movement downward that transfers the signal. This may or may not be the reason for the non-functionality of the NpHAMP domains in the test system.

A sequence comparison of the $NpHAMP_1$ and $HAMP_{Tsr}$ indicated deficits in the sequence of the $NpHAMP_1$ for signal uptake. Accordingly 5 mutations in the $NpHAMP_1$ AS1 ($NpAS1_1$) were introduced. The five point mutations in $NpAS1_1$ clearly did not endow $NpHAMP_1$ with properties sufficient for signal transduction on its own as serine had no effect on the chimera. Nevertheless the changes in amino acids in $NpHAMP_1$ must have resulted in novel structural/mechanical properties which facilitated interactions with $NpHAMP_2$ and formation of a signal transducing HAMP tandem as the $NpH_{1\text{-}mut5}$ tandem was inhibited by serine. This effect of the mutations questioned the predicted signal inversion by HAMPs in tandem. Although it is arguable that maybe the $NpH_{1\text{-}mut5}$ monomer can be activated by serine but a tendency for inhibition was observed which was not significant. This implies that both monomer and tandem chimeras were signaling in the same direction, i.e., inhibition by serine.

5.3 Oppositely signaling tandems.

The $NpHAMP_1$ is placed in the canonical group of HAMP domains [42]. A replacement of the $NpHAMP_1$ with $HAMP_{Tsr}$ or $HAMP_{Af1503}$ was not functional whereas $HAMP_{Af1503mut2}$ was able to combine functionally with the $NpHAMP_2$. The $Af1503_{mut2}$ in tandem with $NpHAMP_2$ was activated by serine. The sign of signal in tandem was opposite to the inhibition by serine

in $Af1503_{mut2}$ monomer [68]. Two tandem HAMP domains were identified which had the opposite sign of signal. Since the $NpHAMP_2$ was common in both tandems, the sign of signal was obviously controlled by $HAMP_1$ that receives the signal input.

To understand the structural details of signal inversion a couple of chimeric tandems were generated wherein combinations of different structural components of the $NpH_{1\text{-}mut5}$, Tsr, Tar and $Af1503_{mut2}$ were used. Replacements of the $NpHAMP_1$ connector and the $NpAS2_1$ were either nonfunctional or inactive. This points out critical interactions between the $NpHAMP_1$ connector and the $NpAS2_1$ in the NpHAMP tandem.

The inhibition to serine was reversed when the $AS1_1$ was replaced with AS_1 from Tsr in $NpH_{1\text{-}mut5}$ tandem. The $AS1_{1\text{-}Tsr}/NpH_1$ in tandem was activated by serine and as a monomer was inhibited by serine. Obviously, depending on the particular module composition of the HAMP tandem the output signal for serine may be activation or inhibition. The data further indicated that $HAMP_1$ in the tandem is set to determine the signal sign independently of $HAMP_2$ as long as a functional interaction with the latter is possible at all. According to the gearbox model of signal transduction one might consider that $HAMP_1$ can rotate in both directions. However, such an interpretation would clash with the fact that the signal emanating from the Tsr membrane receptor certainly is the same irrespective of the type of HAMP domain attached at its membrane exit. It is similarly questionable whether other proposals for signal transduction such as the piston or the dynamic bundle models alone could plausibly explain the above results. Obviously, the NpHAMP tandem operated as a single unit in which signal output could be engineered in both directions. This expands recent observations of behavioral assays with *H. halobium* which reported signal inversion by $NpHAMP_2$ [85].

5.4 Five residues determine the signal sign in tandem.

From the opposite signaling HAMP tandems it is clear that the sign of the signal is determined by the $AS1_1$ that receives the signal. The comparison of the $AS1_1$ of the tandems indicated that all of the conserved residues are identical. A helical wheel diagram of the heptads in the coiled coil indicates that all core residues are similar (Fig. 5-1, identical residues in red). The positions from 'a' to 'g' are indicated below both the sequences. The residues identical are shaded grey and the similar core residues are shaded pink. This indicates that the residues in the periphery of $AS1_1$ are responsible for the sign of signal output. To

explore this possibility an exhaustive mutational analysis of the $AS1_1$ of both the tandems was done.

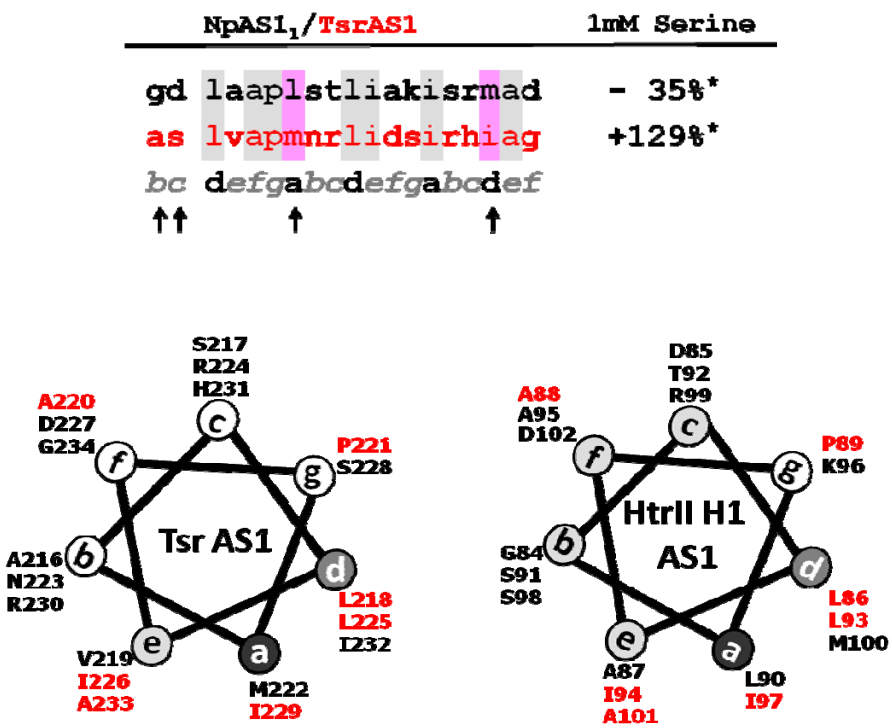

Figure 5-1. ***Above*****, shown is the sequence of the AS1 of NpHAMP-1mut5 (black) and $AS1_{1\text{-}Tsr}$/NpH_1 (red) tandem chimeras which are inhibited and activated by serine respectively.** ***Below*****, helical wheel diagram of the $AS1_1$ of both the tandems. The identical residue at the respective positions are colored red.**

The upshot of the 48 mutations is that four residues in the $AS1_1$ of the tandem determine the sign of the signal output (Fig. 4-16). One of the five positions, the Gly234 in $AS1_{Tsr}$ and Asp102 in $NpAS1_1$ are at a critical position at the hairpin turn merging into the connector sequence, had a greater impact when the sign of signal output was activation (Gly234), but not inhibition (Fig. 5-1, 4-17, [43, 90]). In $AS1_{1\text{-}Tsr}$ tandem the sign of the output can be modulated by four specific amino acid positions whereas in $NpH_{1\text{-}mut5}$ tandem a similar effect was not observed (Fig. 4-17). All constructs included two residues found in the NMR structure but now debated to be part of the proposed control cable. Furthermore, the last amino acid of the control cable seems to have a significant effect on $AS1_{1\text{-}Tsr}$ tandem, but not on $NpH_{1\text{-}mut5}$ tandem as the mutant was highly active and regulated. The residues in the control cable and $AS1_1$ can determine the ground state of the signaling unit and thereby affect the signal sign.

5.4.1 Effect of an M/M or L/I in a/d positions in $AS1_1$.

It is interesting that in the tandem HAMPs two specific core positions have a reversed amino acid pair i.e., I90 and M100 in $NpHAMP_{1\text{-}mut5}$ and M222 and I232 in $AS1_{1\text{-}Tsr}/NpH_1$ tandem (Fig. 5-1). When one of these positions are mutated so that core positions are occupied by the same hydrophobic residue i.e., I90M and M100 or I90 and M100I in $NpHAMP_{1\text{-}mut5}$ tandem and M222 and I232M or M222I and I232 in $AS1_{1\text{-}Tsr}/NpH_1$ tandem, the chimeras were nonfunctional (Table 4-9, 4-10). The I90M mutation in $NpHAMP_{1\text{-}mut5}$ and the I232M mutation in $AS1_{1\text{-}Tsr}/NpH_1$ tandem chimeras rendered the chimeras inactive. A similar effect was observed when core residues were Leu/Ile residues. The M222I and I232 $AS1_{1\text{-}Tsr}/NpH_1$ tandem was unaffected by serine whereas the I90 and M100I $NpHAMP_{1\text{-}mut5}$ tandem was inactive (Table 4-9, 4-10). In $NpHAMP_{1\text{-}mut5}$ tandem when the $AS1_1$ was replaced by either Tar or $Af1503_{mut2}$ were unregulated by serine. Tar AS1 has L120 and I130 and $Af1503_{mut2}$ has I284 and I294 at these core positions. It is reasonable to assume that the presence of same hydrophobic residue L/I pair at these positions rendered the chimeric tandem nonfunctional. It is surprising to observe such an effect at this position as the amino acids methionine, leucine and isoleucine have identical van der Waals volumes (V_r=124 $Å^3$) and they are typical core residues of the coiled coil. These results complicate predictions of HAMP mediated signaling. It is obvious that we are in dire need of additional structural, biochemical and physiological data to get more insight on a mechanism of HAMP signaling which may be generally applicable for this ubiquitous signal transducer.

Taken together, the results strongly suggest that in a HAMP tandem setting the control cable is intricately tuned to the adjacent $AS1_1$ sequence and profoundly affects the basal state of the modular signaling complex. The opposing sign of the output signal from Gly/Asp-$NpAS1_{1mut5}$ and Ala/Ser-$AS1_{Tsr}$ tandem is a reflection of such differing basal states. Substitutions in the transition zone between membrane and cytosol of NpHtrII abrogated signaling indicating a crucial role of the control cable in signal propagation. Our data is in agreement with results obtained from behavioral assays with *N. pharaonis* transducer. The reversal of the signal sign indicated that in one basal state the catalytic AC homodimer is correctly assembled and Tsr receptor stimulation results in inhibition of activity by enhancing disassembly. In the other state, a disassembled AC dimer is favored. By no means does this exclude rotation as an important structural parameter for signaling; rather it puts rotation into perspective with other movements of the modular signaling device which might control four helix bundle stability in essence by regulated unfolding. Addition of serine enables formation of the catalytic centre

assayed as stimulation of AC activity. Unregulated constructs could be considered as having deficits in intra-protein signal transfer from one module to the other thus disabling Tsr regulation. The molecular parameters responsible for these structural transitions remain to be elucidated. The data are compatible with a model of expanded dynamic bundle stability. Stability in this context is not restricted exclusively to the HAMP module but includes adjacent regions as well. The contribution of the control cable to signaling has been reported to be minor in serine or aspartate chemotaxis receptor signaling [46, 81, 89].

5.5 Importance of connector

The flexible loop called connector joins the two alpha helices and is proposed to play a major role in the stabilization of the helices [43, 90]. The connector in $NpHAMP_1$ is 12 amino acids long similar to Tsr HAMP. Based on the structure of the Af1503 HAMP (2) this is the minimum length required to bridge the gap between the C-terminus of AS1 and the N-terminus of AS2. In the structure of Af1503 the connector preferably interacts with AS2 via formation of salt bridges [68].

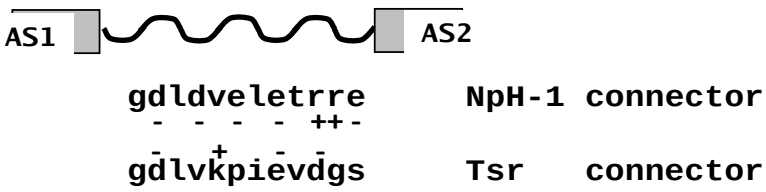

Figure 5-2. The sequence of the connector in $NpHAMP_{1\text{-}mut5}$ and Tsr HAMP.

The connector of $NpHAMP_1$ has the conserved residue pattern "G-X-HR1-X-X-X-HR2" as formerly delineated [48, 90]. The motif is also preserved in divergent HAMP domains [48]. The glycine residue at the beginning of the connector is crucial for flexibility. The other two conserved hydrophobic residues are irreplaceable. Apart from these three positions all other residues are not critical for functioning. In Af1503 the connector residues form salt bridges between the AS1 and AS2 helices [68]. It has also been reported earlier that the replacement of the connector segment is not always possible. This raises the possibility of a specific connector for each HAMP. They may/may not functionally combine with other HAMP domains.

In the $HAMP_1$ connector of NpHAMP tandem 7/12 amino acids are charged (2 positive, 5 negative) whereas in the connector of the Tsr HAMP from E. coli only 4/12 are charged (1

positive, 3 negative) (Fig. 5-2). Analysis of 15 mutants in the $HAMP_1$ connector of $NpH1_{1\text{-}mut5}$ tandem indicated that only an unsuspicious T111V exchange was tolerated as this mutant still retained the inhibition by serine (Table 4-12). Not a single charged amino residue could be replaced by an uncharged one without loss of serine regulation (Table 4-12).

It appeared that each charged amino acid was specifically required for a functional interaction. The connector most probably interacts with AS2 in $NpHAMP_1$ as replacement of AS1 in $NpHAMP_1$ by that from Tsr HAMP did not result in structural disorder interrupting signal transduction but none of the chimeras with replacements of the $NpHAMP_1$ connector or $AS2_1$ were functional. The $NpAS2_1$ is highly charged (7/22 compared to 4/22 in Tsr HAMP AS2). The $HAMP_1$ connector and $NpAS2_1$ may form a salt bridge which stabilizes the $NpHAMP_1$ as both the connector and the AS2 are highly charged. It also indicates a possible $NpAS2_1$ induced stability or a possible interaction to the inter-HAMP linker. This accumulation of charges in the connector and $AS2_1$ segment of $NpHAMP_1$ may mirror peculiar structural and functional requirements in the hypersaline cytoplasm of this archaeon [82]. Further insights into the interactions will be possible only with structural data on these tandem HAMPs.

5.6 Inter-HAMP linker

The tandem HAMPs in *N. pharaonis* and *H. salinarium* has an inter-HAMP linker connecting $HAMP_1$ and -2. The inter-HAMP linker in *N. pharaonis* (20aa) and in *H. salinarium* (42 aa) are predicted to be an α-helix which holds the tandem in a rigid state. Both the linkers are highly charged, 10/20 in NpHtrII and 19/42 in HsHtrII (Fig. 5-3). The linker is a unique coiled coil in the sense that most of the hydrophobic core positions are occupied by alanine. In a canonical coiled coil, the core positions are mostly occupied by larger hydrophobic residues. The presence of alanine residues in the core raises questions on the stability and interaction between two adjacent linkers in the active state wherein the protein is a homodimer. The structure of the NpHtrII inter-HAMP linker was solved [93]. The work done further on the linker stated that the assembly of the homodimers is asymmetric [91]. The asymmetric association of the linker is proposed to stabilize the tandem HAMPs.

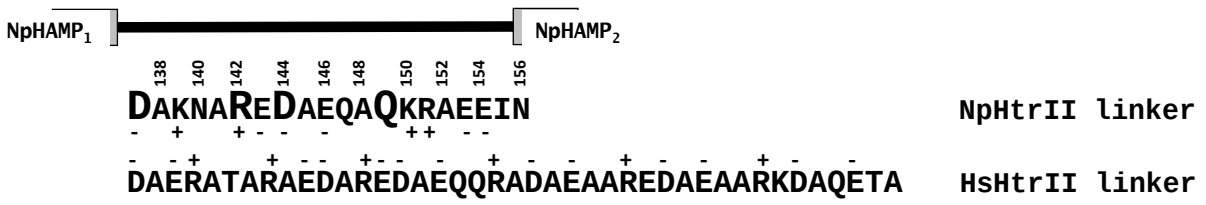

Figure 5-3. Sequence of the inter-HAMP linker of the *N. pharaonis* (number on top of sequence) and *H. salinarium*. Both linkers are highly charged. The residues which are proposed to be interacting in NpHtrII linker are shown with increased font.

It has been reported that in NpHtrII there is an asymmetric association of the protomers. There is a proposed electrostatic interaction between the R142 of one protomer to D144 of the other and this interaction leads to interaction between D137 and R142 of the other protomer. It was also reported that the R142 can either interact with D144 or D147 but not both at the same time [91]. Attraction of R142 in one protomer to D137 in the other leads to a longitudinal displacement, such that R142 comes closer to D144, and vice versa. The resulting shift is additionally stabilized by short-lived bonds between Q149 and D144. It was also assumed that this asymmetrical interaction of the linker maybe an indicator for a role of the linker in acting like a switch to determine the signal sign or just stabilizes the conformations of the HAMP domains.

To validate and to understand the specificity of the linker, several deletions and insertions were done. As the linker is a coiled coil continuous from the AS2 of HAMP 1, two heptads were identified within the sequence. These two heptads were deleted separately and together to check their effect on the linker (Fig. 4-21). Deletions of the heptad from 'AEQAQKR' in the linker lead to a drop in activity and also loss of serine response (Fig. 4-21). Whereas, the deletion of heptad 'AKNARED' retains the serine inhibition but there is also a drop in activity (Fig. 4-21). Both the heptad deletions had similar activities. The double heptad deletion chimera was inactive (Fig. 4-21). If the interactions with the R142 and D144 are critical, the deletion of the heptad 'AKNARED' would have led to an inactive/unregulated chimera but on the contrary the regulation is retained. The regulation is lost in the 'AEQAQKR' heptad deletion. The double deletion is inactive indicating that the most critical residue interactions are in the heptad "**AEQAQKR** " region. Next, alanine residues were introduced in the heptad to check if there are stutter/stammer positions within the linker. One to four alanine residues were introduced at position 137 just in front of the first identified heptad in the linker ('AKNARED'). All chimeras generated with alanine insertions were inactive (Table 4-14). These results indicate that the linker does not necessarily influence the sign of signal although it is essential for retaining the serine response.

Inter-HAMP linker is present in phototaxis receptors of *Natronomonas* and *Halobacterium*. The linkers differ in length; the linker in *H. salinarum* is exactly twice the size of *N. pharaonis* linker. The structure of the linker from NpHtrII is available and it is proposed that the HsHtrII inter-HAMP linker is also an α-helix. Functional replacement of the linkers between the NpHtrII and HsHtrII is possible indicating that although the length of the HsHtrII is longer the functionality or the interactions in between the linkers are identical (Fig. 4-22). Though the swapping of the entire linker worked, mere doubling or even tripling of the linker chimera with the same residues from N. pharaonis linker does not work (Fig. 4-22). This indicates very specific interaction between the residues of the linkers or between the $AS2_1$-linker-$AS1_2$.

The inter-HAMP linker region can be compared to the signaling helix (S-Helix [66, 96]) in that it continues the signal output from the AS2 of the $HAMP_1$ domain to the AS1 of the $HAMP_2$. S-helices also form two helical coiled coils with the core positions occupied by hydrophobic residues and have been reported to influence the sign of signal but as shown in this work, this has not been the case with the inter-HAMP linkers [66]. To be able to influence the sign of signal the linker must be able to undergo longitudinal motions along the protomers. The motions of these two helical coiled coils sandwiched between two HAMP domains would be more rigid. Hence it is unlikely that these protomers influence the signal sign.

5.7 Model for signal transmission via tandem HAMPs

Sensing and adaptation to the present condition is the key to the survival of the organisms. The HAMP being modules, it's quite puzzling the need to have a HAMP tandem. Mutational analysis of the tandem indicated that in $HAMP_1$ AS1, five residues determine the sign of signal output. Never before have the HAMP domains been reported to be functioning like a switch and determining the signal sign. The sign of the signal was determined by five positions: $\mathbf{b}_1$, $\mathbf{c}_2$, $\mathbf{a}_9$, $\mathbf{d}_{17}$ and $\mathbf{f}_{19}$ combinations (Fig. 5-1). The first two amino acids are considered now to be a part of a control cable. The next two are core positions with known significance in forming the core and the last position is the end of the AS1. The last position is not that critical as the signal sign can also be influenced without mutating it. This specific pattern of signal sign determination is quite unique and novel. The changes in the $AS1_1$ are transferred through the tandem HAMPs either with/without a switch in signal sign. These

multiple changes are then accumulated at the end of $HAMP_2$. The region joining the end of $HAMP_2$ to the start of the cyclase domain is a dynamic region undergoing a massive rearrangement which is then sensed by the cyclase in one way or the other leading to changes in the proximity of the cyclase dimers to one another (Fig. 5-4, [97]).

The ability of a protein to switch between signals with subtle changes in the conformation i.e., by a position of $HAMP_2$ relative to $HAMP_1$ is the key to the signal encoding by displacement of the whole cytoplasmic part of the transducer. As we have noted, asymmetry of the inter-HAMP is enforced by electrostatic interactions of oppositely charged side chains of corresponding residues. Flexibility of those side chains allows some longitudinal displacements (up to zero shift) without breaking of the formed electrostatic bonds. Thus, the evolution of the system with time may be different depending on which bonds are formed that is, the history of the system. This means that the inter-HAMP region is in effect a multistate switch. It is worth mentioning that a study of the HAMP domain alone would not provide sufficient information about signal transduction.

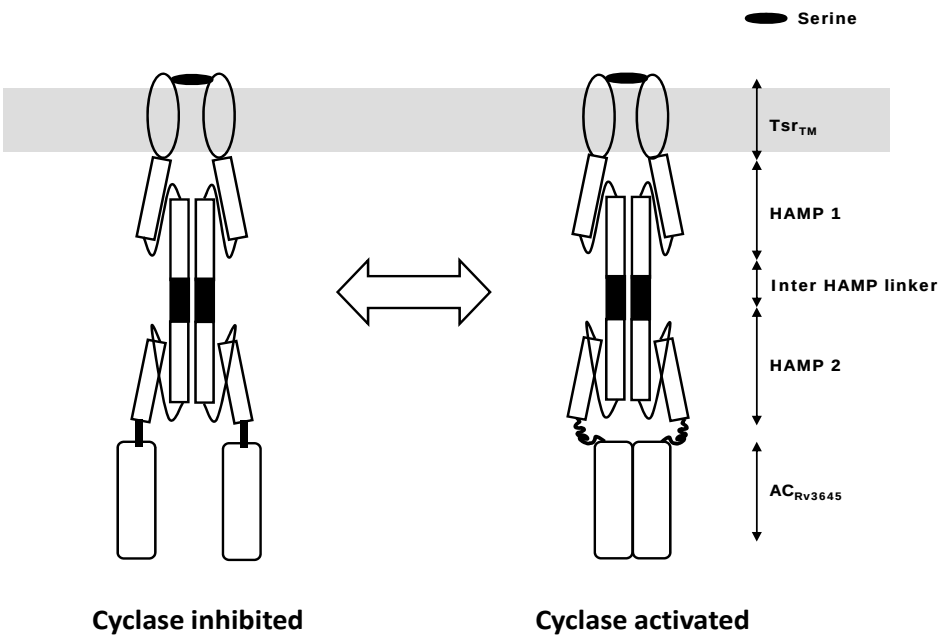

Figure 5-4. A model of the probable conformations of the two oppositely signaling tandems.

6 SUMMARY

The incidence of HAMP tandems in bacterial signaling proteins is low and presently it is unknown what physiological advantage may be gained by using a tandem. Presently a simple general mechanism of HAMP signaling which satisfactorily accounts for all experimental data cannot be presented. To study signal transduction via HAMP domains we used an in vitro biochemical system in which the signal output is affected exclusively by the HAMP domain that is inserted between the Tsr receptor as the input and the Rv3645 adenylyl cyclase as output domain. Initially neither the HAMP tandem nor its respective monomers operated as signal transducers in our system. The introduction of five targeted mutations in the first α-helix of $NpHAMP_1$ which adapted this sequence somewhat to the equivalent Tsr sequence was required to obtain a functional, i.e. signal-transducing HAMP tandem. Replacement of the entire α-helix $NpAS1_{1\text{-}mut5}$ by the equivalent sequence of $HAMP_{Tsr}$ the chimeric HAMP monomer ($AS1_{Tsr}$/NpAS2) was fully operational in that serine strongly inhibited AC activity. Furthermore, in combination with $NpHAMP_2$ in tandem the sign of the output signal was inverted as predicted. This left us with two HAMP tandem constructs with opposite outputs of the serine signal as initiated by serine-binding to the periplasmic domain of Tsr. The differences between both constructs were confined to the first α-helix of the first HAMP domain in the tandem as all other segments remained unchanged. Both constructs received the same conformational signal from Tsr. One might then reasonably speculate that the first α-helix (α-helix-1) is ultimately responsible for formation of different ground states of the output domain which leads to differences in signal output. In a series of experiments, AS1 of $NpHAMP_1$ was extensively mutated to decipher which residues actually might determine such different states. In $NpAS1_{1\text{-}Tsr}$ and $NpAS1_{1\text{-}mut5,}$ five amino acid residues in α-helix-1 were responsible for defining opposite ground states. Just manipulating the α-helix-1 in a HAMP tandem was sufficient to produce opposite signaling outputs. The data do not permit making a similar claim for signal transduction through a HAMP monomer. This finding is hard to explain with rotation as a major HAMP signaling mechanism. In *N. pharaonis* sensory rhodopsin-I and its cognate transducer complex, SRI-HtrI has a dual function by mediating attractant and repellant responses whereas SRII-HtrII mediates only repellant responses. Both transducers have a HAMP tandem. In such a system signal rapid changes in signal input may require a fast track system for adaptation which has been reported for SRI-HtrI complex signaling. Our data allow the speculation that HAMP tandems by virtue of their intrinsic sequences prime a signal transduction system for a distinct organismal response to peculiar

environmental cues such as light in *N. pharaonis*. The results complicate predictions of HAMP mediated signaling based on our current structural knowledge base.

According to the gearbox model of HAMP signal transduction one might consider that $HAMP_1$ may rotate in both directions. However, such an interpretation would clash with the fact that the signal emanating from the Tsr membrane receptor is the same irrespective of the type of HAMP domain attached to its C-terminal membrane exit. It is similarly questionable whether other proposals for signal transduction such as the piston or the dynamic bundle models alone could plausibly explain the above results. Rotation as one structural parameter for HAMP signal transduction is not excluded, rather it ought to be seen in conjunction with other molecular movements which might control four helix bundle stability in essence by regulated unfolding. Stability in this context is not restricted to the HAMP module alone but includes adjacent regions with which the HAMP domain is in a continuous structural balance.

The possibility to switch the sign of the output signal by a single amino acid mutation in a HAMP tandem context may be an evolutionary advantage in the multiplicity of HAMP-mediated signaling systems and may expand the versatility of such units.

7 Zusammenfassung

HAMP* vermittelte Signaltransduktion ist allgegenwärtig (> 28.000 HAMP Datenbank Einträge). In den meisten Fällen ist zwischen einem Sensor und einem Ausgabemodul eine HAMP Domäne (HAMP Monomer) eingesetzt. Sie dient wahrscheinlich als Adapter zwischen der Sensor- und Effektordomäne. Der vorgeschlagene Mechanismus der HAMP Signaltransduktion durch Drehung wurde durch eine Kristallstruktur einer seriellen dreifach-HAMP aus *Pseudomonas aeruginosa* gestärkt. Das Rotationsmodell würde vorhersagen, dass sich mit jeder zusätzlichen HAMP Domäne das Vorzeichen des Ausgangssignals umkehrt. Diese Vorhersage wurde durch biochemische Experimente überprüft, indem eine HAMP-Tandem Domäne des HtrII Photorezeptors aus *N. pharaonis* verwendet wurde. Das grundlegende Design unserer getesteten Konstrukte mit Tsr als Sensor und Rv3645 AC als Effektor wurde beibehalten. Das grundlegende Design unserer getesten Konstrukte war jeweils Tsr als Sensor und Rv3645 AC als Effecktor mit der zu untersuchenden HAMP Domäne dazwischen. Es war nicht verwunderlich, dass zunächst weder das HAMP-Tandem noch seine jeweiligen Monomere in den getesteten Konstrukten als Signalgeber fungierten, weil in NpHtrII das Lichtsignal zwischen sensorischem Rhodopsin II und der Chemotaxiseinheit HtrII innerhalb der Membran weiter gegeben wird. Die Einführung von fünf gezielten Mutationen in der ersten α-Helix von $NpHAMP_1$, die deren Sequenz stärker an die von Tsr angleicht, war erforderlich, um eine funktionale, d.h. signaltransduzierende HAMP-Tandem Domäne zu erhalten. Beide HAMP Monomere allein waren inaktiv als Signalgeber. Der überraschende Befund war, dass das Vorzeichen des Ausgangssignals nicht wie vorhergesagt umgedreht wurde.Wenn die gesamte erste α-Helix (AS1) im NpHAMP Monomer durch die äquivalente α-Helix von $HAMP_{Tsr}$ ersetzt wurde ($AS1_{1\text{-}Tsr}/NpH_1$), wurde das Konstrukt gehemmt. Mit $NpHAMP_2$ als HAMP-Tandem allerdings wurde das Vorzeichen des Ausgangssignals invertiert, d.h. das Tandem-Konstrukt wurde aktiviert. Die Unterschiede im Ausgangssignal zwischen beiden Konstrukten können der ersten α-Helix der ersten HAMP Domäne im Tandem zugerechnet werden, da alle anderen Segmente unverändert blieben. Man kann annehmen, dass die erste α-Helix letztlich verantwortlich ist für die Bildung von unterschiedlichen Grundzuständen der Effektordomäne.In einer Serie von Experimenten wurde durch zahlreiche Mutationen in AS1 von $NpHAMP_1$ untersucht, welche Aminosäuren die verschiedenen Zustände bestimmen. Das Ergebnis von 48 Mutationen in $NpAS1_{1\text{-}mut5}$ und

*- **H**istidine kinases, **A**denylyl cyclases, **M**ethyl-accepting chemotaxis proteins and **P**hosphatases.

$AS1_{1\text{-}Tsr}/NpH_1$ Tandem Konstrukten war, dass fünf Aminosäuren für die gegensätzlichen Grundzustände verantwortlich waren. Dies würde dafür sprechen, dass das Signal, das vom Tsr Membranrezeptor ausgeht, immer das gleiche ist, unabhängig von der Art der angeschlossenen HAMP Domäne. So ist es fraglich, ob andere Modelle der Signaltransduktion wie z.B. das Kolben-Modell oder das "dynamic bundle model" die obigen Ergebnisse plausibel erklären. Rotation als alleiniger struktureller Parameter für die HAMP Signaltransduktion wird kaum ausreichen, sondern sollte in Verbindung mit anderen molekularen Bewegungen gesehen werden, welche Einfluss auf die Stabilität des Vierhelixbündels der HAMP Domäne nehmen können. Hierzu lässt sich z.B. das „regulated unfolding'' nennen. Bei dieser These ist die Stabilität nicht auf das HAMP Modul allein beschränkt, sondern umfasst auch benachbarte Bereiche, mit denen sich die HAMP Domäne in einem kontinuierlichen Strukturgleichgewicht befindet. Eine plausible Interpretation wäre, dass HAMP Domänen verschiedene Grundzustände eines sensorischen Systems definieren und entsprechend gegensätzliche physiologische Reaktionen auslösen können. In dem einen Grundzustand lagert sich das katalytische AC Homodimer richtig zusammen, sodass bei Stimulation des Tsr Rezeptors sich die Untereinheiten voneinander distanzieren, wodurch es zu einer Hemmung der Enzymaktivität kommt. Im Gegensatz dazu kommen im anderen Grundzustand die Untereinheiten durch ein Serinsignal zusammen, was zu einer erhöhten Enzymaktivität führt.

8 References

1. Abdel Motaal, A., et al., *Fatty acid regulation of adenylyl cyclase Rv2212 from Mycobacterium tuberculosis H37Rv.* Febs J, 2006. **273**(18): p. 4219-28.
2. Stoeckenius, W., E.K. Wolff, and B. Hess, *A rapid population method for action spectra applied to Halobacterium halobium.* J Bacteriol, 1988. **170**(6): p. 2790-5.
3. Armitage, J.P., *Bacterial tactic responses.* Adv Microb Physiol, 1999. **41**: p. 229-89.
4. Falke, J.J., et al., *The two-component signaling pathway of bacterial chemotaxis: a molecular view of signal transduction by receptors, kinases, and adaptation enzymes.* Annu Rev Cell Dev Biol, 1997. **13**: p. 457-512.
5. Stock, A.M., V.L. Robinson, and P.N. Goudreau, *Two-component signal transduction.* Annu Rev Biochem, 2000. **69**: p. 183-215.
6. Hoff, W.D., K.H. Jung, and J.L. Spudich, *Molecular mechanism of photosignaling by archaeal sensory rhodopsins.* Annu Rev Biophys Biomol Struct, 1997. **26**: p. 223-58.
7. Zhang, X.N., J. Zhu, and J.L. Spudich, *The specificity of interaction of archaeal transducers with their cognate sensory rhodopsins is determined by their transmembrane helices.* Proc Natl Acad Sci USA, 1999. **96**(3): p. 857-62.
8. Hazelbauer, G.L., J.J. Falke, and J.S. Parkinson, *Bacterial chemoreceptors: high-performance signaling in networked arrays.* Trends Biochem Sci, 2008. **33**(1): p. 9-19.
9. Porter, S.L., G.H. Wadhams, and J.P. Armitage, *Signal processing in complex chemotaxis pathways.* Nat Rev Microbiol, 2011. **9**(3): p. 153-65.
10. Suzuki, D., et al., *Phototactic and chemotactic signal transduction by transmembrane receptors and transducers in microorganisms.* Sensors (Basel), 2010. **10**(4): p. 4010-39.
11. Tso, W.W. and J. Adler, *Negative chemotaxis in Escherichia coli.* J Bacteriol, 1974. **118**(2): p. 560-76.
12. Li, M. and G.L. Hazelbauer, *Cellular stoichiometry of the components of the chemotaxis signaling complex.* J Bacteriol, 2004. **186**(12): p. 3687-94.
13. Grebe, T.W. and J. Stock, *Bacterial chemotaxis: the five sensors of a bacterium.* Curr Biol, 1998. **8**(5): p. R154-7.
14. Manson, M.D., et al., *Bacterial locomotion and signal transduction.* J Bacteriol, 1998. **180**(5): p. 1009-22.
15. Yamamoto, K. and Y. Imae, *Cloning and characterization of the Salmonella typhimurium-specific chemoreceptor Tcp for taxis to citrate and from phenol.* Proc Natl Acad Sci USA, 1993. **90**(1): p. 217-21.
16. Weerasuriya, S., B.M. Schneider, and M.D. Manson, *Chimeric chemoreceptors in Escherichia coli: signaling properties of Tar-Tap and Tap-Tar hybrids.* J Bacteriol, 1998. **180**(4): p. 914-20.
17. Kim, K.K., H. Yokota, and S.H. Kim, *Four-helical-bundle structure of the cytoplasmic domain of a serine chemotaxis receptor.* Nature, 1999. **400**(6746): p. 787-92.
18. Milburn, M.V., et al., *Three-dimensional structures of the ligand-binding domain of the bacterial aspartate receptor with and without a ligand.* Science, 1991. **254**(5036): p. 1342-7.
19. Weis, R.M., et al., *Electron microscopic analysis of membrane assemblies formed by the bacterial chemotaxis receptor Tsr.* J Bacteriol, 2003. **185**(12): p. 3636-43.
20. Falke, J.J. and G.L. Hazelbauer, *Transmembrane signaling in bacterial chemoreceptors.* Trends Biochem Sci, 2001. **26**(4): p. 257-65.
21. Maddock, J.R. and L. Shapiro, *Polar location of the chemoreceptor complex in the Escherichia coli cell.* Science, 1993. **259**(5102): p. 1717-23.

22. Briegel, A., et al., *Universal architecture of bacterial chemoreceptor arrays.* Proc Natl Acad Sci USA, 2009. **106**(40): p. 17181-6.
23. Kentner, D., et al., *Determinants of chemoreceptor cluster formation in Escherichia coli.* Mol Microbiol, 2006. **61**(2): p. 407-17.
24. Sourjik, V., *Receptor clustering and signal processing in E. coli chemotaxis.* Trends Microbiol. , 2004. **12**: p. 569-576.
25. Ames, P., et al., *Collaborative signaling by mixed chemoreceptor teams in Escherichia coli.* Proc Natl Acad Sci USA, 2002. **99**(10): p. 7060-5.
26. Studdert, C.A. and J.S. Parkinson, *Crosslinking snapshots of bacterial chemoreceptor squads.* Proc Natl Acad Sci USA, 2004. **101**(7): p. 2117-22.
27. Homma, M., et al., *Attractant binding alters arrangement of chemoreceptor dimers within its cluster at a cell pole.* Proc Natl Acad Sci USA, 2004. **101**(10): p. 3462-7.
28. Sourjik, V. and H.C. Berg, *Functional interactions between receptors in bacterial chemotaxis.* Nature, 2004. **428**(6981): p. 437-41.
29. Oesterhelt, D., *The structure and mechanism of the family of retinal proteins from halophilic archaea.* Curr Opin Struct Biol, 1998. **8**(4): p. 489-500.
30. Schmies, G., et al., *Electrophysiological characterization of specific interactions between bacterial sensory rhodopsins and their transducers.* Proc Natl Acad Sci USA, 2001. **98**(4): p. 1555-9.
31. Sudo, Y., et al., *Photo-induced proton transport of pharaonis phoborhodopsin (sensory rhodopsin II) is ceased by association with the transducer.* Biophys J, 2001. **80**(2): p. 916-22.
32. Vonck, J., *A three-dimensional difference map of the N intermediate in the bacteriorhodopsin photocycle: part of the F helix tilts in the M to N transition.* Biochemistry, 1996. **35**(18): p. 5870-8.
33. Kamikubo, H., et al., *Structure of the N intermediate of bacteriorhodopsin revealed by x-ray diffraction.* Proc Natl Acad Sci U S A, 1996. **93**(4): p. 1386-90.
34. Luecke, H., et al., *Structural changes in bacteriorhodopsin during ion transport at 2 angstrom resolution.* Science, 1999. **286**(5438): p. 255-61.
35. Xiao, W., et al., *Light-induced rotation of a transmembrane alpha-helix in bacteriorhodopsin.* J Mol Biol, 2000. **304**(5): p. 715-21.
36. Subramaniam, S. and R. Henderson, *Molecular mechanism of vectorial proton translocation by bacteriorhodopsin.* Nature, 2000. **406**(6796): p. 653-7.
37. Shibata, M., et al., *High-speed atomic force microscopy shows dynamic molecular processes in photoactivated bacteriorhodopsin.* Nat Nanotechnol, 2010. **5**(3): p. 208-12.
38. Sasaki, J., A.L. Tsai, and J.L. Spudich, *Opposite displacement of helix F in attractant and repellent signaling by sensory rhodopsin-Htr complexes.* J Biol Chem, 2011. **286**(21): p. 18868-77.
39. Gordeliy, V.I., et al., *Molecular basis of transmembrane signalling by sensory rhodopsin II-transducer complex.* Nature, 2002. **419**(6906): p. 484-7.
40. Jin, T. and M. Inouye, *Transmembrane signaling. Mutational analysis of the cytoplasmic linker region of Taz1-1, a Tar-EnvZ chimeric receptor in Escherichia coli.* J Mol Biol 1994. **244**: p. 477–481.
41. Aravind, L. and C.P. Ponting, *The cytoplasmic helical linker domain of receptor histidine kinase and methyl-accepting proteins is common to many prokaryotic signalling proteins.* FEMS Microbiol Lett, 1999. **176**(1): p. 111-6.
42. Dunin-Horkawicz, S. and A.N. Lupas, *Comprehensive Analysis of HAMP Domains: Implications for Transmembrane Signal Transduction.* J Mol Biol, 2010. **397**: p. 1156-1174.

43. Hulko, M., et al., *The HAMP domain structure implies helix rotation in transmembrane signaling.* Cell 2006. **126**(5): p. 929-940.
44. Crick, F.H.C., *The Packing of a-Helices: Simple Coiled-Coils.* Acta Crystallogr., 1953. **6**: p. 689-697.
45. Mason, J.M. and K.M. Arndt, *Coiled coil domains: stability, specificity, and biological implications.* Chembiochem, 2004. **5**(2): p. 170-6.
46. Zhou, Q., P. Ames, and J.S. Parkinson, *Mutational analyses of HAMP helices suggest a dynamic bundle model of input–output signalling in chemoreceptors.* Mol Microbiol, 2009. **73**(5): p. 801-814.
47. Parkinson, J.S., *Signaling mechanisms of HAMP domains in chemoreceptors and sensor kinases.* Annu Rev Microbiol, 2010. **64**: p. 101-22.
48. Airola, M.V., et al., *Structure of concatenated HAMP domains provides a mechanism for signal transduction.* Structure, 2010. **18**(4): p. 436-48.
49. Barzu, O. and A. Danchin, *Adenylyl cyclases: a heterogeneous class of ATP-utilizing enzymes.* Prog Nucleic Acid Res Mol Biol, 1994. **49**: p. 241-83.
50. Cases, I. and V. de Lorenzo, *Expression systems and physiological control of promoter activity in bacteria.* Curr Opin Microbiol, 1998. **1**(3): p. 303-10.
51. Yahr, T.L., et al., *ExoY, an adenylate cyclase secreted by the Pseudomonas aeruginosa type III system.* Proc Natl Acad Sci U S A, 1998. **95**(23): p. 13899-904.
52. Cotta MA, W.T., Wheeler MB., *Identification of a novel adenylate cyclase in the ruminal anaerobe, Prevotella ruminicola D31d.* FEMS Microbiol Lett., 1998. **164**: p. 257-60.
53. Sismeiro, O., et al., *Aeromonas hydrophila adenylyl cyclase 2: a new class of adenylyl cyclases with thermophilic properties and sequence similarities to proteins from hyperthermophilic archaebacteria.* J Bacteriol, 1998. **180**(13): p. 3339-44.
54. Tellez-Sosa, J., et al., *The Rhizobium etli cyaC product: characterization of a novel adenylate cyclase class.* J Bacteriol, 2002. **184**(13): p. 3560-8.
55. Linder, J.U. and J.E. Schultz, *The class III adenylyl cyclases: multi-purpose signalling modules.* Cell Signal, 2003. **15**: p. 1081–1089.
56. Tesmer, J.J., et al., *Crystal structure of the catalytic domains of adenylyl cyclase in a complex with Gsalpha.GTPgammaS.* Science, 1997. **278**(5345): p. 1907-16.
57. Tesmer, J.J., et al., *Two-metal-Ion catalysis in adenylyl cyclase.* Science, 1999. **285**(5428): p. 756-60.
58. Sunahara, R.K., et al., *Exchange of substrate and inhibitor specificities between adenylyl and guanylyl cyclases.* J Biol Chem, 1998. **273**(26): p. 16332-8.
59. Bai, G., G.S. Knapp, and K.A. McDonough, *Cyclic AMP signalling in mycobacteria: redirecting the conversation with a common currency.* Cell Microbiol, 2011. **13**(3): p. 349-58.
60. McCue, L.A., K.A. McDonough, and C.E. Lawrence, *Functional classification of cNMP-binding proteins and nucleotide cyclases with implications for novel regulatory pathways in Mycobacterium tuberculosis.* Genome Res, 2000. **10**(2): p. 204-19.
61. Shenoy, A.R. and S.S. Visweswariah, *Mycobacterial adenylyl cyclases: biochemical diversity and structural plasticity.* FEBS Lett, 2006. **580**(14): p. 3344-52.
62. Linder, J.U., A. Hammer, and J.E. Schultz, *The effect of HAMP domains on class IIIb adenylyl cyclases from Mycobacterium tuberculosis.* Eur J Biochem, 2004. **271**: p. 2446–2451.
63. Ohmori, M. and S. Okamoto, *Photoresponsive cAMP signal transduction in cyanobacteria.* Photochem Photobiol Sci, 2004. **3**(6): p. 503-11.
64. Fujisawa, T., et al., *Genomic structure of an economically important cyanobacterium, Arthrospira (Spirulina) platensis NIES-39.* DNA Res, 2010. **17**(2): p. 85-103.

65. Kasahara, M., et al., *CyaG, a novel cyanobacterial adenylyl cyclase and a possible ancestor of mammalian guanylyl cyclases.* J Biol Chem, 2001. **276**(13): p. 10564-9.
66. Winkler, K., A. Schultz, and J.E. Schultz, *The s-helix determines the signal in a tsr receptor/adenylyl cyclase reporter.* J Biol Chem, 2012. **287**(19): p. 15479-88.
67. Krupinski, J., et al., *Adenylyl cyclase amino acid sequence: possible channel- or transporter-like structure.* Science, 1989. **244**(4912): p. 1558-64.
68. Mondejar, L.G., et al., *HAMP Domain-mediated Signal Transduction Probed with a Mycobacterial Adenylyl Cyclase as a Reporter.* J Biol Chem, 2012. **287**(2): p. 1022-31.
69. Kanchan, K., et al., *Transmembrane signaling in chimeras of the Escherichia coli aspartate and serine chemotaxis receptors and bacterial class III adenylyl cyclases.* J Biol Chem, 2010. **285**(3): p. 2090-2099.
70. Porath, J., et al., *Metal chelate affinity chromatography, a new approach to protein fractionation.* Nature, 1975. **258**(5536): p. 598-9.
71. Laemmli, U.K., *Cleavage of structural proteins during the assembly of the head of bacteriophage T4.* Nature, 1970. **227**(5259): p. 680-5.
72. Towbin, H., T. Staehelin, and J. Gordon, *Electrophoretic transfer of proteins from polyacrylamide gels to nitrocellulose sheets: procedure and some applications.* Proc Natl Acad Sci U S A, 1979. **76**(9): p. 4350-4.
73. Salomon, Y., C. Londos, and M. Rodbell, *A highly sensitive adenylate cyclase assay.* Anal Biochem, 1974. **58**(2): p. 541-8.
74. Lupas, A., M. Van Dyke, and J. Stock, *Predicting coiled coils from protein sequences.* Science, 1991. **252**(5009): p. 1162-4.
75. Hofmann, K. and W. Stoffel, *TMbase - A database of membrane spanning proteins segments.* Biol. Chem. Hoppe-Seyler 1993. **374**: p. 166.
76. Tusnady, G.E. and I. Simon, *The HMMTOP transmembrane topology prediction server.* Bioinformatics, 2001. **17**(9): p. 849-50.
77. Cserzo, M., et al., *Prediction of transmembrane alpha-helices in prokaryotic membrane proteins: the dense alignment surface method.* Protein Eng, 1997. **10**(6): p. 673-6.
78. Schultz, J., et al., *SMART, a simple modular architecture research tool: identification of signaling domains.* Proc Natl Acad Sci U S A, 1998. **95**(11): p. 5857-64.
79. Marchler-Bauer, A. and S.H. Bryant, *CD-Search: protein domain annotations on the fly.* Nucleic Acids Res, 2004. **32**(Web Server issue): p. W327-31.
80. Letunic, I., et al., *SMART 5: domains in the context of genomes and networks.* Nucleic Acids Res, 2006. **34**(Database issue): p. D257-60.
81. Kitanovic, S., P. Ames, J.S. Parkinson, *Mutational analysis of the control cable that mediates transmembrane signaling in the E. coli serine chemotaxis receptor.* Journal of Bacteriology, 2011. **193**(19): p. 5062-5072.
82. Doebber, M., et al., *Salt-driven equilibrium between two conformations in the HAMP domain from Natronomonas pharaonis: the language of signal transfer?* J Biol Chem, 2008. **283**(42): p. 28691-701.
83. Bayley, S.T. and R.A. Morton, *Recent developments in the molecular biology of extremely halophilic bacteria.* CRC Crit Rev Microbiol, 1978. **6**(2): p. 151-205.
84. Lanyi, J.K., *Salt-dependent properties of proteins from extremely halophilic bacteria.* Bacteriol Rev, 1974. **38**(3): p. 272-90.
85. Wang, J., et al., *HAMP domain signal relay mechanism in a sensory rhodopsin-transducer complex.* J Biol Chem, 2012. **287**(25): p. 21316-25.
86. Eisenbach, M., et al., *Repellents for Escherichia coli operate neither by changing membrane fluidity nor by being sensed by periplasmic receptors during chemotaxis.* J Bacteriol, 1990. **172**(9): p. 5218-24.

87. Tisa, L.S. and J. Adler, *Cytoplasmic free-Ca2+ level rises with repellents and falls with attractants in Escherichia coli chemotaxis.* Proc Natl Acad Sci U S A, 1995. **92**(23): p. 10777-81.
88. Khan, S. and D.R. Trentham, *Biphasic excitation by leucine in Escherichia coli chemotaxis.* J Bacteriol, 2004. **186**(2): p. 588-92.
89. Wright, G.A., et al., *Mutational analysis of the transmembrane helix 2-HAMP domain connection in the Escherichia coli aspartate chemoreceptor tar.* J Bacteriol, 2011. **193**(1): p. 82-90.
90. Ames, P., Q. Zhou, and J.S. Parkinson, *Mutational analysis of the connector segment in the HAMP domain of Tsr, the Escherichia coli serine chemoreceptor.* J Bacteriol, 2008. **190**(20): p. 6676-6685.
91. Gushchin, I.Y., V.I. Gordeliy, and S. Grudinin, *Role of the HAMP domain region of sensory rhodopsin transducers in signal transduction.* Biochemistry, 2011. **50**(4): p. 574-80.
92. Kouyama, T., et al., *Crystal structure of the light-driven chloride pump halorhodopsin from Natronomonas pharaonis.* J Mol Biol, 2010. **396**(3): p. 564-79.
93. Hayashi, K., et al., *Structural analysis of the phototactic transducer protein HtrII linker region from Natronomonas pharaonis.* Biochemistry, 2007. **46**(50): p. 14380-90.
94. Greenfield, N.J., *Using circular dichroism spectra to estimate protein secondary structure.* Nat Protoc, 2006. **1**(6): p. 2876-90.
95. Watts, K.J., B.L. Taylor, and M.S. Johnson, *PAS/poly-HAMP signalling in Aer-2, a soluble haem-based sensor.* Mol Microbiol, 2011. **79**(3): p. 686-99.
96. Anantharaman, V., S. Balaji, and L. Aravind, *The signaling helix: a common functional theme in diverse signaling proteins.* Biol Direct, 2006. **1**: p. 25.
97. Schultz, J.E. and J. Natarajan, *Regulated unfolding: a basic principle of intraprotein signaling in modular proteins.* Trends Biochem Sci, 2013. **38**(11): p. 538-45.